SOME GEOTECHNICAL ASPECTS OF ICEBERG GROUNDING

TUPPAL RAMANUJA CHARI

SOME GEOTECHNICAL ASPECTS OF ICEBERG GROUNDING

by

© Tuppal Ramanuja Chari, B.E., M.Tech.,

A Thesis Submitted in Partial Fulfillment

of the Requirements for the Degree of

Doctor of Philosophy

Faculty of Engineering and Applied Science

Memorial University of Newfoundland

March 1975

St. John's Newfoundland

ABSTRACT

On Canada's eastern seaboard where hydrocarbon deposits have now been determined, the operational hazards are numerous. Damage by icebergs to installations on and in the ocean floor is one of the major threats. An understanding of the interaction of an iceberg with the continental shelf surface sediment during the process of grounding is needed to establish safe design standards for bottom structures in offshore drilling operations. Knowledge of icebergs, their size, shape and drift, is still very limited and so is the engineering behaviour of the surface sediment of the oceans.

In this thesis, the behaviour of an iceberg of idealized shape is analyzed while it grounds in a uniform slope of very weak and compressible sediment. An expression was derived for the theoretical size of the scour that could be caused and this was substantiated by laboratory experiments.

A tiltable towing tank was fabricated in which a 9" wide plexiglas model of the idealized iceberg was tested. Forces and pressures on the model were measured during the process of its scouring into an artificially sedimented slope. The frontal soil resistance was found to be the predominating force confirming the assumptions made. Soil failure was dominantly local. A soil front of about 5 feet was under compression during the gouging process and a similiar phenomenon was also noticed below the maximum scour depth. About 30% of the pushing effort was computed to be

lost in this compression. Observations in a small tank with 2" wide models confirmed the soil compression phenomenon and also led to a qualitative understanding of the effects of iceberg shape.

Scour sizes, computed and compared with reported side-scan observations off the Newfoundland coast showed that the predictions made by the analytical model are realistic.

ACKNOWLEDGMENTS

This dissertation was completed at Memorial University of Newfoundland, as part of a project sponsored by the National Research Council of Canada Negotiated Grant to the Faculty of Engineering and Applied Science for research in Ocean Engineering. The writer wishes to acknowledge the receipt of a Memorial University Fellowship during this study.

The writer is deeply indebted to Dr. J.H. Allen, Professor and Chairman of the Supervisory Committee, for his mature advice, guidance and contribution to the progress of this study. The writer would like to express his gratitude to Dr. J.J. Sharp and Mr. E. Moore, Associate Professors in Engineering, for their keen interest in the progress of this work and their willingness to help. Dr. J.M. Jones, Associate Professor in Engineering, assisted to a great extent in the instrumentation for which the writer expresses his grateful appreciation.

As with all research of this type, many individuals contributed to this study. In particular, the writer wishes to acknowledge the assistance and express his appreciation to Dr. R.M. Slatt, Mrs. C. Allen, Mr. J.F. Johnstone, Mr. H. Jacobs and Mr. J. Tucker.

The typing of this thesis was done by Miss D. Woodland and drafting by Mr. T.F. Dyer.

TABLE OF CONTENTS

LIST OF TABLES

LIST OF FIGURES

NOTATIONS

The symbols used in this thesis generally confirm to those suggested by the American Society of Civil Engineering (Nomenclature for soil mechanics, Journal of the soil mechanics division, June 1962) and are defined when they first appear in the text. This list will serve as a general reference and guide

A = Projected area of an iceberg normal to wind/current, cross-sectional area at the water line.

a = acceleration

B = width of an iceberg scour track, width of an idealized iceberg

c = soil cohesion

c_a = soil-structure adhesion

c_v = coefficient of consolidation

C_d = coefficient of drag (fluid/wind)

D = depth, maximum scour depth

d = any representative depth, usually an intermediate scour depth

e_o = initial void ratio

e_1 = final void ratio

F = force due to soil resistance

g = acceleration due to gravity

H = maximum height of surcharged soil

h = any representative height of the surcharge

K_1, K_2	=	constants
L	=	length, maximum length of gouge
ℓ	=	any representative gouge length
L_1	=	maximum length of soil surcharge in front of an iceberg
ℓ_1	=	any representative length of the surcharge
M		mass
P, P_1, P_2	=	force due to soil pressure
P_p	=	coefficient of passive soil pressure
q	=	rate of sediment deposition
S, S_1	=	shear force
t	=	time
U	=	degree of consolidation of a sediment deposit
u	=	excess hydrostatic pressure in pore water
$\bar{U}$	=	average degree of consolidation of a sediment deposit
V	=	velocity, velocity of an iceberg at the commencement of scouring.
V_s	=	velocity of soil in front of an iceberg
W	=	weight of an iceberg, weight of soil particle
W_s	=	weight of soil wedge
z	=	any representative depth
α	=	slope of surcharged soil
β, β'	=	slope of a sediment deposit
γ	=	unit weight of soil
γ'	=	submerged unit weight of soil
γ_w	=	unit weight of water
δ	=	angle of soil/structure friction

θ = angle of inclination of the soil wedge to the horizontal

λ = scale ratio of a model

μ = coefficient of friction

ρ = density of any medium in which a body moves

τ = shear stress in soil

τ_f = shear strength of soil

ϕ = angle of internal friction in soil

CHAPTER I

INTRODUCTION

Engineering research problems usually arise out of an immediate need of industry and are mostly unique because of their environment. Study of icebergs in recent years is one such example. The search for mineral resources on the continental shelves and slopes has resulted in a spurt of ocean engineering research since the late nineteen fifties. With an area nearly 2½ times the land surface, the ocean environment is vast, invariably hostile and varied. Winds, waves, tides and currents are usually to be contended with in addition to all the other problems encountered on land. On Canada's eastern seaboard where the petroleum finds are now promising, there are two additional hostile elements, sea ice and icebergs. The main thrust of research activity in ocean engineering at Memorial University of Newfoundland has been on the special problems of this region. Iceberg study has been one of these.

TYPES OF ICEBERG THREAT

The types of threat by icebergs in general can be classified as (Fig. 1):

1. To navigation - a direct collision with a moving ship,
2. To offshore structures - a direct collision with a fixed or semifixed offshore drill rig, and
3. To ocean bottom installations - through scouring and bottom dragging icebergs.

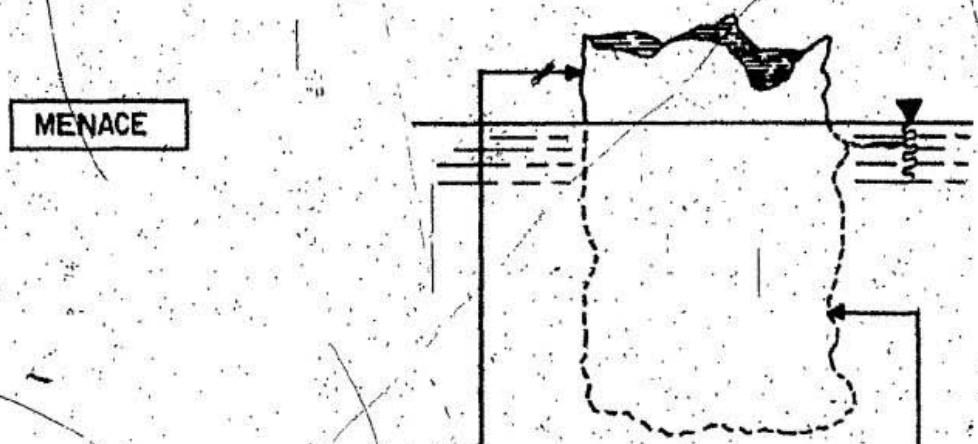

FIG. 1.- TYPES OF ICEBERG THREAT

Navigation: The real threat to navigation from icebergs was demonstrated after the 'Titanic' disaster of 1912, when 1517 lives were lost. This resulted in the formation of the International Ice Patrol mainly to warn the ships sailing across the iceberg alley in the Grand Banks region. A forewarned ship can thus watch for icebergs and steer clear of their course.

Offshore installations: Offshore installations such as oil rigs are more vulnerable to collision with icebergs because of their relative immobility. Even if the rig is a mobile drill ship, the process of dismantling and moving away from the iceberg path takes time. In terms of the unproductive days till the rig is reinstalled in the same location, the loss is reportedly estimated[5,19*] at about 40,000 dollars per day. Some of the solutions suggested[19] to prevent the collision of a drifting berg with an offshore rig include

1. Deflecting the iceberg from the collision course,
2. Designing the rig so that it can be quickly moved and reinstalled after the berg moves off,
3. Making the offshore installation strong enough to withstand collision forces, and
4. Locating the operation within a suitable bunded protection.

Detailed studies have already been done at Memorial University[18] to demonstrate that icebergs could be deflected off the collision course by applying a suitable external towing force. This method

---

* Numerals in parentheses refer to corresponding items in the bibliography.

seems to have met with appreciable success by some oil companies during the latest drilling season.

Sea bottom structures: The present investigation is concerned with the iceberg threat to sea bed installations such as blowout preventer stacks, pipe lines and underground storage facilities through scouring and bottom dragging bergs. Side-scan sonar images of the ocean floor northeast of Newfoundland[37] (Fig. 2) and in the Beaufort Sea[65] show definite scour marks attributed to icebergs. Observations even in the Northeast Atlantic west of the British Isles and the Norwegian coast show tracks[13,48] believed caused by icebergs. These later scours were said to have been formed when bergs were common in this area thousands of years ago. It thus appears from these reports that some of the geomorphological features of the sea bed could be quite ancient. The scours observed in the Labrador Sea could therefore be recent or ancient, and it is difficult to correlate these to the iceberg sizes seen at the present time.

THE PURPOSE AND SCOPE OF THE INVESTIGATION

From the literature surveyed during the course of this investigation, it appears that no research has been done till recently on the mechanics of iceberg grounding although there have been speculations on the damage that could be caused by a grounding iceberg. A comprehensive project on iceberg grounding was commenced at Memorial University aimed at predicting the design standards for ocean bottom structures to enable them to be located safely in specified offshore location in the iceberg-infested waters. This

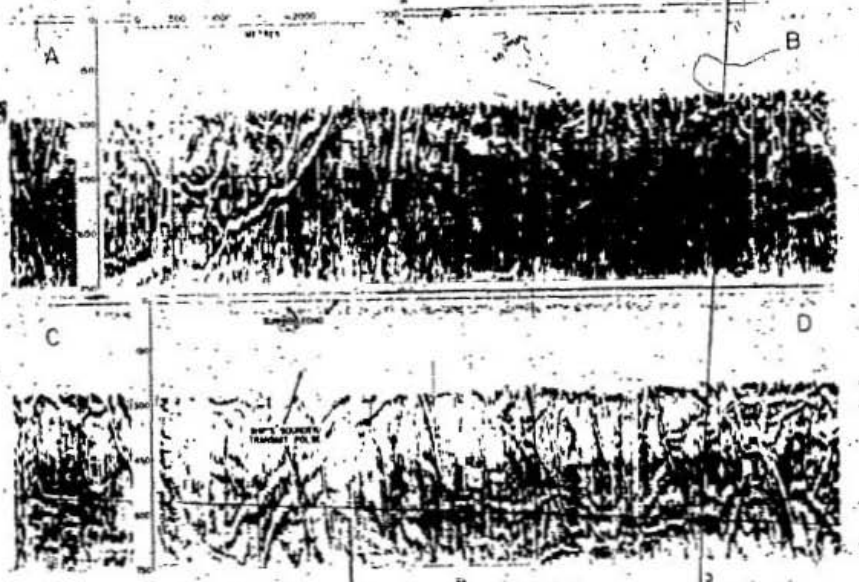

FIG. 2. - SIDE SCAN SONAR IMAGE OF ICEBERG SCOUR MARKS ON THE NORTHEASTERN COAST OF NEWFOUNDLAND (From Harris and Jollymore[37])

presentation is a first step towards this goal and is confined to:

1. Studying the implications of the problem in reference to the current state-of-the-art on,

   a) Icebergs, their shape, size and propelling forces,

   b) The engineering properties of the sea floor surface deposits, and

   c) The iceberg-sediment interaction.

2. Developing an analytical model for an idealized iceberg scouring into soft and weak sediment, and

3. Testing the analytical model after designing a suitable test facility.

The safety of the sea bed installations is the main theme of this discussion. Deep scours are likely when the iceberg is rigid in comparison with the sediment. In fact this would be the actual situation for most areas of the continental shelf.

Icebergs are huge in mass, generally weighing millions of tons and travel at relatively low velocities in the range of 0.25 knots (0.42 ft/sec) to 1 knot (1.68 ft/sec). The scouring potential of an iceberg is primarily from its kinetic energy. At these low velocities any gain in the potential energy of the berg through a rise in its level greatly reduces the scouring capacity. Such a possibility will be shown to be unlikely when an iceberg interacts with very soft sediments. The grounding phenomenon will therefore be considered as one where an iceberg ploughs into a sediment slope, spreads the gouged soil in front and to the side and dissipates its entire kinetic energy as it slowly ploughs deeper. The consequent interaction between the sediment and the iceberg will be analyzed.

CHAPTER II

THE STATE-OF-THE-ART AND REVIEW OF LITERATURE

Engineering research on icebergs is a relatively novel area. The general characteristics of icebergs will therefore be reviewed in detail. Some of the available data on the engineering properties of ocean floor surface deposits will be discussed along with the mechanics of soil movement and cutting with tillage equipment which bears some resemblance to iceberg grounding.

EARLY STUDIES ON ICEBERGS

Recorded observations on icebergs date back to the year 1859 when one Rev. Louis L. Noble[58] went on a voyage along the Labrador coast for the purpose of "studying and sketching icebergs". A vivid description of the different shapes and also the dangers in approaching too close to an iceberg are described in this work. Bergs were observed grounded in 40 and 50 fathom waters. In a more scientific study in 1876, Milne[52] examined the geological features of Newfoundland and attributed the parallel markings on outcrops to iceberg action. It is known that fishermen identified[12] fertile fishing and sealing grounds from grounded bergs. Damage to cod traps by icebergs was always a recognized threat.

Formation of the International Ice Patrol in 1914 may be said[87] to be the first step in the study of iceberg drift, shape, size and draft. Though the Ice Patrol was primarily intended to warn

ships sailing through the iceberg-infested waters, the U.S. Oceanographic department which operates the Ice Patrol has been conducting scientific studies correlating the berg movement with the ocean currents and winds. The Marion expedition report[70] is a significant early contribution in this effort followed by other periodical publications.

Fig. 3 is a map of the Northwest Atlantic Ocean showing the normal iceberg drift paths and also the oil exploration lease area which lies along the iceberg alley. The need for understanding the movement of these *ice mountains* for a safe offshore operation is obvious.

ORIGIN OF ICEBERGS

Practically all icebergs of the North Atlantic Ocean originate from the Greenland ice cap. From about 100 glaciers on the Greenland coast, 21 major ones[29,69,70] located between the Melville Bugt and Disko Bugt on the west coast contribute the maximum discharge, accounting for about 85% of the bergs reaching the Newfoundland coast. East Greenland glaciers account for 10% of the numbers and the remaining 5% are said to come from[29] Northern Ellesmere Island. While the estimates of the berg count dumped into the ocean varies from 15,000 to 40,000 bergs per year[32,55,63,70] it is generally agreed that a vast number are permanently grounded near their birth place. A large percentage are trapped in the bays and indentations of the Baffin Island and Labrador coasts. An average of 2,500 icebergs per year[56] cross the 60th parallel of latitude near

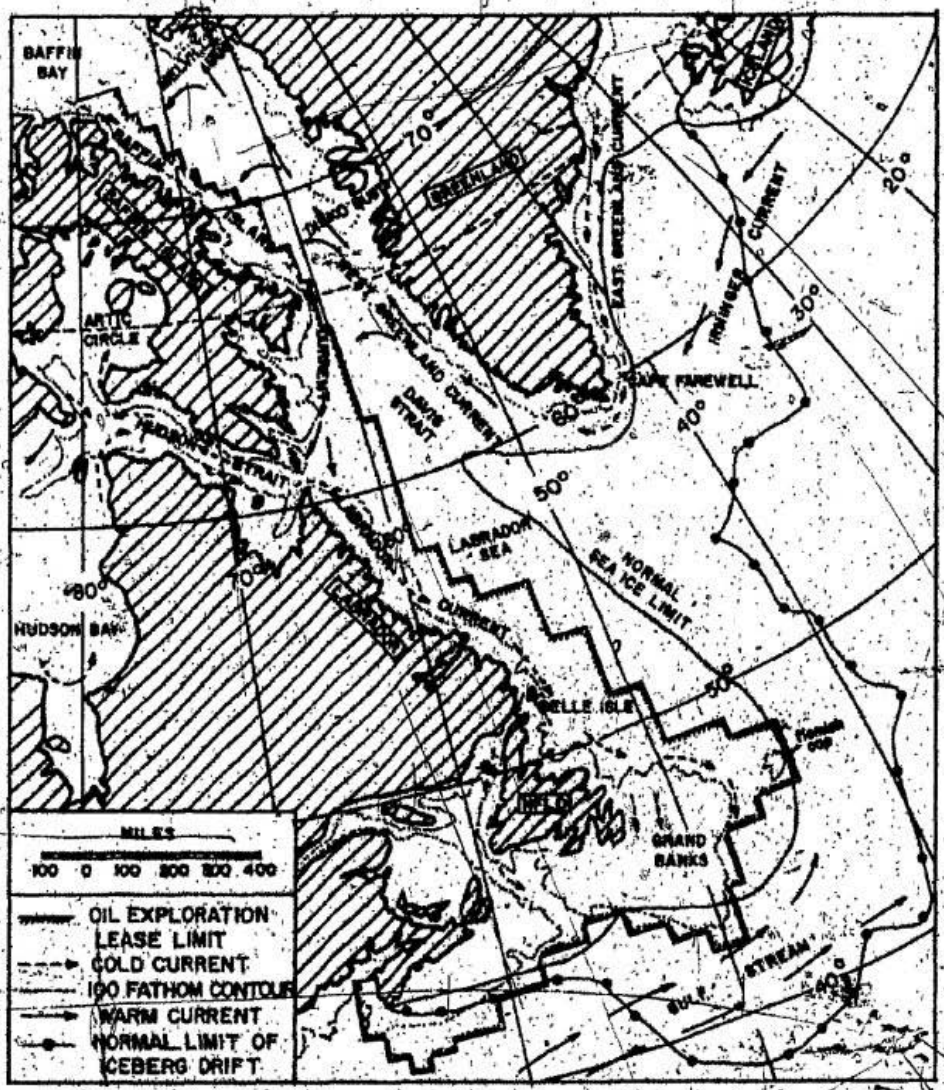

FIG. 3 -- REGION OF ICEBERG PROBLEMS

This map shows the offshore exploration lease limit, the normal limit of iceberg and sea ice occurrence and the ocean circulation in the Northwest Atlantic Ocean.

the northern tip of Labrador, nearly 1,000 bergs are seen off Belle Isle[29] and an average of 400 peaking around 1,000 during severe ice years reach the Grand Banks off Newfoundland. Fig. 4 is adapted from the International Ice Patrol record[77] of the berg count crossing the 48th parallel. The southern edge of the Grand Banks, where the Gulf Stream flows, is the limit up to which icebergs are a threat in any number.

Iceberg production: Glaciers and glacier movement form a separate field of study. Glaciers originate from snow accumulation which consolidate and form a nucleus. These increase in thickness and mass while the forces of gravity cause the edges of the sheet to creep forward and outward along paths of least resistance. Greenland glaciers are said to be rapid ice streams flowing at a rate of about 35 to 60 feet per day with wide fronts. The mean tidal range along the West Greenland coast is[21] between 6.2 and 10.5 feet and the maximum 10.1 to 17.5 feet. The glacier flow comes out of the fjords into the sea and at spring tides about twice a month the end breaks off in great calving (Fig. 5). Iceberg calving has been broadly classified[32,70] into four types.

1. The largest iceberg is calved when the front end of a glacier outlet enters water deep enough to float it. The end of the glacier is slowly raised by the buoyancy of water and is then torn loose.

2. The second type of calving occurs when the glacier front is subjected to faster disintegration in air forming a toe-like projection. This is subsequently undermined by sea water, breaks off

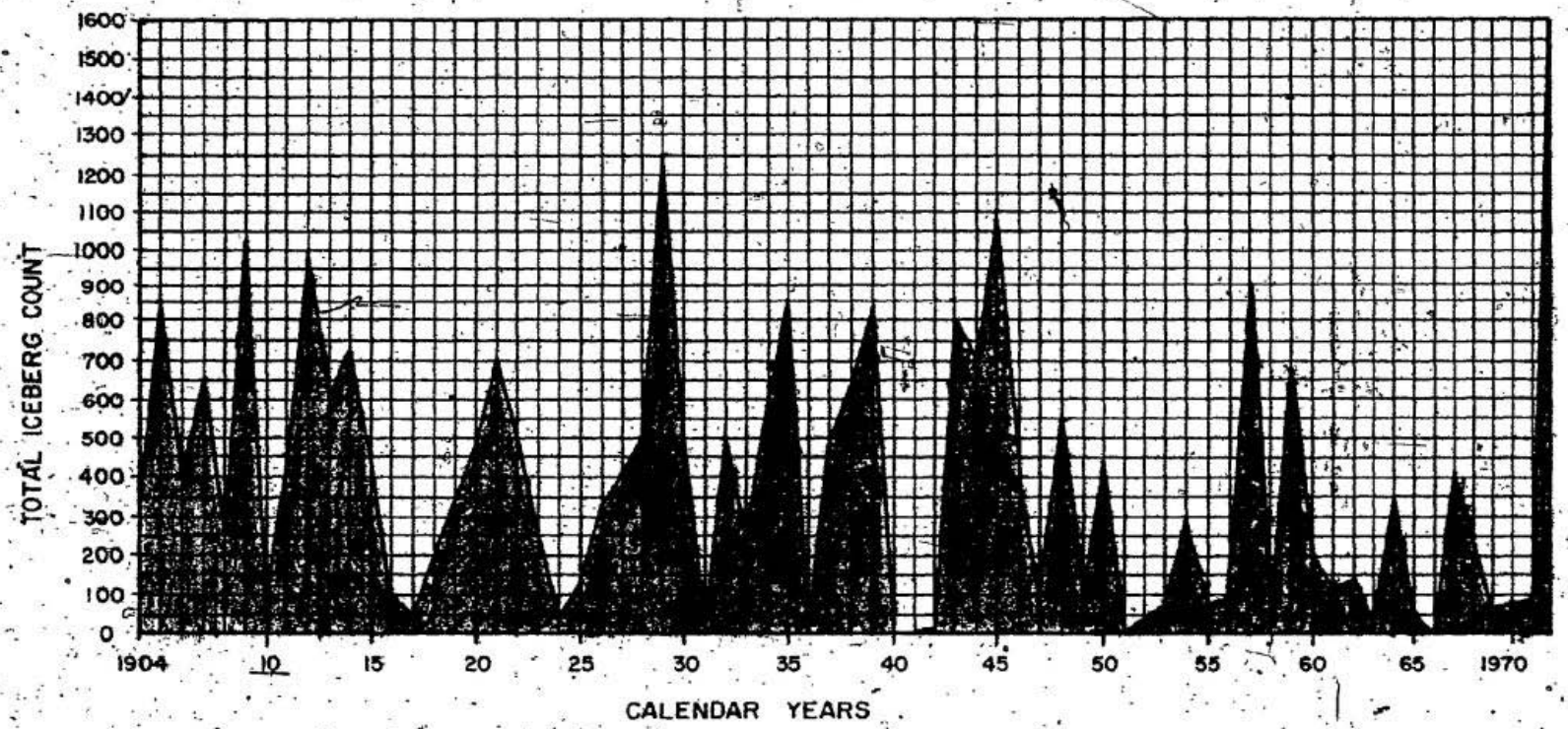

FIG. 4.- YEARLY COUNT OF ICEBERGS CROSSING THE 48TH PARALLEL OF LATITUDE OFF NEWFOUNDLAND.

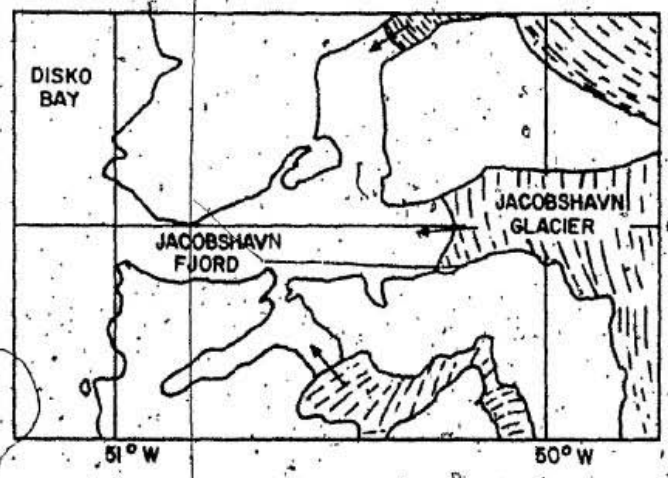

FIG. 5a.- GLACIER FLOW INTO JACOBSHAVN FJORD

Other fjords have a similar topography.

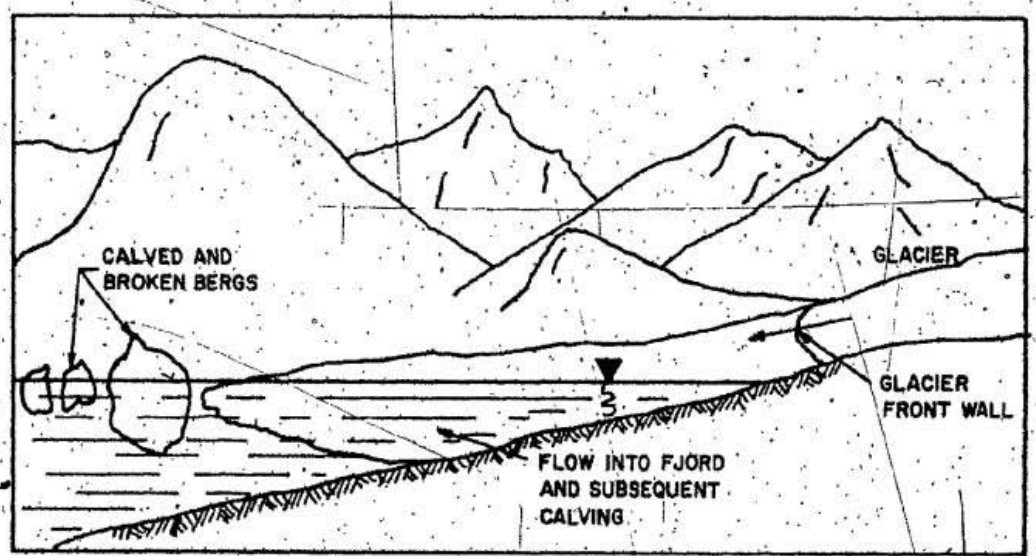

FIG. 5b.- ICEBERG CALVING

(Modified from Smith[70])

usually with a great noise and then bobs up and down till an equilibrium is reached.

3. Sometimes the underwater portion disintegrates faster than the above-water portion and the glacier breaks off when the projecting weight is sufficient to cause a fracture. The berg then plunges beneath, bobs up and down and reaches equilibrium.

4. The fourth type of calving is caused by pieces of ice breaking off and falling from the upper body of the glacier. This results in the smallest of the bergs.

Generally once calved, the bergs are contained inside the fjords and are packed row upon row. It has been stated[70] that an ice dam is formed at the fjord mouths by the jamming of icebergs. Approximately ten times a year, without any warning, the icebergs start moving out into the sea in trains, slowly at first and then attain an incredible speed of 5 to 8 miles per hour accompanied by a thundering noise. This phenomenon termed *offshoot* is attributed to the breaking of the ice dam by the pentup iceberg meltwater and the subsequent discharge of bergs into the bay.

Ice Islands: Ice islands are formed by the combination of land-fast ice and glacier ice. These are common in the Beaufort Sea and are believed to come from[16] the Ellesmer Island ice shelf. Ice islands have been reported grounded[4,65] in the Beaufort Sea and on the Alaskan continental shelf. This problem is of concern to the Arctic oil and gas exploration program. The draft of ice islands is generally in the 100 to 150 feet range which is less than a quarter of that of some of the Atlantic icebergs and hence they ground in relatively shallower

waters.

Antarctic Icebergs: It is relevant to mention here that icebergs are also calved in the Antarctic. Fig. 6 is a comparison of the topography of the Antarctic and Greenland glaciers. The Greenland icecap is believed to be comprised of two or three dome shapes with the edge contained within the land mass while the Antarctic icecap is one huge mass overflowing into the sea. Summers are also believed less severe in Antarctic. These glaciers therefore flow and spread over large areas before being fractured. A huge tabular shape is characteristic of Antarctic bergs. Icebergs of Antarctic origin, 60 miles wide and 208 miles long, have been observed and reported[32]. However, they have not so far been considered any threat to civilization as the drift path of these bergs does not cross any major commercial shipping lanes and the resource potential of the Antarctic is still to be explored.

PHYSICAL PROPERTIES OF ICEBERGS

The specific gravity of an iceberg varies depending on the relative degree of consolidation at the parent glacier. The voids in the structure of snow precipitated in the glacier regions contain air. In the process of snow accumulation and consolidation, this air is trapped inside and finally becomes part of the glacier structure. Iceberg ice thus contains significant quantity of entrapped air[10] estimated as varying from 7 to 15 percent. As the berg drifts and slowly melts, the release of entrapped air can be generally noticed[2] by the upwelling and bubbling all around the berg. Depending on the

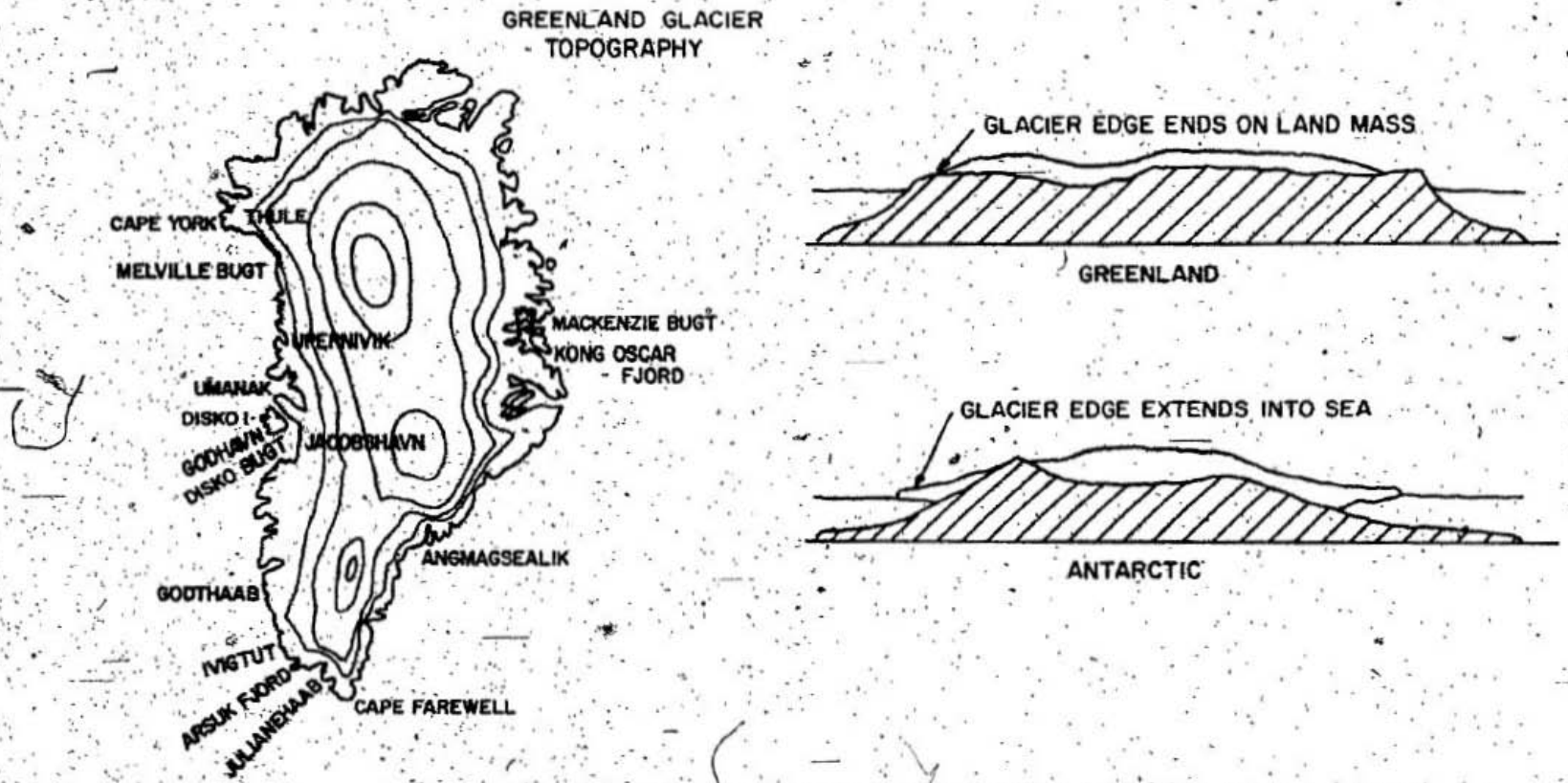

FIG. 6.- COMPARISON OF ARCTIC AND ANTARCTIC GLACIER CAPS

Note the protrusion of the Antarctic glacier edge into the sea
(Adapted from Smith[70])

porosity, a glacier can have[70] a specific gravity as low as 0.6 upto 0.905, compared to 0.92 for frozen fresh water. An iceberg embraces the entire glacier front, top to bottom and hence the specific gravity may vary over a wide range. For the bergs that float on the Labrador and Newfoundland coasts an average specific gravity of 0.89 is generally assumed reasonable. Data on the strength of icebergs were not noticed in the literature examined. Limited tests on compressive strength of cylindrical specimens conducted at room temperature (about 70°F) showed a value of about 180 p.s.i.

ICEBERG CLASSIFICATION - SHAPE, HEIGHT AND DRAFT

Icebergs vary very greatly in form and size. Views from two directions of typical icebergs with their prominent dimensions are shown in Fig. 7. No two bergs are alike. The shape of an iceberg will change as it drifts, disintegrates and rolls over. Even a particular iceberg viewed from various angles often looks different. After observing a number of icebergs, the International Ice Patrol broadly classified icebergs based on the size and above-water shape. These classifications and their suggested draft to height ratios are given in Tables I to III.

One of the major parameters in either iceberg towing or iceberg grounding is its draft. When a berg with an average specific gravity of 0.89 floats in sea water of specific gravity 1.03, the volume of the berg hidden below would be nearly 7 times the above-water portion. However, the draft in relation to the exposed height depends on the shape of the berg. While a prismatic block

TABLE I

ICEBERG TYPES BY SIZE[55]

NOMENCLATURE	HEIGHT	LENGTH
TABULAR BERGS:		
S - small	20 ft.	Less than 300 ft.
M - medium	20 to 50 ft.	300 to 700 ft.
L - large	More than 50 ft.	More than 700 ft.
OTHER TYPES:		
S - small	Less than 50 ft.	Less than 200 ft.
M - medium	50 to 150 ft.	200 to 400 ft.
L - large	150 to 255 ft.	400 to 700 ft.
VL - very large	More than 255 ft.	More than 700 ft.

NOTE: Sizes refer to the above-water dimensions. When the length and height fall into two different classifications, the larger one is used.

could have a draft of 7 times its height, a pyramidal berg will only have a draft almost equal to its height.

Based on observations, the International Ice Patrol suggested the draft/height ratios for bergs of different shape (Table III).

Theoretical ratios of draft to height for stable icebergs of regular shapes were computed by Allaire[1]. These are reproduced in Table IV. From these data it is seen that the draft of an iceberg can vary from 1 to 9 times its exposed height depending on

TABLE II

ICEBERG TYPES BY SHAPE[55]

TYPE	DESCRIPTION
B - Blocky	Steep precipitous sides with horizontal or flat top, very solid berg, length/height ratio 5:1.
DK - Drydock	Eroded such that a large U-shaped slot is formed with twin columns or pinnacles, slot extends into the water line or close to it.
D - Dome	Large smooth rounded top, solid type berg.
P - Pinnacled	Large central spire or pyramid of one or more spires dominating the shape, less massive than dome shaped bergs of similar dimensions.
T - Tabular	Horizontal or flat-topped berg with length/height ratio of 5:1.
Bergy Bit	A mass of glacial ice smaller than a berg but larger than a growler, about the size of a small cottage, small berg or large growler is preferred usuage.
Growler	A mass of glacial ice that has calved from a berg or is the remains of a berg. Less than 8 ft height and 20 ft length.

TABLE III

DRAFT/HEIGHT RATIOS SUGGESTED BY ICE PATROL[70]

TYPE	DRAFT/HEIGHT RATIO
Tabular or rectangular (Blocky)	5:1
Rounded (domed)	4:1
Pyramidal	3:1
Pinnacled	2:1
Winged or horned (drydocked)	1:1

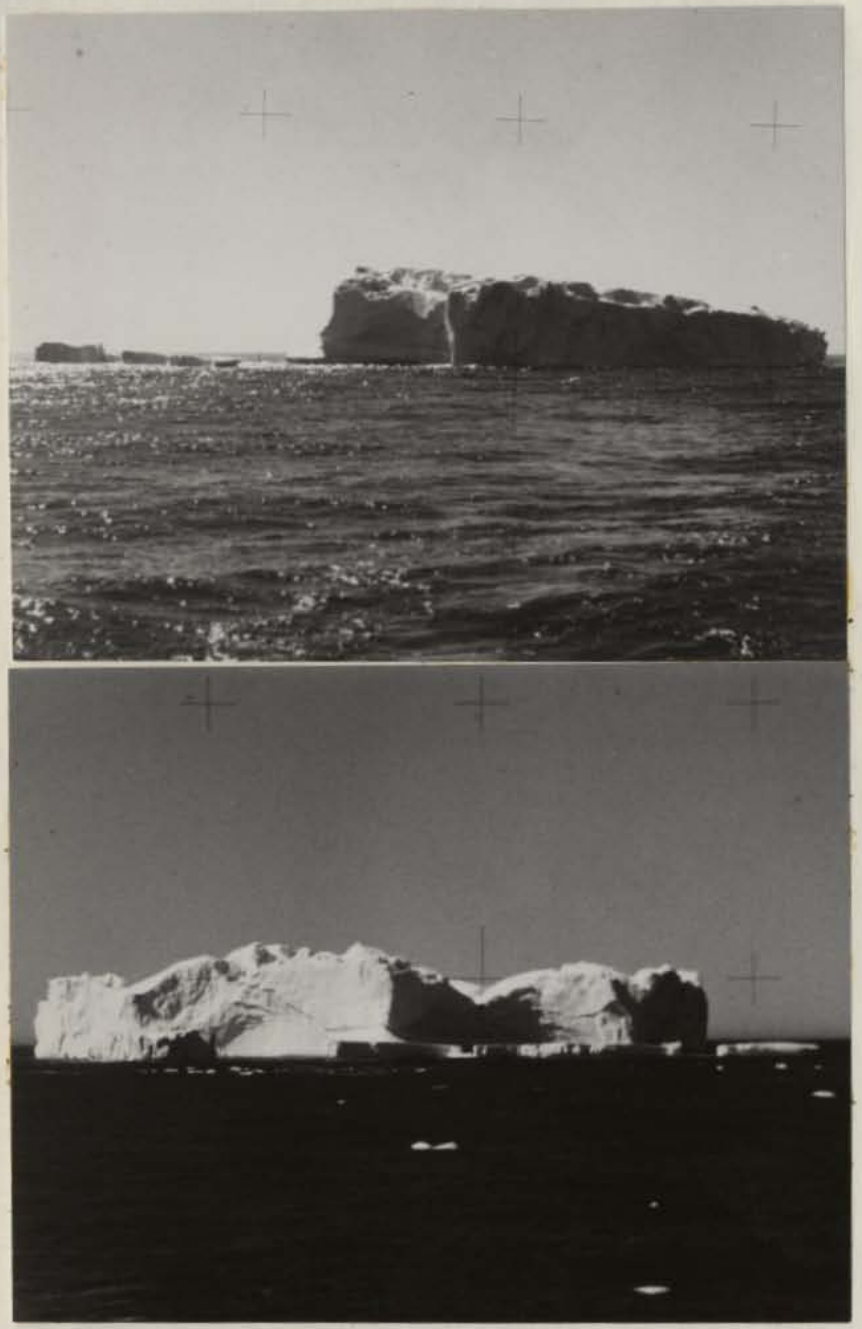

FIG. 7a.- PHOTOGRAPHS OF A TABULAR ICEBERG

Estimated Dimensions:

Height = 170 ft.
Length = 1100 ft.
Width = 950 ft.
Draft = 700 ft.
Weight = 20-25 million tons

FIG. 7b.- PHOTOGRAPHS OF A PINNACLED CRESCENT ICEBERG

This berg is crescent shaped in plan
Estimated Dimensions:

Height	=	170 ft.
Length	=	700 ft.
Width	=	400 ft.
Draft	=	450 ft.
Weight	=	3-3.5 million tons

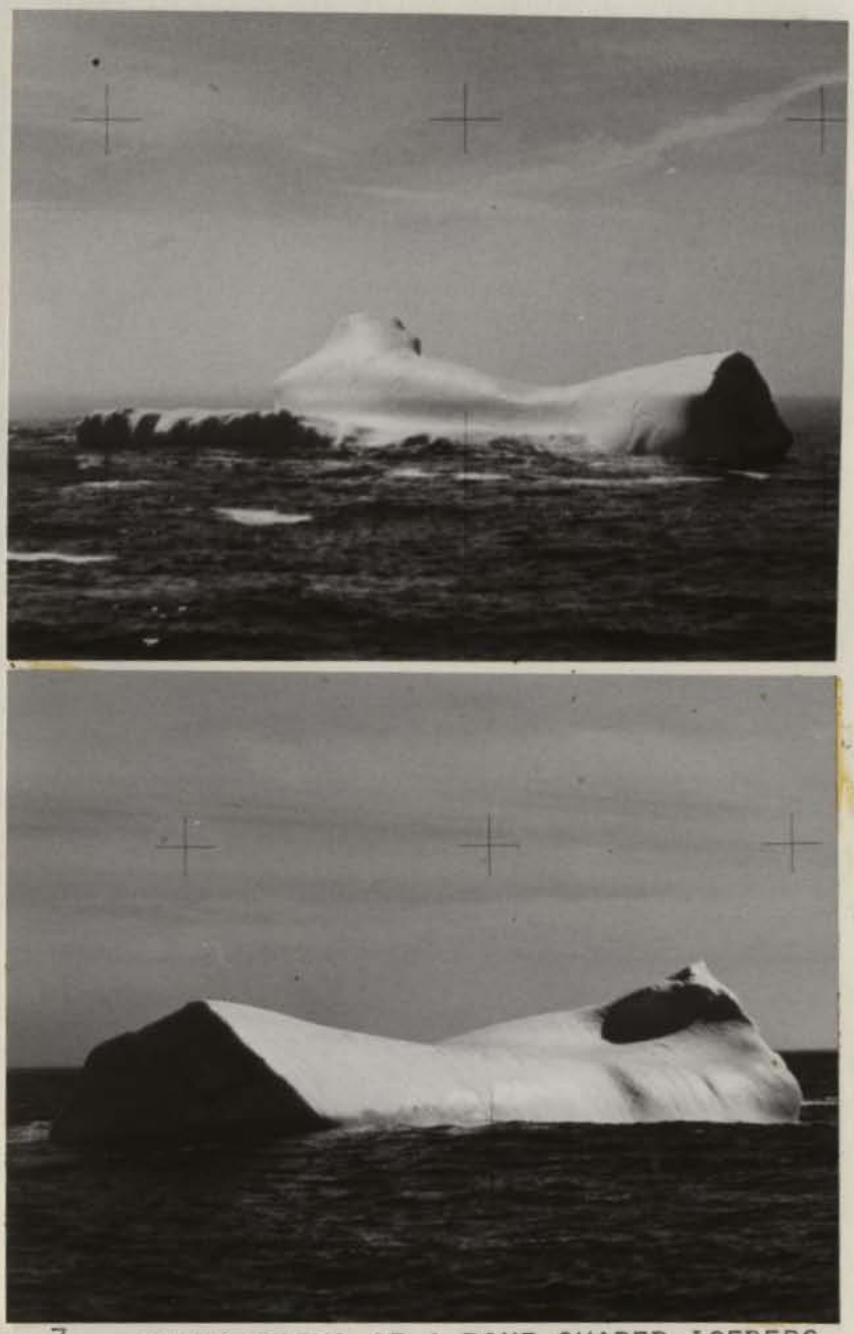

FIG. 7_c.- PHOTOGRAPHS OF A DOME SHAPED ICEBERG

Estimated Dimensions:

Height	=	40 ft.
Length	=	200 ft.
Width	=	100 ft.
Draft	=	150 ft.
Weight	=	50-70 thousand tons

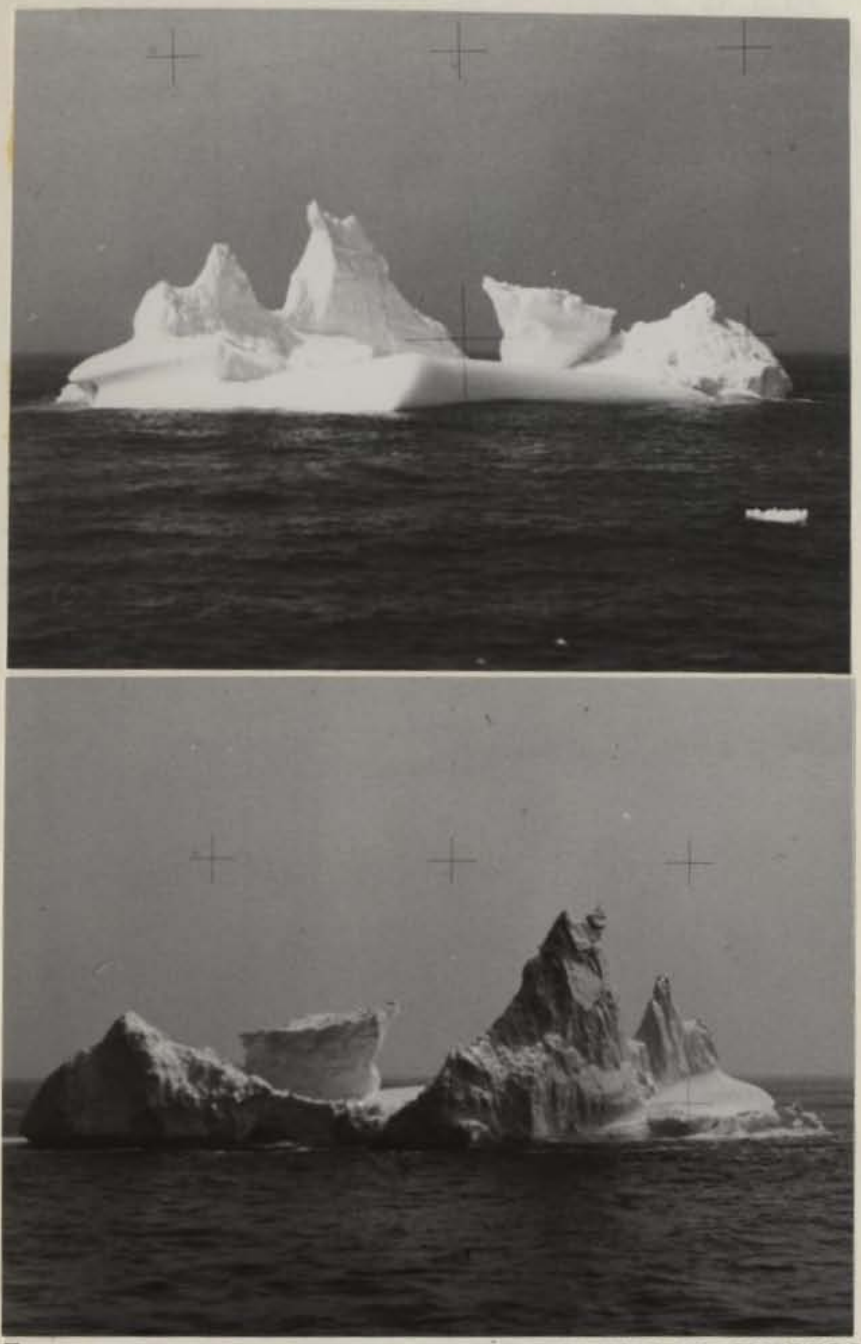

FIG. 7d.- PHOTOGRAPHS OF A MULTI-PINNACLED ICEBERG

Estimated Dimensions:

Height = 90 ft.
Length = 300 ft.
Width = 100 ft.
Draft = 200 ft.
Weight = 150-200 thousand tons

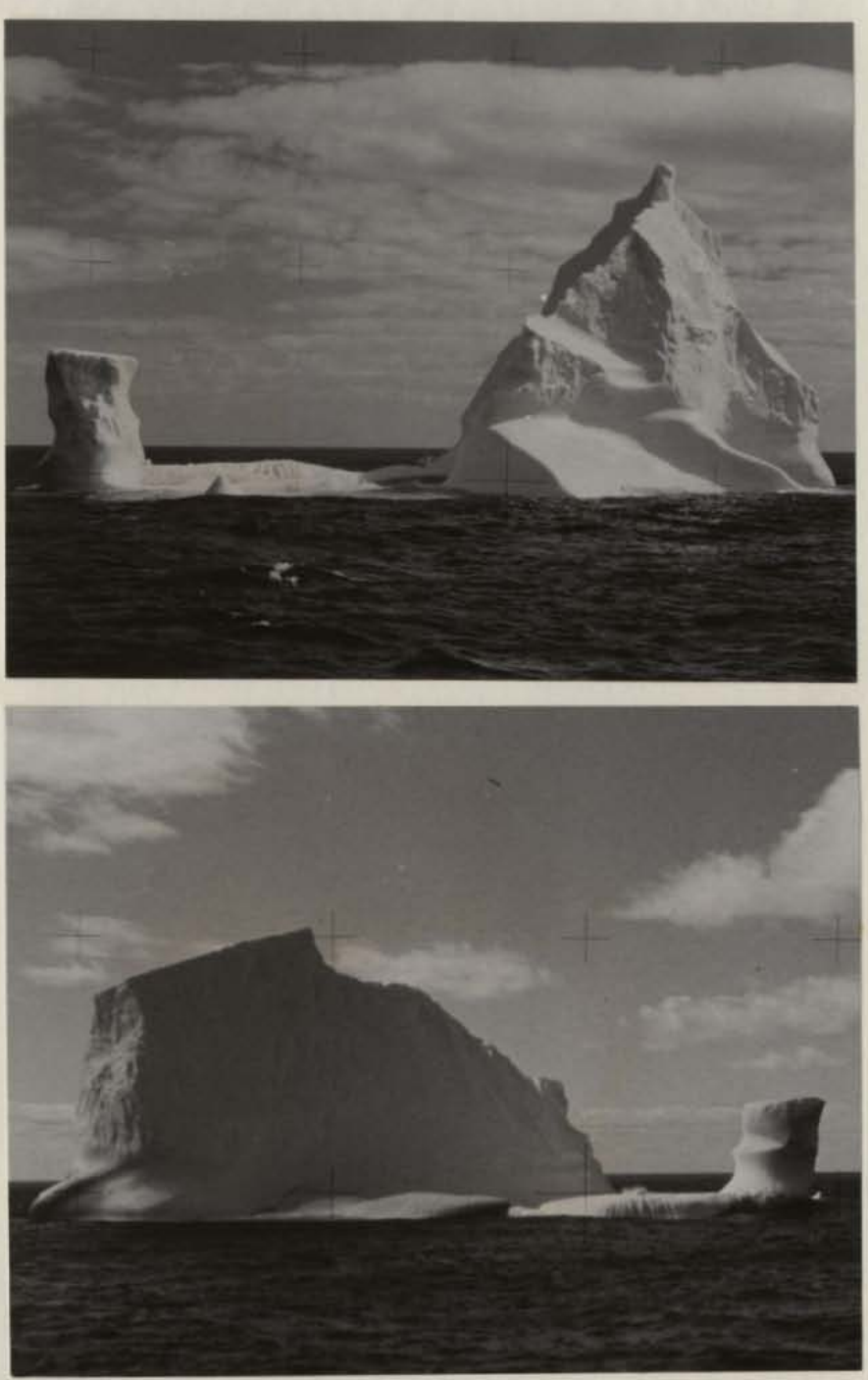

FIG. 7e.- PHOTOGRAPHS OF A DRYDOCKED ICEBERG

Estimated Dimensions:

Height	=	250 ft.
Length	=	570 ft.
Width	=	300 ft.
Draft	=	300 ft.
Weight	=	1½-2 million tons

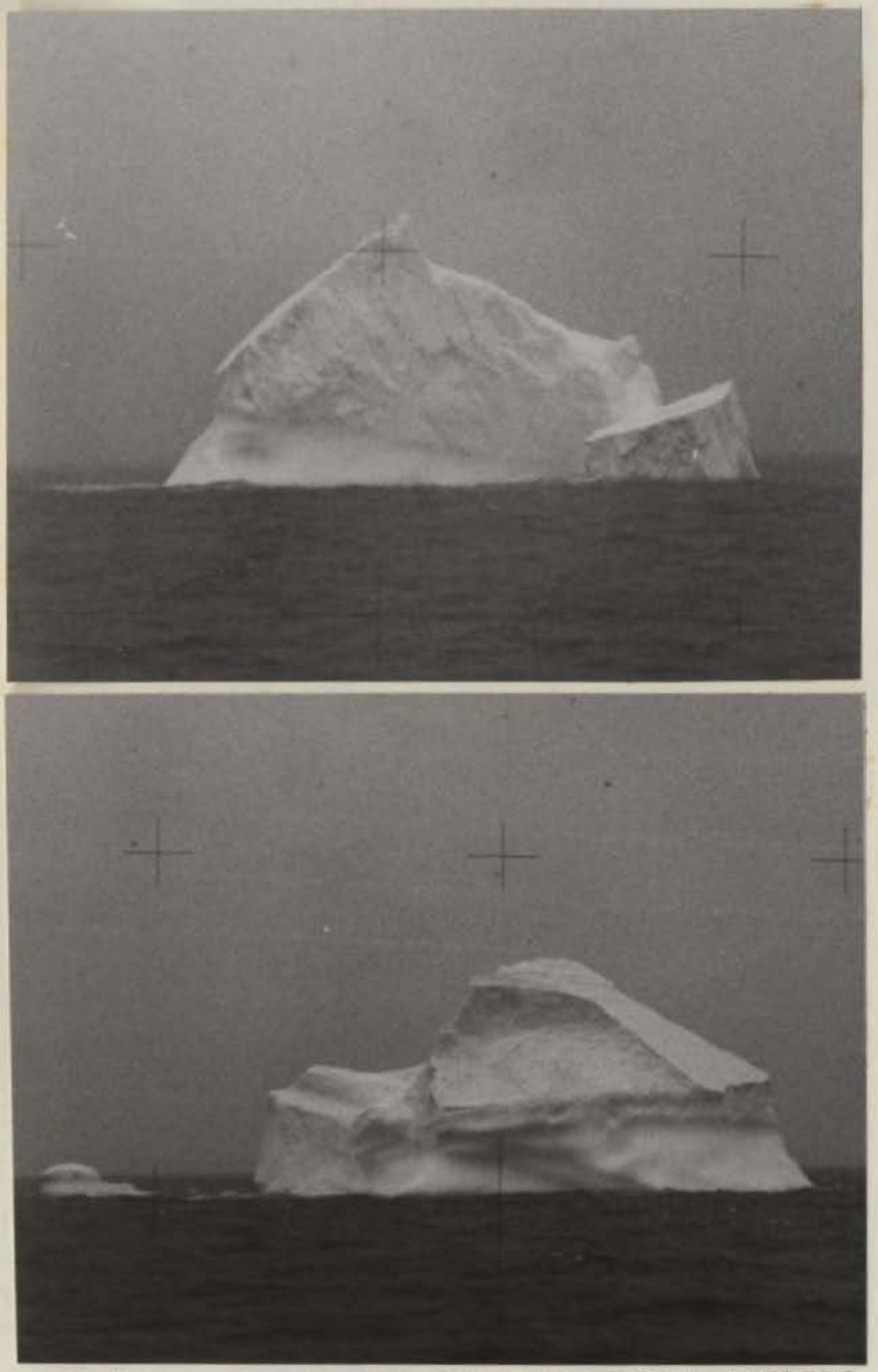

FIG. 7f.- PHOTOGRAPHS OF A PINNACLED ICEBERG

The general shape of the berg is pyramid with a pinnacle on top.

Estimated Dimensions:

Height	=	200 ft.
Length	=	650 ft.
Width	=	450 ft.
Draft	=	300 ft.
Weight	=	4-5 million tons

TABLE IV

COMPUTED DRAFT/HEIGHT RATIOS FOR REGULAR SHAPED ICEBERGS[1]

ICE PATROL CLASSIFICATION	ASSUMED SHAPE	MEASURED DRAFT/HEIGHT	CALCULATED DRAFT/HEIGHT
Blocky or Tabular	Half Ellipsoid	6.7:1 to 5.1:1	9:1
	Rectangular		7.2:1
	Cross		4:1
	Inverted T		3:1
	Star		2.6:1
Drydock	Deep dry dock I		4.9:1
	Deep dry dock II		3.8:1
	Shallow dry dock I		3:1
	Shallow dry dock II		2.5:1
	Pinnacled dry dock		1.3:1
Dome	Ellipsoid	3.4:1 to 4:1	3.6:1
	Domed Cylinder		3:1
Pinnacled	Diamond	2.2:1 to 3.1:1	2.2:1
	Pyramid		1:1

its overall shape. A berg which has not deteriorated is likely to be blocky with a higher draft/height ratio while one in the last stages of decay is likely to have small ratios.

ICEBERG DRIFT

Icebergs are propelled by the combined effect of ocean currents, wind, wind-generated currents and tidal currents. However ocean currents have a greater influence particularly on deep drafted bergs.

Ocean circulation in the Northwest Atlantic: The pattern of ocean circulation in the Northwest Atlantic is shown in Fig. 3. The East Greenland Current is a polar current having its origin in the Arctic Ocean and flows south along the East Greenland coast as far as Cape Farewell. At this point it mixes with the warm Atlantic Irminger Current and the resulting West Greenland Current flows north along the west coast of Greenland with velocities of about 1 knot and steadily loses volume through westward branching. The main stream continues into Baffin Bay where it feeds the eastern edge of Baffin Island forming the Baffin Island Current. Part of this current enters the Hudson Strait along the northern side and leaves by the southern side. The Labrador Current is formed by the confluence of the south-flowing Baffin Island Current with the westward branching of the East Greenland Current and the cold flow from the Hudson Strait. The resulting stream flows in two components, one frigid on the coast side and the other slightly warmer on the offshore side with an axis parallel to the continental slope. These characteristics are retained

till the current reaches the Grand Banks where it divides into two branches. One branch flows south along the Avalon peninsula of Newfoundland and the other, usually the major branch, flows along the eastern edge of the Grand Banks. A portion of the frigid component flows through the Strait of Belle Isle.

Iceberg drift: Icebergs of East Greenland origin drift southwards along the coast to Cape Farewell and are then caught in the West Greenland current and drift north. A few escape across the Davis Strait to Baffin Island and the Labrador coast and join the main stream drifting south. Usually East Greenland bergs disintegrate rapidly while they drift in the warm west Greenland Current. West Greenland bergs are prodigious in number and huge in size. After coming out of the fjords they travel up the West Greenland coast and around to the western side of Baffin Bay. Bergs are seen on the Baffin Island coast throughout the year. South of Hudson Strait they become scarce by December due to heavy disintegration during the preceding summer and early fall. Later, protected by the colder temperature and advancing sea ice, bergs from Baffin Bay move south and berg counts along the Labrador coast reach a peak by May-June. A number of bergs are eliminated by being driven out of the Baffin Island-Labrador Current system to the open sea where they quickly disintegrate. The Hudson Strait, the Strait of Belle Isle and other indentations along the coast trap a number of icebergs.

Wind and wind generated currents also influence[20] the iceberg movement. Smith[70] estimated that a moderate to fresh wind (15 to 20 m.p.h.) blowing continuously for a day or two will induce movement

of water layers up to 200 feet deep, the mean velocity being that at 80 feet depth. Icebergs with deep draft and propelled by ocean currents are usually not influenced by a direct wind force while those in their last stages with smaller drafts are more susceptible to the direct influence of winds.

Icebergs which survive their long and tortuous travel of 1900 to 2700 miles may journey down to about 40°N. latitude, where the warm Gulf Stream water quickly disintegrates them. Occasionally icebergs have been sighted near the Azores, the British Isles and Bermuda, but this is a very rare phenomenon occurring only in exceptionally bad ice years. Fig. 8 shows some of these freak iceberg sightings.

Drift forces: As discussed earlier, an iceberg moves under the combined effect of the ocean currents, wind, wind-generated currents and tidal currents. Under a steady state there will be no force on the iceberg and the direction of the iceberg motion will be along the resultant of all the external forces. The total force on a berg can be written[55] as:

$$\Sigma F = 0 = M.a \qquad \ldots\ldots\ldots [1]$$

where ΣF = Sum of all external forces

M = Mass of the berg and

a = acceleration.

The hydrodynamic drag on an immersed body can be in general expressed[27] as:

$$F = \frac{1}{2} C_d \rho A V^2 \qquad \ldots\ldots\ldots [2]$$

where F = force

C_d = the drag coefficient which depends on the shape of the body and the medium

ρ = Density of the medium

A = Area exposed normal to the wind/current

V = Relative velocity between the body and wind/current.

The effect of the earth's rotation is accounted for (Coriolis effect) either implicitly in the motion of the fluid or explicitly in the motion of the iceberg. The resultant direction of motion can be found from[70] principles of elementary mechanics.

Sea ice also plays some role in influencing the iceberg drift. Fast ice is known to hold icebergs[70] stationary for one or more seasons and such icebergs may taken 2 or 3 years after calving to reach the Newfoundland shores. Icebergs are also known to move along the Baffin Island coast with the protection pack ice. The influence of pack ice on iceberg drift has not been defined. Kovacs[43] has concluded that the force exerted by sea ice on ice islands is possibly the major component in supplying the energy to induce such long scours in what are comparatively strong sediments. Other reported observations[4] attribute the grounding of those same islands primarily to their kinetic energy. The only reference found in the literature regarding North Atlantic bergs is by Milne[52] where he stated that icebergs have maintained courses at variance with wind, surface currents or ice push. This has been confirmed many times orally by people familiar with iceberg behaviour.

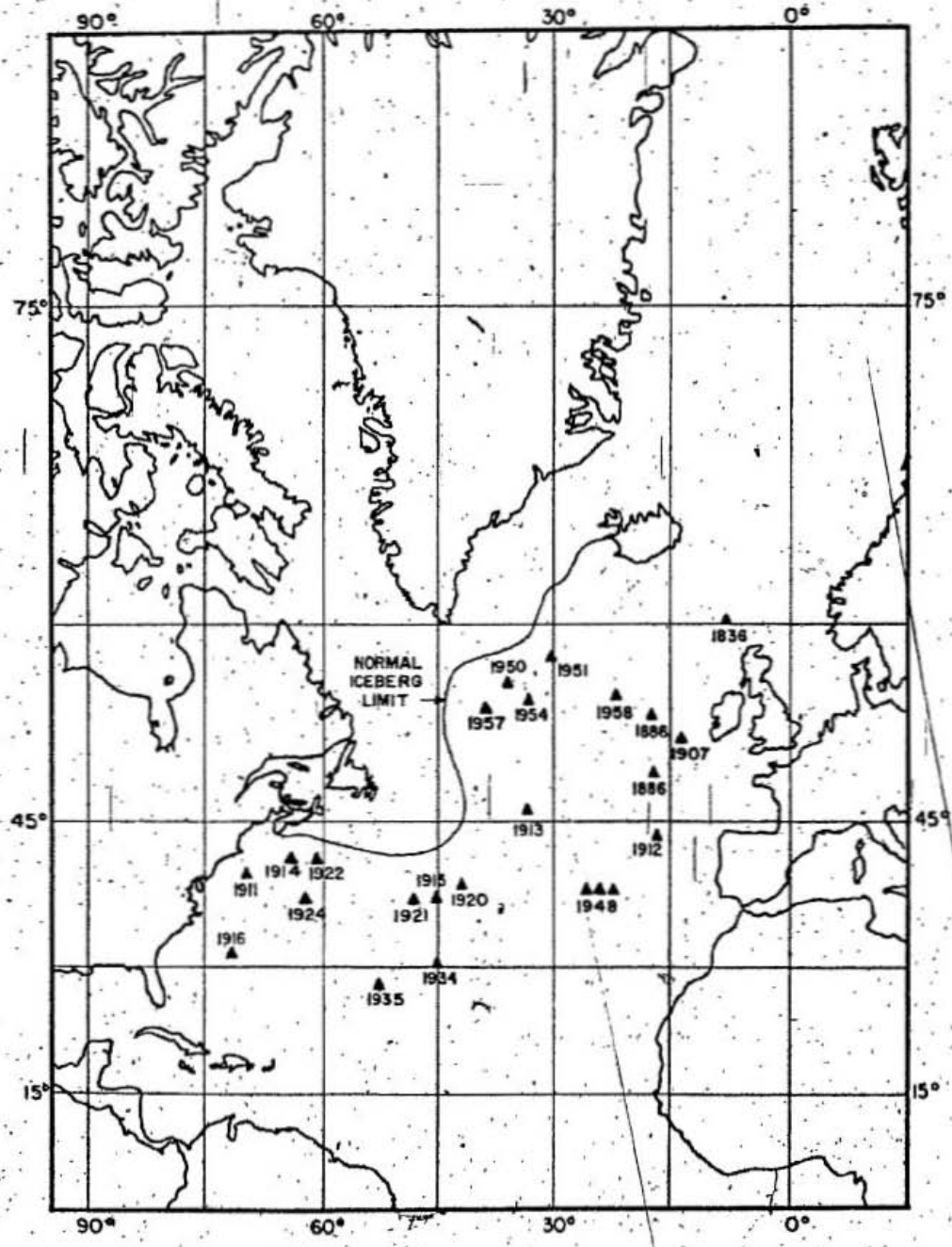

FIG. 8.- UNUSUAL ICEBERG SIGHTINGS
(Adapted from reference #76)

ICEBERG DETERIORATION

Icebergs are subjected to deterioration in three[70] ways: 1. melting, 2. erosion by waves, swells and rain, and 3. calving. All the three methods are usually at work in different degrees. Melting processes are always at work on all icebergs, but they are slowest in winter and are speeded up during warmer months and also as the iceberg drifts further south. Melt water can usually be seen[3] all over the iceberg in tracks but melting proceeds fastest at the water line. Washing by waves and ocean swell is the most effective of the destructive agents. As the seas continuously wash back and forth, irregularities on the berg are enlarged and valleys are eroded which grow larger till this becomes a prominent feature as can be seen in most of the bergs in their last stages. Melting and erosion set up strains in the berg which results in prominances and overhanging ledges to fall away. This upsets the stability and causes the berg to roll. Crisscross water line marks seen on icebergs are a clear evidence of rolling. During the travel from Greenland to the Grand Banks, the deterioration process reduces an iceberg to about $\frac{1}{9}$ th of its original height and about one half of its original[70] volume. The rate of wastage is maximum near the Grand Banks in the Gulf Stream where the disintegration is nearly six times faster than in the cold Arctic waters.

Artificial destruction: Artificial destruction of icebergs, using dynamite, thermit[8,10,11] and even incendiary bombs[78,79], has so far not proved very successful.

PROPERTIES OF SUBMARINE SOIL DEPOSITS

The bulk of published literature on submarine soils is oriented towards the geology of the oceans. Although several oil exploration companies and consulting firms have collected information on the engineering behaviour of sea floor sediments, relatively little is available through publications. Most of the unpublished data are considered proprietory.

Reviews of the state-of-the-art of marine soil mechanics presented by Ling[46] and Noornay and Gizienski[59] summarize most of the published material in this field. The characteristics of the ocean floor surface sediments relevant to the present study will be discussed below.

Structure: When a sinking particle of weight W arrives at the surface of a sediment deposit (Fig. 9) it tends to settle in the most stable position, but as soon as the particle touches the deposit, the adhesion between the particle and sediment at the first point of contact resists further movement of the particle. The resisting couple M_2 due to adhesion is independent of the grain size while the overturning couple $M_1 = W \cdot r$ decreases as the fourth power of the grain size. This accounts for the varying void ratios with grain size. Any vibration or disturbance causes a rearrangement of the particles. Terzaghi[74] termed this type of structure as "metastable". He also experimented with crushed quartz of different sizes and measured the void ratios after sedimentation and subsequent disturbance. These results are reproduced in Table V. Particles with grain size

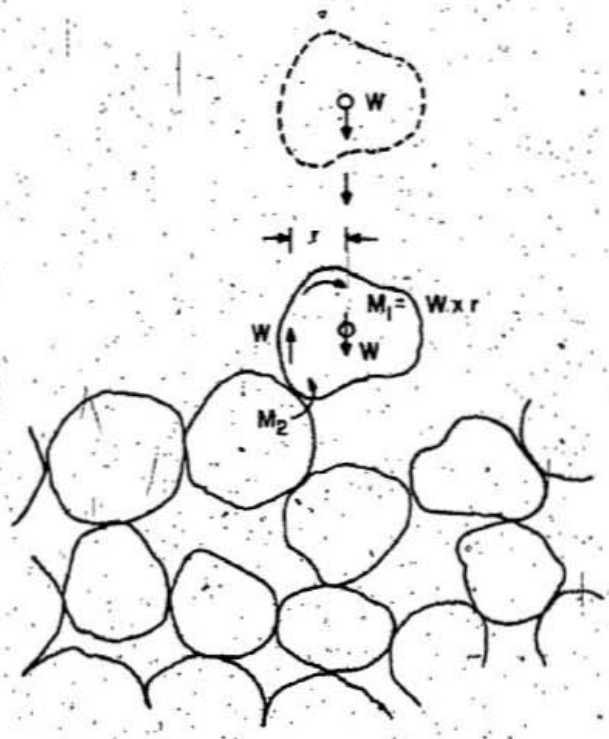

FIG. 9.- THE CONCEPT OF METASTABLE SEDIMENT
(From Terzaghi[74])

TABLE V

VOID RATIO VARIATION WITH GRAIN SIZE[74]

GRAIN SIZE (MICRONS)	700-250	100-20	20-6	6-2	Less than 2
Void ratio e_o after sedimentation	1.0	1.21	2.23	2.57	2.66
Void ratio e_1 after vibration	0.67	0.80	1.10	1.50	2.16
Ratio $\frac{e_1}{e_o}$	0.67	0.66	0.40	0.58	0.81

between 20 and 6 microns corresponding to the conventional silt size are most sensitive to disturbance. At higher grain sizes the initial void ratio is low while at higher initial void ratios the sediment composed of fine grained size particles exhibits greater cohesion.

The shearing resistance τ_f at any point in the submerged sediment is given by

$$\tau_f = c + (\gamma' z - u) \tan\phi \quad \ldots\ldots\ldots [3]$$

where c = cohesion

γ' = submerged unit weight of the sediment

z = depth below the free surface of the sediment

u = excess hydrostatic pressure in pore water, and

ϕ = True angle of internal friction.

At the instant of collapse of the metastable structure, the weight of the solid particles is temporarily transferred from the

point of contact to the water. Consequently the hydrostatic pressure at any depth z increases by $\gamma' z$ resulting in liquifaction and flow of the soil. However, this is temporary. The flow of sediment is followed by expulsion of excess water and gradual increase in consolidation. The time required for the recovery is related to the permeability and grain size of the particle. The distance to which the sediment can travel during liquifaction increases with decreasing grain size. Flows of this type on gentle slopes result in fan shaped deposits. However, this does not assume the character of a turbidity current as the liquifaction is followed by an increase in viscosity due to the expulsion of water. After testing several samples, Finn et al[34] and Winterkorn and Fang[83] have come to a similar conclusion on the structure and type of ocean floor surface deposits.

Consolidation: The degree of consolidation U of a sediment deposit has been defined as

$$U = \frac{\gamma' z - u}{\gamma' z} \qquad \ldots\ldots\ldots [4]$$

or

$$u = \gamma' z \, (1 - U) \qquad \ldots\ldots\ldots [5]$$

When the excess pore water pressure u = 0, the degree of consolidation is 1. The variation of the pore water pressure in the soil and the total stress can be represented as shown in Fig. 10. $\bar{U}$ the average degree of consolidation of the deposit is defined as

$$\bar{U} = \text{area } A_p \; / \; \text{Area } (A_p + A_u)$$

The progressive consolidation of such a sediment with time was expressed by Terzaghi[74] as:

$$\frac{d\bar{U}}{dt} + \frac{3}{t^2}\left(\frac{t}{2} + \frac{C}{3}\right)\bar{U} = \frac{C}{t^2} \qquad \ldots\ldots\ldots [6]$$

where $C = \frac{3\gamma'^2 C_v}{\gamma_w q^2}$

q = sediment deposition rate in gm/sq cm/sec

γ' = average submerged unit weight of soil

γ_w = unit weight of water, and

C_v = coefficient of consolidation

The solution of the above equation[60] is shown in Fig. 11. It can be stated that:

1. If sedimentation takes place in an ocean environment at a constant rate, the degree of consolidation decreases with increasing time. This naturally implies that the surface sediment will always be highly underconsolidated.

2. If sedimentation stops at any time t_1, the value of $\bar{U}$ increases as shown by the rising curves marked t_1/C. In an environment where sedimentation has ceased, the material will gradually reach normal consolidation.

Shear strength: The shearing resistance of a clay deposit sedimenting at a constant rate q is represented in Fig. 12 at two stages during its deposition. If the average value of $\bar{U}$ is low, the curves marked τ_f descend very steeply and consequently the shearing resistance tends to be almost independent of depth and close to cohesion c. Metastable soils are said[54] to show very large volume decrease during shear. Shear strengths of some of the sediments measured in the Gulf of Mexico[35] and the North Pacific Ocean[53] were as low as 8 lb/sft. Deposits 360 feet thick with such properties were found in some locations. Keller's tests[42] on North Atlantic

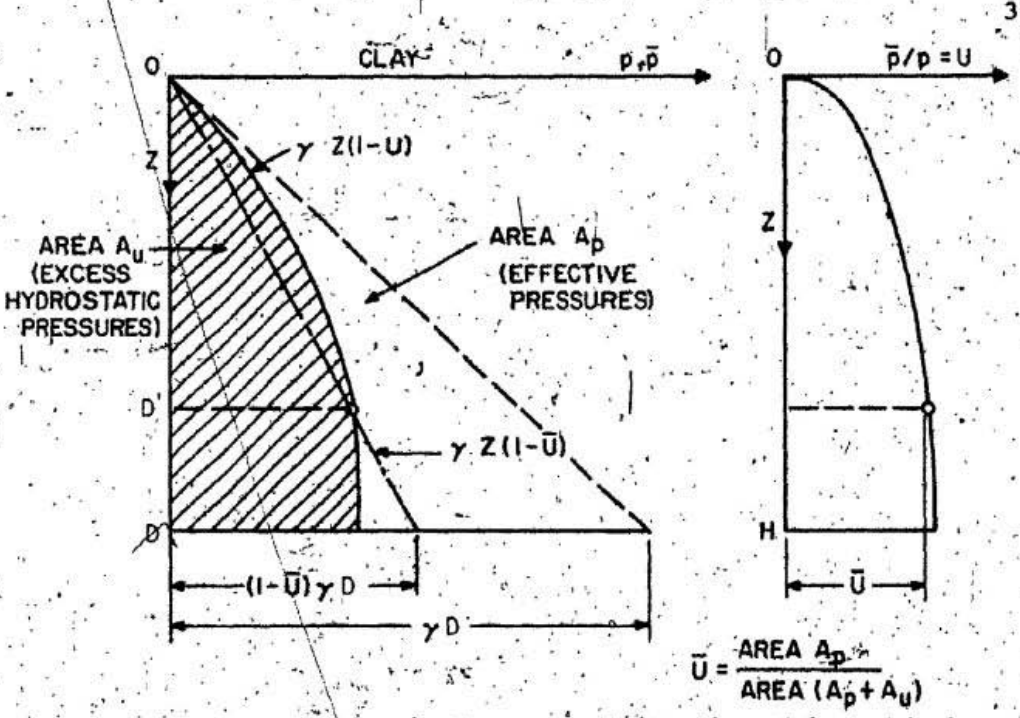

FIG. 10.- TOTAL AND EFFECTIVE PRESSURE IN A CLAY DEPOSIT UNDER PROGRESSIVE CONSOLIDATION (From Terzaghi[74])

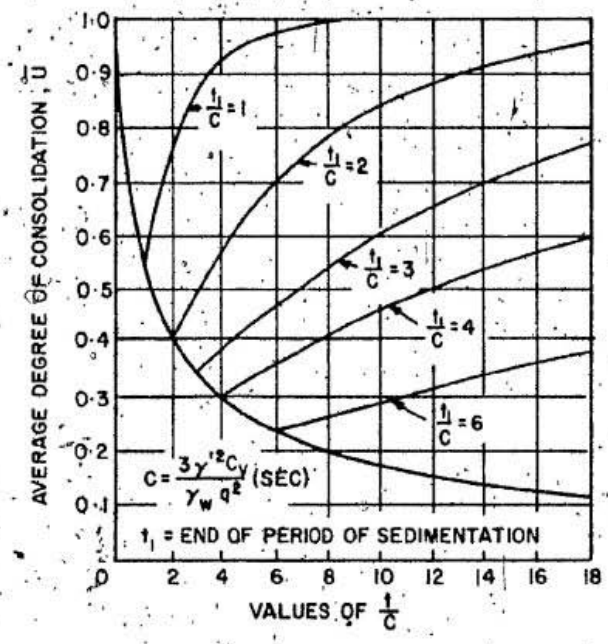

FIG. 11.- RELATIONSHIP BETWEEN TIME FACTOR AND DEGREE OF CONSOLIDATION

(From Olsson[60])

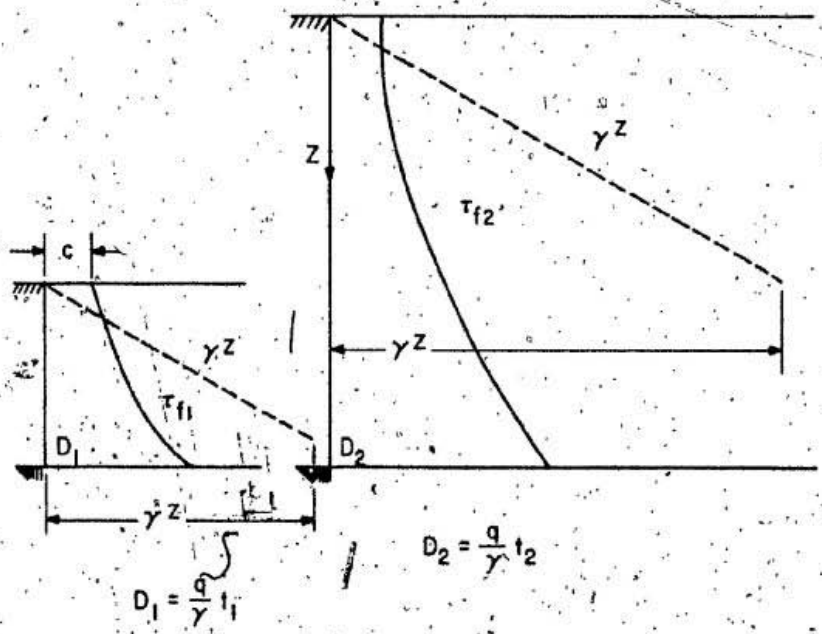

FIG. 12.- SHEAR STRENGTH VARIATION IN A COHESIVE DEPOSIT UNDER PROGRESSIVE CONSOLIDATION

(From Terzaghi[74])

sediments showed that sediment with strengths less than 74 lb/sft are common in this area.

Although experiments by Vey and Nelson[81] to assess the environmental effects of the ocean on the shear strength of the sediments did not yield conclusive results, these tests appeared to indicate that the frictional component of the shear decreased with increasing environmental pressure.

While the information on ocean floor sediments at present is still very limited it appears reasonable to infer that the surface deposits are generally likely to be highly compressible with low shear strengths.

Meyerhof[50] has shown that the critical angle of flat continuous slopes can be expressed as

$$\beta' = \frac{c}{\gamma D} \qquad \ldots\ldots\ldots [7]$$

where β' = slope of the deposit (radians)

c = cohesion

γ = unit weight of the soil and

D = depth of the sediment.

For a value of c even as small as 10 lb/sft, D would be 135 feet on a 1:500 slope. Thus the ocean floor sediments in spite of being weak, could retain 1:500 and flatter slopes common to the continental shelves.

North Atlantic sediments: On the basis of analysis of nearly 200 samples and from other published data, Keller[42] summarized the general engineering properties of North Atlantic surface deposits. Figs. 13, 14 and 15 were redrawn from Keller's data and show the

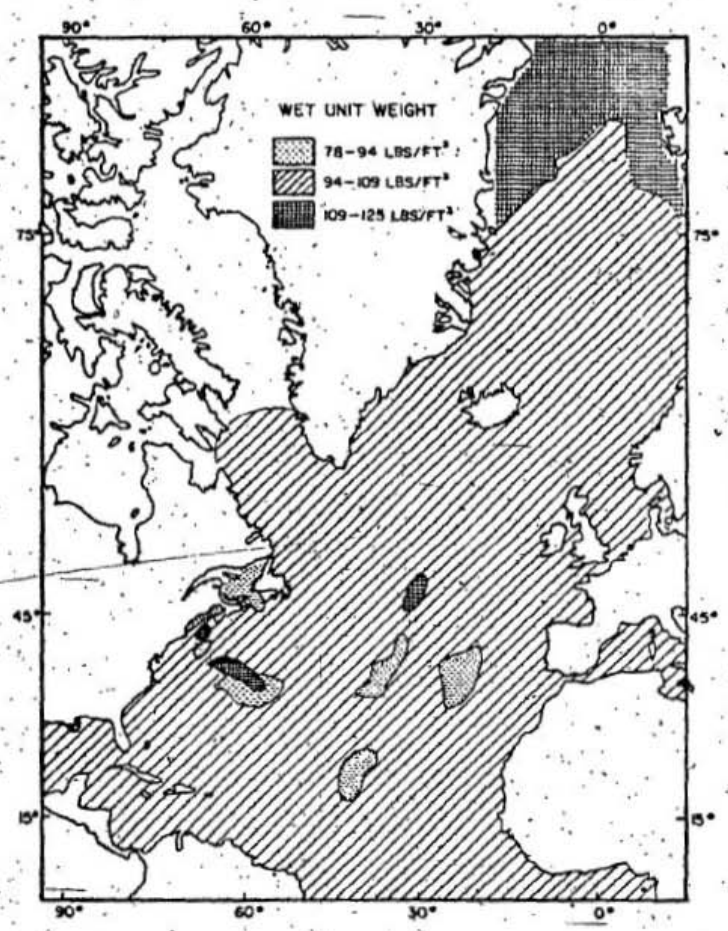

FIG. 14.- WET UNIT WEIGHT VARIATION OF NORTH ATLANTIC SURFACE SEDIMENTS (From Kellor[42])

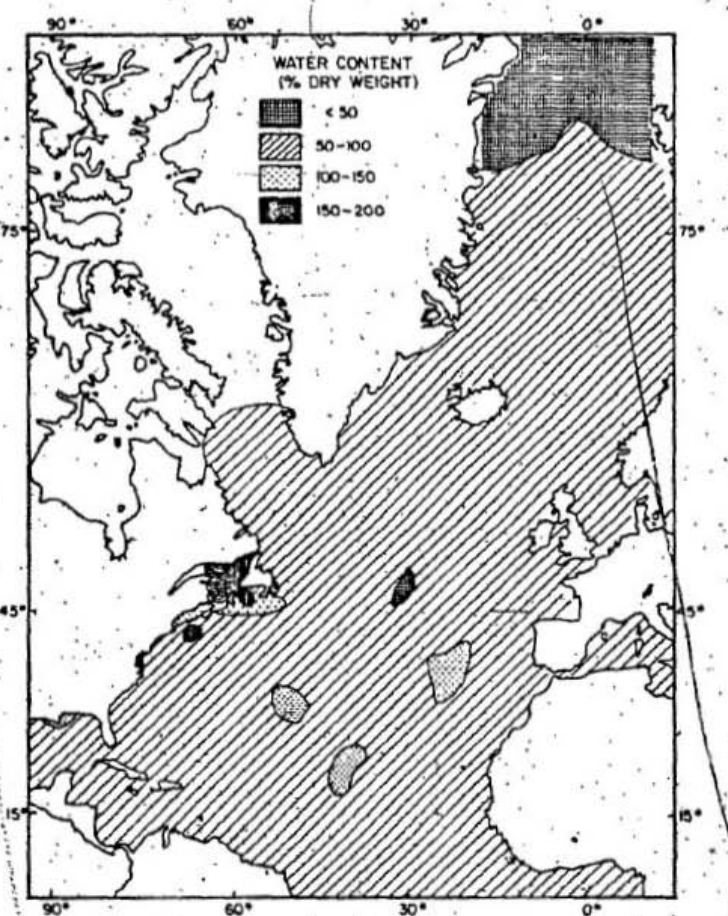

FIG. 13.- WATER CONTENT VARIATION OF NORTH ATLANTIC SURFACE SEDIMENTS (From Kellor[42])

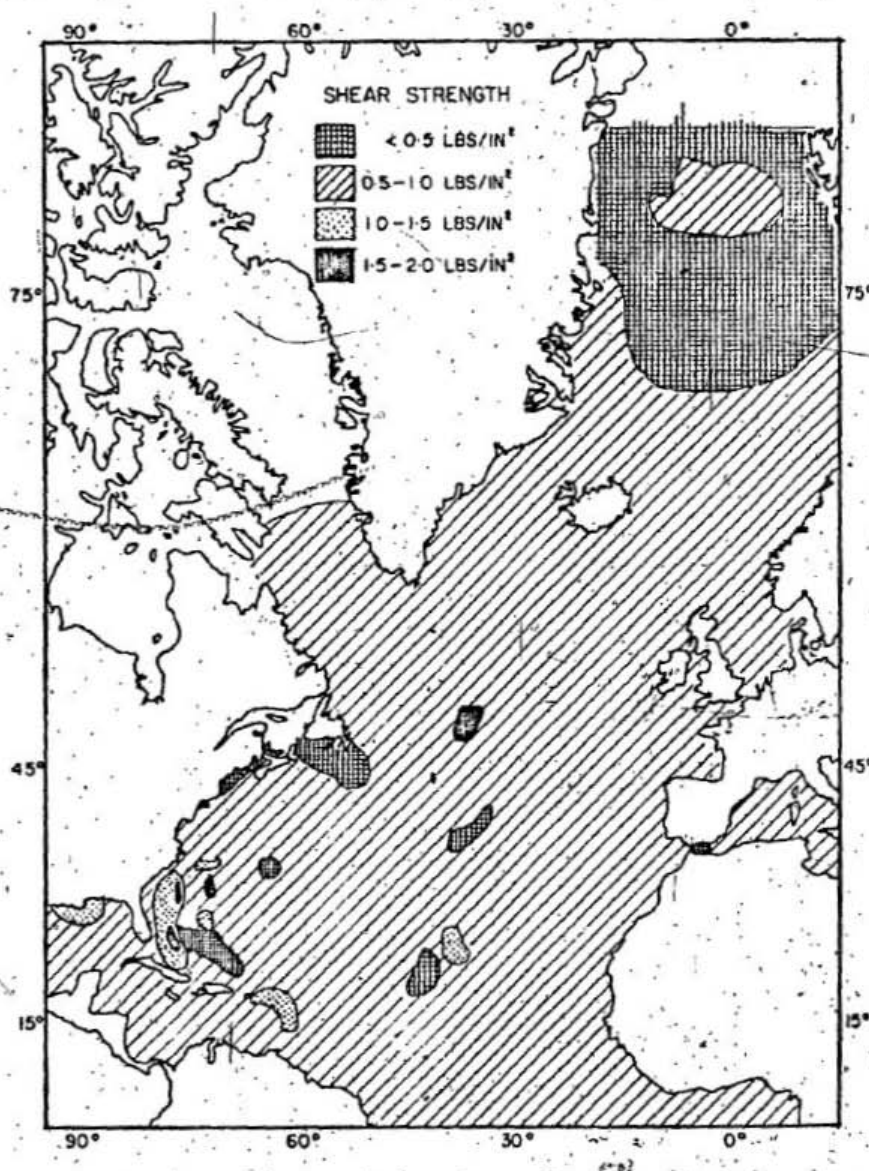

FIG. 15.- SHEAR STRENGTH VARIATION OF NORTH ATLANTIC SURFACE SEDIMENTS

(From Kellor[42])

variation of the natural water content, wet unit weight and shear strength. It is to be cautioned that this is highly generalized information based on representative data. Even for subaerial soils where there is easy access to visual inspection and sampling, a comprehensive summary of this type is very difficult to prepare as the soil properties vary greatly from place to place. The sediment type on the Labrador coast along a small stretch of about 30 miles varied[3] from rock outcrop to very soft and loose mud as observed during the *Dawson* cruise. The values for the entire North Atlantic represented in Figs. 13-15 can be considered reasonably accurate for use in any preliminary analysis. In the final solution of problems relating to a specific area, detailed study of that area is necessary. Geological aspects of the sediments on the Newfoundland and Labrador continental shelf are now being researched actively. Slatt and Lew[68] analyzed the texture of the Labrador shelf sediments and classified those as sand-silt-clay and silty-sand. It is learnt (Slatt - personal communications) that on the Labrador shelf, the silt content (0.063 mm to 0.004 mm) varies from 15 to 70% and clay (less than 0.004 mm) from 1 to 30%. The Northern Newfoundland shelf sediments are said to be similar while the Grand Banks are predominantly gravel (coarser than 2 mm) and sand (2 to 0.063 mm). Similar studies by Avilov showed that the Newfoundland and Labrador shelf surface deposits vary in texture from clay to rocks. Grant[36] conducted extensive geophysical studies of the same area and proved mud deposits of up to 328 feet (100 meters) in some areas. Those studies showed that the shelf sediments were moraínal and reworked in a number of places.

The range of geotechnical properties for marine clays as summarized by Winterkorn and Fang[83] is reproduced in Table VI below.

TABLE VI[83]

GEOTECHNICAL DATA ON MARINE CLAYS

Clay content (less than 2 microns)	35-60%
Silt	40-60%
Sand	Less than 10%
Insitu moisture	60-150%
Activity PI/Clay content	0.33 - 1.33
Void ratio	0.5 - 0.8
Sensitivity	8 - 19

SEDIMENT RESISTANCE TO GROUNDING ICEBERGS

Iceberg gouging can be visualized as a process (Fig. 20) where an iceberg drifts along, comes to a soil bank or slope and ploughs into the slope horizontally without significant change in elevation. Iceberg scouring starts on the sediment surface and may extend finally 10 to 20 feet below at the end of the travel. From the presently available knowledge, sediments in this depth range can be assumed to be soft and weak. This sediment will offer resistance to the moving iceberg in finally bringing the berg to a stop.

In soil mechanics literature, earth pressure problems are classified as active and passive cases. Ever since Coulomb first formulated the limit equilibrium solutions, earth pressure problems

on rigid retaining walls have been studied in great detail. The conventional active and passive earth pressure situations are illustrated in Fig. 16. The front of an iceberg moving into a sediment slope is similar to the inward movement of a rigid retaining wall when the earth pressure is passive.

The limit equilibrium solution of Coulomb assumes a shear plane inside the soil starting from the toe of the retaining wall. By considering the equilibrium of the wedge (Fig. 17) the force on the wall can be computed. Assumption of a plane shear surface is however not a generalized solution. It is also known[75] that the failure surface would be curved when there is friction between the wall and soil. Graphical procedures such as the logarithmic spiral method and friction circle method are available to determine the surface of shear. During the course of studies in earth pressure problems, procedures such as the numerically integrated slip line method[72], the limit analysis solution[25], the method of slices[66] and the finite element solution[22,47] have all been applied to obtain a general solution. When there is no wall friction, the solutions by all these methods converge with Coulomb's results. For angles of skin friction less than one third the soil internal friction, the error in assuming a plane shear surface is reported[73] not to be significant. Chen and Rosenfarb[26] computed the earth pressure coefficients assuming different failure mechanisms (Fig. 18) and compared the results with those from other types of solution. The comparison for the passive case for a vertical wall is reproduced in Table VII from which it can be concluded that for small angles of wall friction the

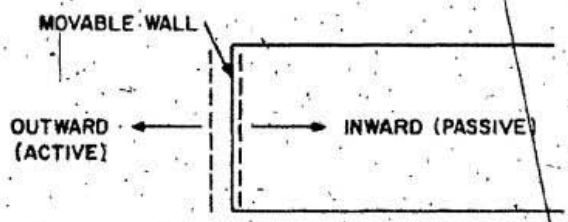

(a) ACTIVE AND PASSIVE PRESSURE CONDITIONS IN SOILS

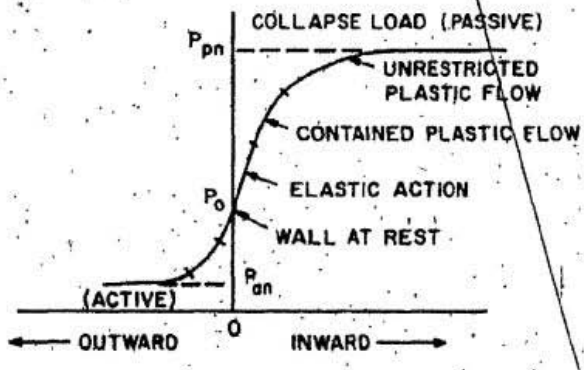

(b) LOAD DISPLACEMENT RELATIONSHIP

FIG. 16.- ACTIVE AND PASSIVE PRESSURE CONDITIONS IN SOILS
(From Chen and Scawthorn[25])

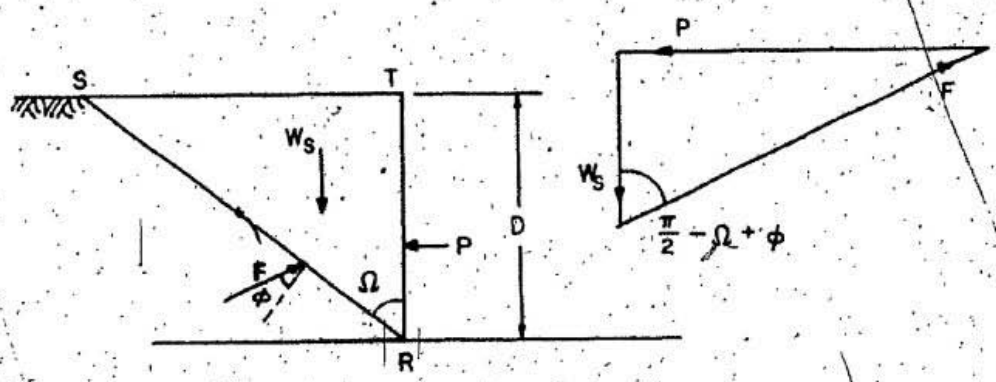

FIG. 17.- COULOMB'S IDEALIZED SHEAR WEDGE FOR PASSIVE PRESSURE CONDITIONS

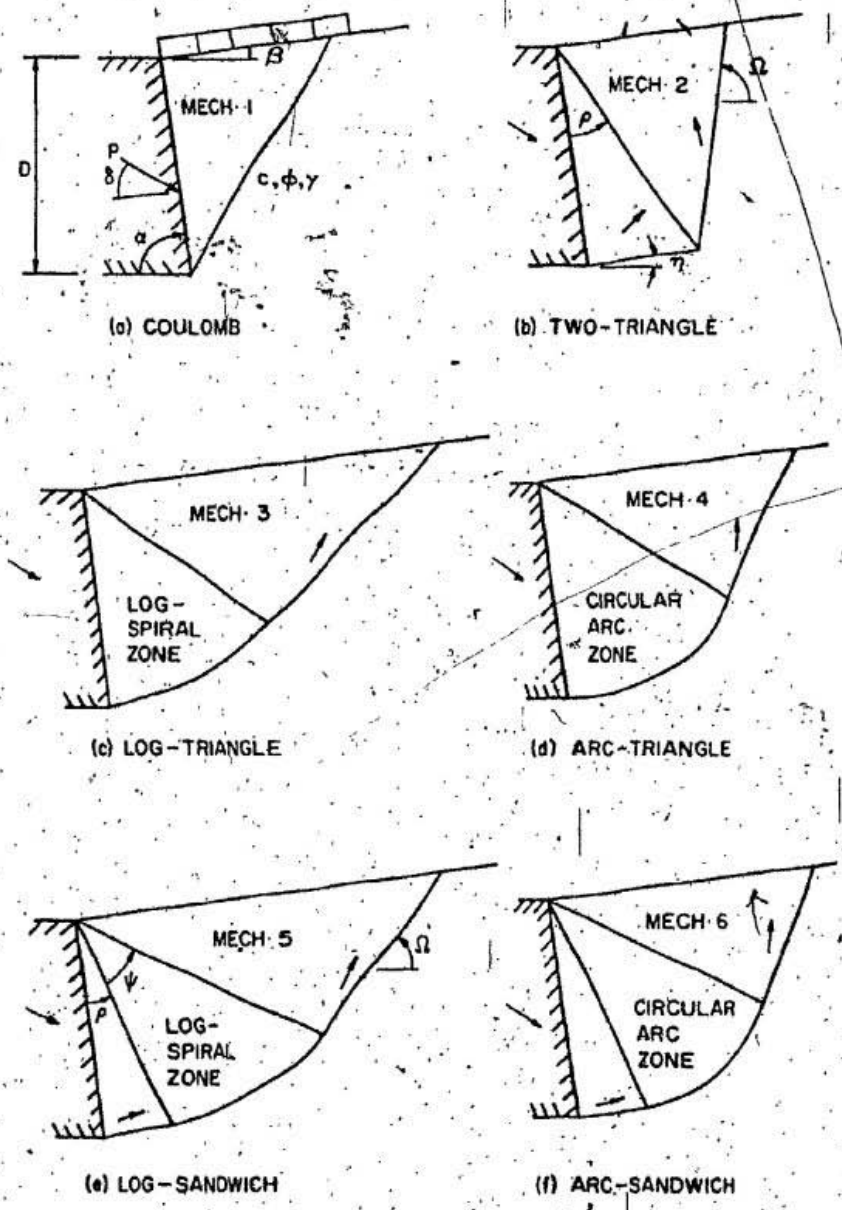

FIG. 18.- DIFFERENT TYPES OF FAILURE SURFACES IN PASSIVE PRESSURE

(From Chen and Rosenfarb[26])

TABLE VII[26]

PASSIVE PRESSURE COEFFICIENTS K_p

		Mechanism						Sokolovskii
ϕ	δ	(a)	(b)	(c)	(d)	(e)	(f)	
10	0	1.42	1.42	1.68	1.60	1.42	1.42	1.42
	5	1.57	1.56	1.69	1.63	1.56	1.56	1.56
	10	1.73	1.68	1.71	1.68	1.68	1.67	1.66
20	0	2.04	2.04	3.07	2.60	2.04	2.04	2.04
	10	2.64	2.58	3.12	2.82	2.58	2.61	2.55
	20	3.53	3.18	3.27	3.19	3.17	3.19	3.04
30	0	3.00	3.00	6.38	4.80	3.00	3.01	3.00
	15	4.98	4.71	6.61	5.88	4.71	4.97	4.62
	30	10.10	7.24	7.37	8.31	7.10	8.31	6.55
40	0	4.60	4.61	16.10	15.40	4.60	4.67	4.60
	20	11.80	10.10	17.70	23.60	10.10	12.50	9.69
	40	92.60	22.70	21.70	67.90	20.90	--	18.20

computation by Coulomb's method gives results which are comparable to that given by the more complicated slip line method.

LARGE DISPLACEMENTS IN EARTH PRESSURES PROBLEMS

Conventional civil engineering designs are based on the failure loads which, in the case of retaining walls, correspond to the development of the first failure surface. Deformations beyond

the first slip are not of interest in design. Large displacement in soils was examined for the first time in agricultural engineering in the study of the forces on moving plough-shares and blades. Soil mechanics theory was applied by Wells[82] to solve the problem by considering the passive pressure on the front. It was proposed that a series of failure planes develop as the tool moves forward (Fig. 19). Payne[61] and Shone[71] measured the forces on model tillage equipment and observed that the variation was in the form of a wave. Selig and Nelson[64] also came to similar conclusions after obtaining oscillographic records of the total force. Siemens[67] built a glass sided bin and using highspeed photography observed failure patterns. Effects of tool speed[85], variation of tool angle[38] and variation of soil types have also been investigated.

In a level surface, the force on a moving blade was due to the passive earth resistance and was in a wave form corresponding to the failure of the soil, subsequent mobilization of strength and the development of the next failure surface. Speed was found to influence the resistance in cohesive soils while granular materials were not influenced by the soil cutting rate. It has also been observed that the accumulation of the soil surcharge in front of the blade reached an equilibrium after a short travel.

The front face of an iceberg scouring into the ocean bed is likely to behave similarly to a scraper or bulldozer blade. The solid shape of an iceberg would however influence the total force and the type of soil surcharge in front. The sloping bed, the movement of the iceberg under its own momentum and the low strength of the sediment

are the other variations whose effects on iceberg grounding will have to be examined.

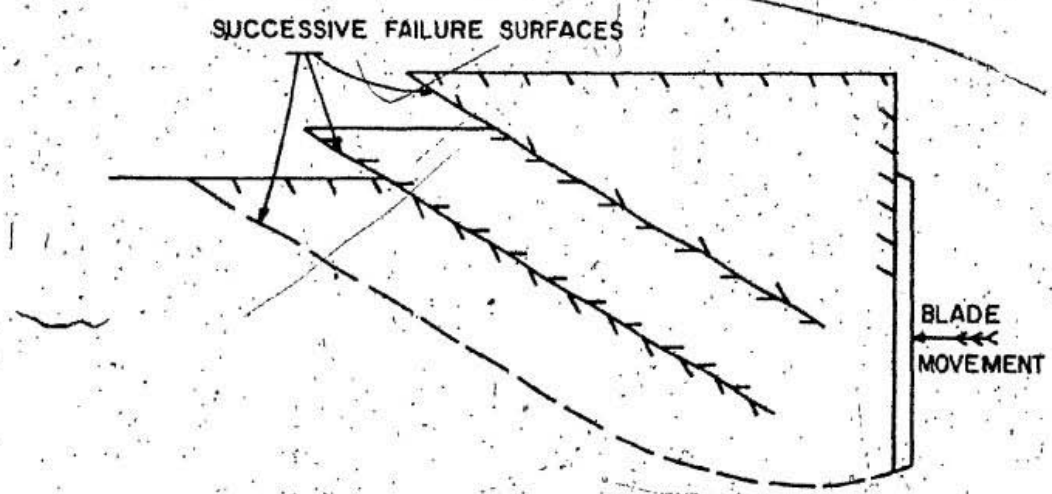

FIG. 19.- SOIL FAILURE ALONG SUCCESSIVE SHEAR PLANES IN FRONT OF EARTHMOVING MACHINES

(From Siemens[67])

CHAPTER III

ANALYTICAL MODEL

The general shape of an iceberg can at best be described as random. Data on ocean floor surface deposits, particularly strength and consolidation properties are limited. The variables which affect the iceberg scouring process are numerous. It is, therefore, necessary to make a number of assumptions in formulating a theoretical model for iceberg gouging. At the present time, the only method of verifying these assumptions is through laboratory experiments. After some field observations at a later stage, results of the theoretical and laboratory models could be extended to cover most of the variables encountered in actual iceberg grounding.

ASSUMPTIONS

In this analysis the iceberg is considered to be a prismatic block (Fig. 20) rectangular in plan with the shorter side perpendicular to the direction of travel. This model will be referred as the idealized berg. The berg is supposed to move under steady state conditions with a constant draft. Grounding of such a berg would occur only when it meets a bank or slope. Uniform slopes between 1:250 and 1:1000 similar to those existing on the continental shelf are considered and the berg movement assumed to be normal to the slope during the grounding process. The sediment is assumed to be loose and weak with shear strengths of about 50 lb/sft. The idealized iceberg-

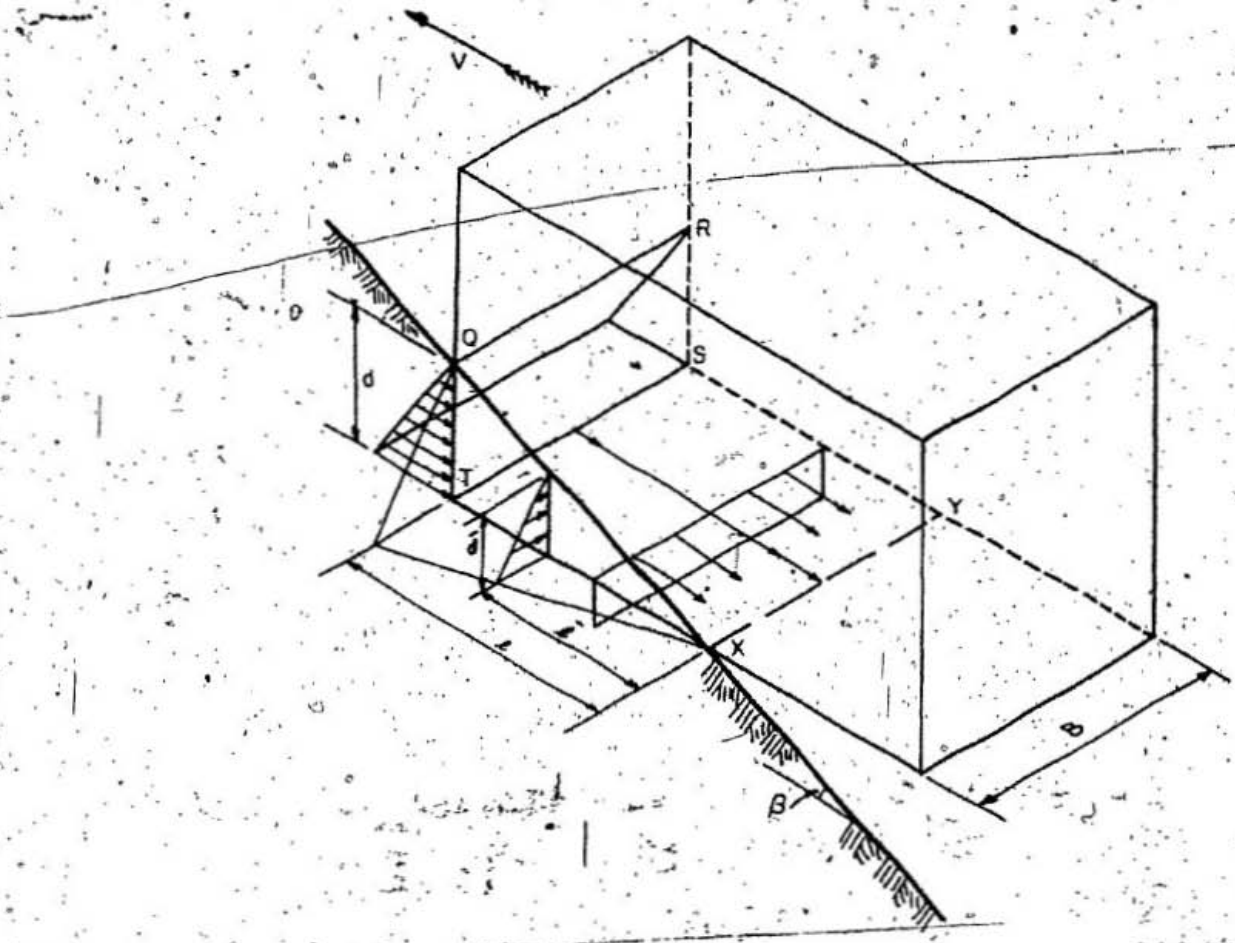

FIG. 20.- THE IDEALIZED ICEBERG IN THE PROCESS OF SCOURING

soil interface is assumed to be smooth.

VERTICAL MOVEMENT OF ICEBERG DURING GROUNDING

A rigid body moving steadily with an initial velocity V and meeting a rigid slope would continue to move up the slope finally coming to rest at some point on the slope where the gain in the potential energy of the body equals its initial kinetic energy. From elementary principles of dynamics, the distance L travelled by the body up the slope (Fig. 21) can be computed.

If W = The weight of the body,

β = slope angle,

V = the initial velocity, and

μ = coefficient of friction along the surface,

$$\text{The deceleration} = \frac{(V\cos\beta)^2}{2L}$$

$$\text{Deceleration force} = (\mu W\cos\beta + W\sin\beta) = \frac{W}{g}\cdot\frac{(V\cos\beta)^2}{2L}$$

$$\text{or } L = \frac{V^2\cos^2\beta}{2g(\sin\beta + \mu\cos\beta)} \qquad \ldots\ldots\ldots [8]$$

Equation [8] cannot be applied directly to the iceberg problem since an iceberg is buoyant and the entire weight of the berg does not come into action in the potential energy computation. Referring to Fig. 22, if A is the area of cross section of the iceberg at the water surface and γ_w the unit weight of water, the height z to which the berg would theoretically rise before completely converting its kinetic energy can be computed from

$$\frac{\gamma_w}{2}\int A.z.dz = \frac{WV^2}{2g} \qquad \ldots\ldots\ldots [9]$$

where W = the weight of the berg,

V = the initial velocity of the berg and

g = the acceleration due to gravity

For a one million ton spherical berg travelling at 1 ft/sec this rise would be about 4.5 feet and for a blocky berg of the same weight, 500 feet long and 250 feet wide, it would be 4.2 feet. Every foot rise of a blocky berg corresponds to an increase in soil pressure of 64 lb/sft if the entire base is in contact with the soil. This pressure would however be far greater for other shapes and also for blocky bergs with only part of the base in contact with the soil as would happen when the berg starts travelling up a slope. A rise in level of the order of 5 feet is, however, not likely because a large portion of the ocean surface sediments are very weak and compressible incapable of carrying these bearing pressures.

Observations on the sea floor support the assumption of a horizontal travel of an iceberg. Long gouge tracks are seen with raised shoulders on either side which can be caused only when the berg shears through and spreads the soil in front and around.

Further, with the present lack of knowledge about iceberg grounding it would be prudent to locate the ocean bottom structures at a depth where the effect of iceberg scour is not felt. Since maximum scour depths would occur when the buoyant berg travels horizontally into the slope, calculations based on such an assumption would be safe for the bottom structure.

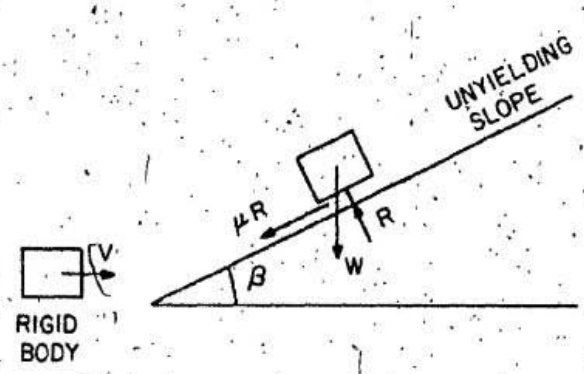

FIG. 21.- MOVEMENT OF A NON-BUOYANT OBJECT UP A SLOPE

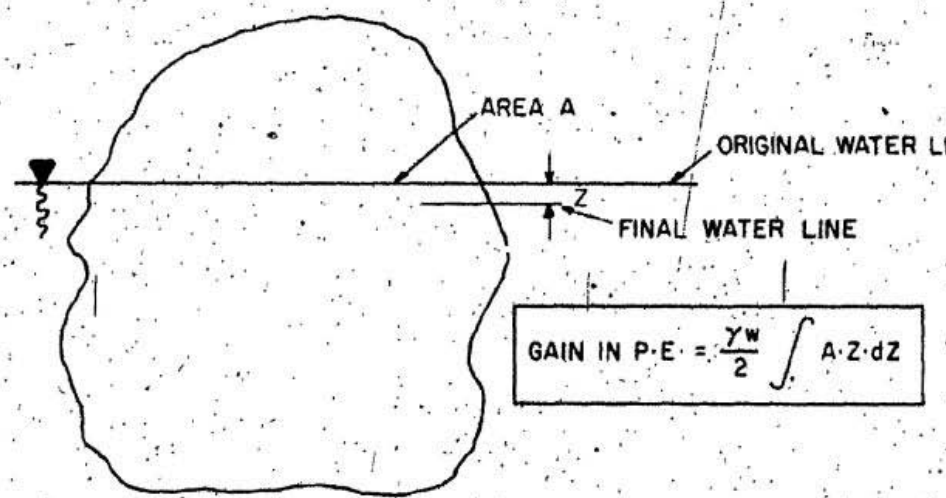

FIG. 22.- GAIN IN POTENTIAL ENERGY OF A BUOYANT BODY

THE PRELIMINARY MODEL

For simplicity, the effect of the displaced soil and the consequent surcharge in front of the iceberg has been neglected in the first approximation. The idealized berg can be assumed to be subjected to a passive soil resistance on the front face, a tangential force on the sides due to a passive soil pressure on the sides and a basal shear resistance as shown in Fig. 20.

The passive earth pressure can be computed as

$$p_p = \gamma' d . N_\phi + 2c\sqrt{N_\phi} \quad \ldots\ldots [10]$$

where p_p = passive earth pressure at

d = any depth below the soil surface,

γ' = submerged unit weight of the soil,

c = cohesion in the soil,

$N_\phi = \text{Tan}^2 (45 + \frac{\phi}{2})$, and

ϕ = angle of internal friction in the soil.

Assuming the soil to be cohesive and neglecting the effect of ϕ which is considered very small, the force P_1 on the front face of the idealized berg of width B can be computed as

$$P_1 = \frac{1}{2} d.B[\gamma' d + 4c] \quad \ldots\ldots [11]$$

The resistance on the two sides would be

$$P_2 = 2[\tfrac{1}{2} . d . \ell (\gamma' d + 4c)]\mu \quad \ldots\ldots [12]$$

where ℓ = length of contact at the sides with the slope,

μ = coefficient of friction between the soil and berg.

The basal shear S will be

$$S = \ell.B.c. \quad \ldots\ldots [13]$$

If β is the angle of the slope, the depth d can be expressed as

$$d = \ell \, \mathrm{Tan}\beta$$

The work done by the resisting forces along the length of the gouge can be equated to the initial kinetic energy of the iceberg which results in the following expression

$$\frac{WV^2}{2g} = \int \frac{1}{2} \beta \ell \, \mathrm{Tan}\beta(\gamma' d + 4c) \, d\ell + \int d.\ell(\gamma' d + 4c)\mu \, d\ell + \int \ell.B.c.d\ell$$

$$= \int \frac{1}{2}.B.\ell \, \mathrm{Tan}\beta(\gamma' \ell \, \mathrm{Tan}\beta + 4c)d\ell + \int \ell^2 \, \mathrm{Tan}\beta(\gamma' \ell \, \mathrm{Tan}\beta + 4c)\mu d\ell$$

$$+ \int \ell.B.c.d\ell$$

$$= \frac{1}{2} B \, \mathrm{Tan}\beta\left[\gamma' \frac{\ell^3}{3} \mathrm{Tan}\beta + \frac{4c\ell^2}{2}\right]_0^L + \mathrm{Tan}\beta\left[\frac{\gamma' \ell^4}{4} \mathrm{Tan}\beta + \frac{4c\ell^3}{3}\right]_0^L \mu$$

$$+ \left[\frac{\ell^2}{2} B.c\right]_0^L$$

$$= \frac{1}{2} B.L.D \left(\frac{\gamma' D}{3} + 2c\right) + L^2 D \left(\frac{\gamma' D}{4} + \frac{4c}{3}\right)\mu + \frac{L^2}{2} B.c. \quad \ldots\ldots [14]$$

where W = the weight of the berg,

V = its velocity at the commencement of gouging,

L = the total gouge length,

D = the final gouge depth and other symbols as defined earlier.

On a closer examination, this simplified expression is seen to over estimate the resisting forces. The pressure on the sides could be zero, active or at-rest, but not passive as the sides do not

push the soil any further. The contribution of the active pressure on the sides in resisting the forward movement of the berg would be negligible as the iceberg is continuously lubricated and friction is virtually absent. Further, if the iceberg moves with a constant draft without exerting any downward pressure, there is not likely to be any basal shear.

If this is the case, then it is more realistic to consider the equilibrium of a soil wedge continuously sheared and pushed in front of the idealized berg. The height of the soil surcharge can be calculated assuming that the scoured sediment settles to a simple geometric shape in front and the sides of the iceberg.

SOIL DISPLACED BY A GOUGING ICEBERG

An idealized iceberg progressively scouring into a slope would bite deeper as it advances into the soil. The soil removed in front would flow around the front edge and slope down from the berg body. The slope to which the displaced soil settles would depend on its physical properties. The gouged channel would have a central depression with raised side ridges and an outward slope from the ridge top. Fig. 23 is a representation of such a concept.

Let β = slope of the ocean surface sediment,

α = slope of the displaced soil,

B = width of iceberg,

ℓ = length of the gouge at any instant during gouging

d = the corresponding depth of the gouge,

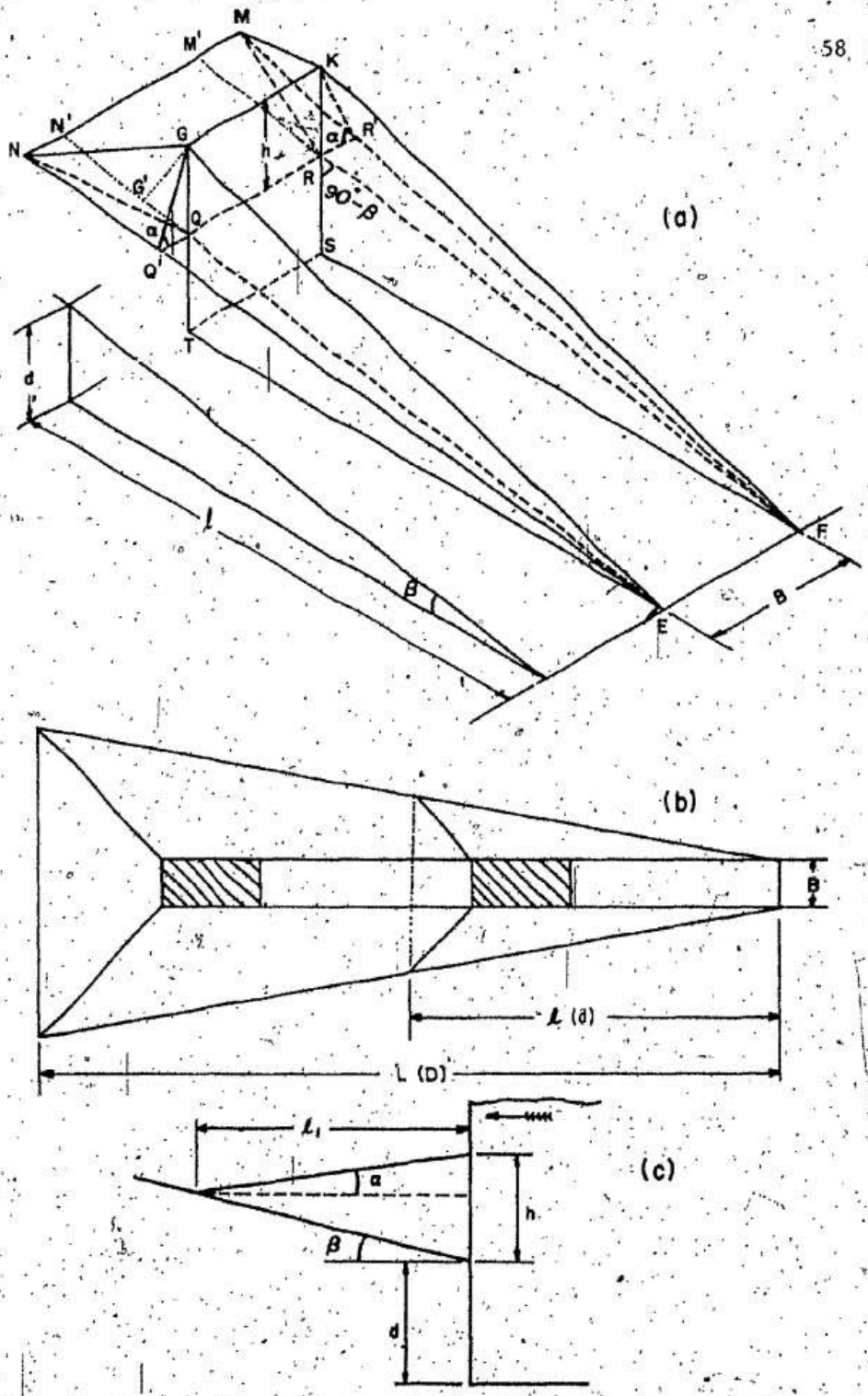

FIG. 23.- SURCHARGE OF DISPLACED SOIL AROUND AN IDEALIZED ICEBERG

ℓ_1 = length of the surcharge in front of the iceberg,

and h = height of the surcharge at the front face of the berg.

From Fig. 23,

The volume of soil scoured = EFSTQRFE

The volume of soil spread on the sides = EQNGE + FRMKF

Volume of soil in front = QRMNGKM.

Assuming no change in the volume of the scoured material,

$$\text{Volume EFSTQRFE} = \text{Volume (EQNGE + FRMKF)} + \text{Volume QRMNGKM} \quad \ldots\ldots\ldots [15]$$

$$= 2\,(EN'NGE) + N'M'RQGKM'$$

$$EFSTQRFE = \frac{1}{2}\,\ell.B.D. \quad \ldots\ldots\ldots [16]$$

$$2(EN'NGE) = 2\left(\tfrac{1}{2}\,EN'.NN'.\frac{GG'}{3}\right) = 2\left(\tfrac{1}{2}EN'.QQ'.\frac{(\ell+\ell_1)}{\ell}\frac{GG'}{3}\right)$$

$$= \frac{(\ell+\ell_1)}{\cos\beta}\cdot\frac{h}{\tan\alpha}\cdot\frac{(\ell+\ell_1)}{\ell}\cdot\frac{h\cos\beta}{3}$$

$$= \frac{h^2(\ell+\ell_1)^2}{3\ell}\cot\alpha \quad \ldots\ldots\ldots [17]$$

$$N'M'RQGKM' = \tfrac{1}{2}\,QN'.GG'.QR$$

$$= \tfrac{1}{2}.\frac{\ell_1}{\cos\beta}.h.\cos\beta.B$$

$$= \frac{\ell_1 hB}{2} \quad \ldots\ldots\ldots [18]$$

$$\text{From [15]} \quad \tfrac{1}{2}\,\ell Bd = \frac{h^2(\ell+\ell_1)^2}{3\ell}\cot\alpha + \frac{\ell_1 hB}{2} \quad \ldots\ldots\ldots [19]$$

Put $\tan\alpha + \tan\beta = K_1$

From Fig. 23c, $h = \ell_1 K_1$

Equation [19] can be rewritten as

$$\tfrac{1}{2}\ell BD = \frac{\ell_1^2 K_1^2}{3\ell}(\ell + \ell_1)^2 \cot\alpha + \frac{\ell_1^2 K_1 B}{2}$$

$$\text{or } 2K_1^2\ell_1^4 + 4K_1^2\ell\ell_1^3 + (2K_1^2\ell^2 + 3K_1\ell B \tan\alpha)\ell_1^2 - 3\ell^2 d.B\tan\alpha = 0 \quad \ldots\ldots [20]$$

If L = the final gouge length L_1 = the corresponding length of the surcharge in front, and D = the final gouge depth,

$$2K_1^2 L_1^4 + 4K_1^2 L L_1^3 + (2K_1^2 L^2 + 3K_1 LB \tan\alpha)L_1^2 - 3L^2 DB \tan\alpha = 0 \quad \ldots\ldots [21]$$

from which L_1 can be solved in terms of L.

EQUILIBRIUM OF THE SHEARED SOIL WEDGE

Fig. 24 shows the idealized iceberg in the process of gouging and the shearing wedge of sediment (Fig. 24 b) in front. The scoured sediment will not be assumed to contribute any shear resistance as it is remolded and would not be settled for sufficient enough time to regain its strength before being moved again by the iceberg.

From Fig. 24(b) $\dfrac{d + h - x \sin\theta}{x\cos\theta} = \tan\alpha$

$$x = \frac{(d + h)}{(\cos\theta \tan\alpha + \sin\theta)} \quad \ldots\ldots [22]$$

$$x_1\cos\theta \tan\beta + d = x_1 \sin\theta$$

$$x_1 = \frac{d}{(\sin\theta - \cos\theta \tan\beta)} \quad \ldots\ldots [23]$$

If P = the total soil resistance

W_s = weight of the wedge of soil

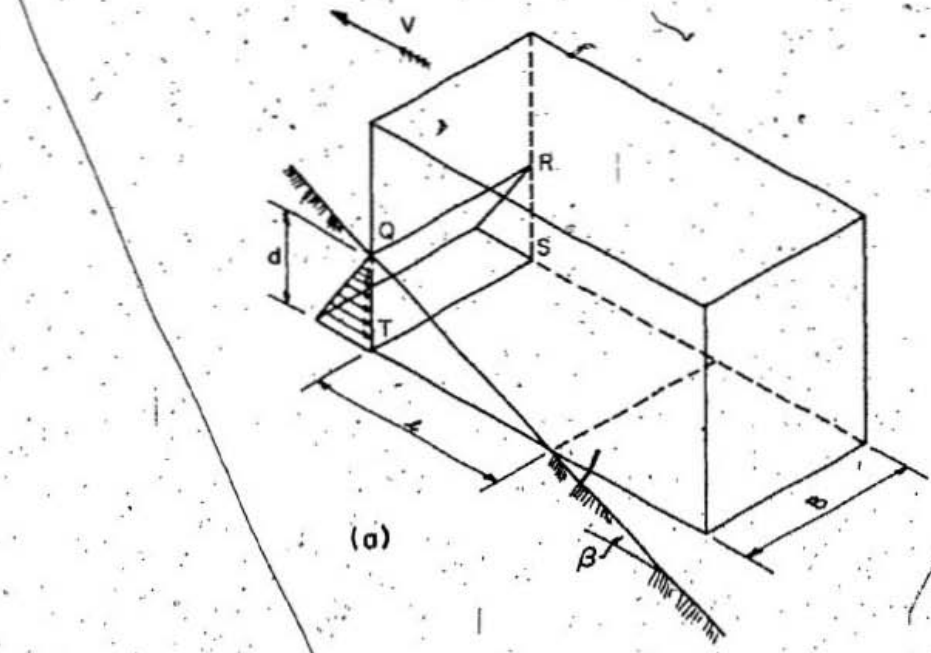

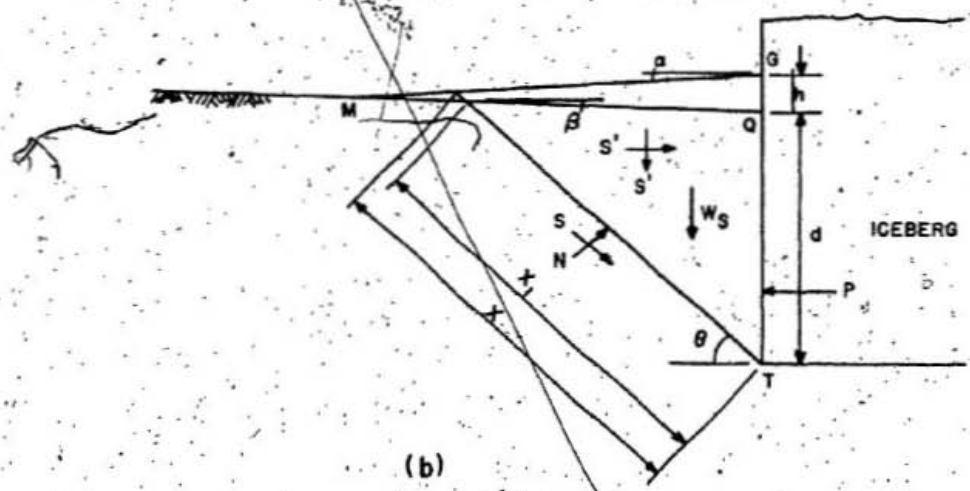

FIG. 24.- ASSUMED TYPE OF SOIL FAILURE IN FRONT OF AN IDEALIZED ICEBERG

S = shear resistance along the failure plane

N = normal reaction on the inclined surface

S' = the shear resistance on each side

τ_f = the shear strength of the soil,

resolving the forces along the X and Y axes,

$$P = S \cos\theta + N \sin\theta + 2S' \qquad \ldots\ldots [24]$$

$$N \cos\theta = W_s + 2S' + S \sin\theta \qquad \ldots\ldots [25]$$

$$W_s = \tfrac{1}{2}\gamma' (h+d)^2 \frac{B \cos\theta}{(\cos\theta \tan\alpha + \sin\theta}$$

$$S' = (\tfrac{1}{2} d.x_1 \cos\theta)\, \tau_f$$

$$= \tfrac{1}{2}d^2 \frac{\cos\theta}{(\sin\theta - \cos\theta \tan\beta)} \tau_f$$

$$S = \frac{d}{(\sin\theta - \cos\theta \tan\beta)} \tau_f B$$

From [25]

$$N = \frac{1}{\cos\theta}\left[\frac{\gamma' (h+d)^2}{2} B \frac{\cos\theta}{(\cos\theta \tan\alpha + \sin\theta} + \frac{\tau_f d^2 \cos\theta}{(\sin\theta - \cos\theta \tan\beta)} + \frac{\tau_f d.B \sin\theta}{(\sin\theta - \cos\theta \tan\beta)}\right] \ldots [26]$$

From [24] and [26]

$$P = \frac{d.B.\tau_f}{(\sin\theta - \cos\theta \tan\beta)} \cos\theta + \frac{\sin\theta}{\cos\theta}\left[\frac{\gamma'(h+d)^2}{2}.B. \frac{\cos\theta}{(\cos\theta. \tan\alpha + \sin\theta)} + \frac{\tau_f.d^2 \cos\theta}{(\sin\theta - \cos\theta . \tan\beta)} + \frac{\tau_f.d.B. \sin\theta}{(\sin\theta - \cos\theta.\tan\beta)}\right] + \frac{\tau_f.d^2. \cos\theta}{(\sin\theta - \cos\theta.\tan\beta)}$$

$$= \frac{\gamma'(h+d)^2}{2} B \left[\frac{\sin\theta}{(\cos\theta \tan\alpha + \sin\theta)}\right]$$

$$+ \tau_f . d . B \left[\frac{\cos\theta}{\sin\theta - \cos\theta \tan\beta} + \frac{\sin^2\theta}{\cos\theta (\sin\theta - \cos\theta \tan\beta)}\right]$$

$$+ \tau_f d^2 \left[\frac{\sin\theta + \cos\theta}{\sin\theta - \cos\theta \tan\beta}\right] \quad \ldots\ldots [27]$$

Tan α and Tan β being very small, the above equation can be rewritten as

$$P = \frac{\gamma'(h+d)^2}{2} . B + \tau_f d . B(\cot\theta + \tan\theta) + \tau_f d^2 (1 + \cot\theta)$$

$$= \frac{\gamma'(h+d)^2}{2} . B + \frac{2\tau_f d . B}{\sin 2\theta} + \tau_f d^2 (1 + \cot\theta) \quad \ldots\ldots [28]$$

AN EQUATION FOR ICEBERG GOUGE SIZE

The work done by the sediment resistance P, as the iceberg moves forward and develops a series of failure wedges, can be equated to the initial kinetic energy of the iceberg and expressed as

$$\frac{WV^2}{2g} = \int P d\ell$$

$$= \int \left[\frac{\gamma'(h+d)^2}{2} . B + \frac{2\tau_f d . B}{\sin 2\theta} + \tau_f d^2 (1 + \cot\theta)\right] d\ell \quad \ldots [29]$$

To make the above expression easily integrable, h can be approximated to vary linearly with d and written as

$$h = (\text{constant } K_2) . d$$

and $d = \ell \text{ Tan } \beta$

$$\frac{WV^2}{2g} = \frac{\gamma'(H+D)^2}{6} BL + \frac{\tau_f DLB}{\sin 2\theta} + \frac{\tau_f D^2 L}{3}(1 + \cot\theta) \quad \ldots\ldots [30]$$

where W = the weight of the berg

V = the velocity of the berg at the commencement of the scouring

and the other terms are as defined earlier.

If $\theta = 45^\circ$, equation [30] reduces to

$$\frac{WV^2}{2g} = \frac{\gamma'(H+D)^2}{6} BL + \tau_f DLB + \frac{2}{3}\tau_f D^2 L \quad \ldots\ldots [31]$$

This equation ignores the energy input from currents and winds during the iceberg deceleration. This aspect is discussed on page 70.

Figs. 25 and 26 are two sets of solutions of the above equation for a set of assumed soil properties. Fig. 25 represents the variation of the gouge length with the $\frac{W}{B}$ ratio. As can be anticipated the length of scour is longer with flatter slopes for a given kinetic energy.

Fig. 26 shows the variation of the maximum gouge depth. It is noted that deeper scours occur in steeper slopes. The sediment resistance increases as the square of the depth and the work done is a linear function of the length. Scours in steep slopes therefore tend to be deep and short in length.

The effect of the variations in the wet density of the sediment and also the shear strength is shown in these figures. The scour size is more sensitive to a change in the soil density and to a lesser degree to the variation in the shear strength.

To verify the error in assuming a linear variation for h, gouge lengths were computed by a numerical integration of equation [29].

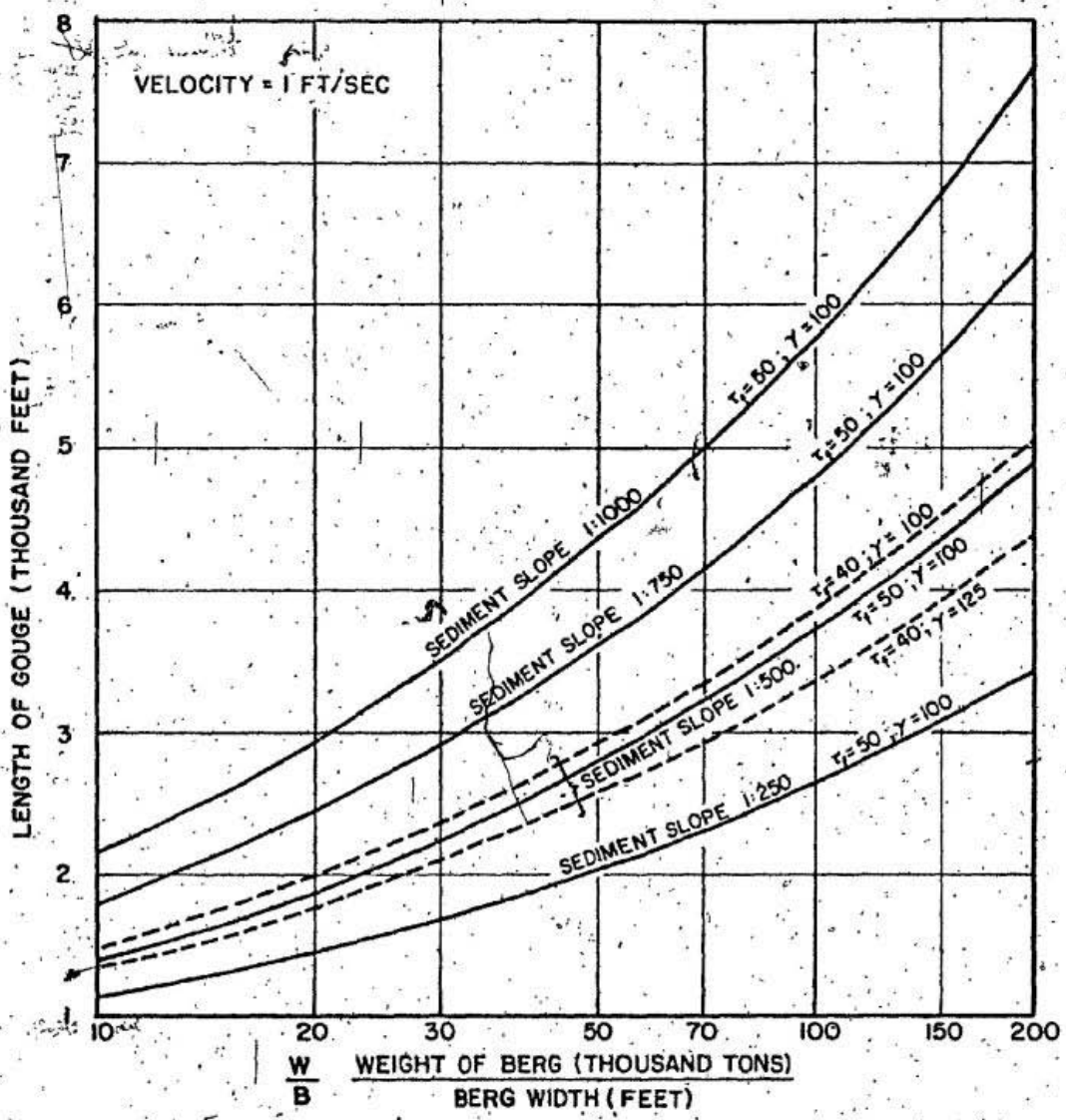

FIG. 25.- THEORETICAL ICEBERG GOUGE LENGTHS

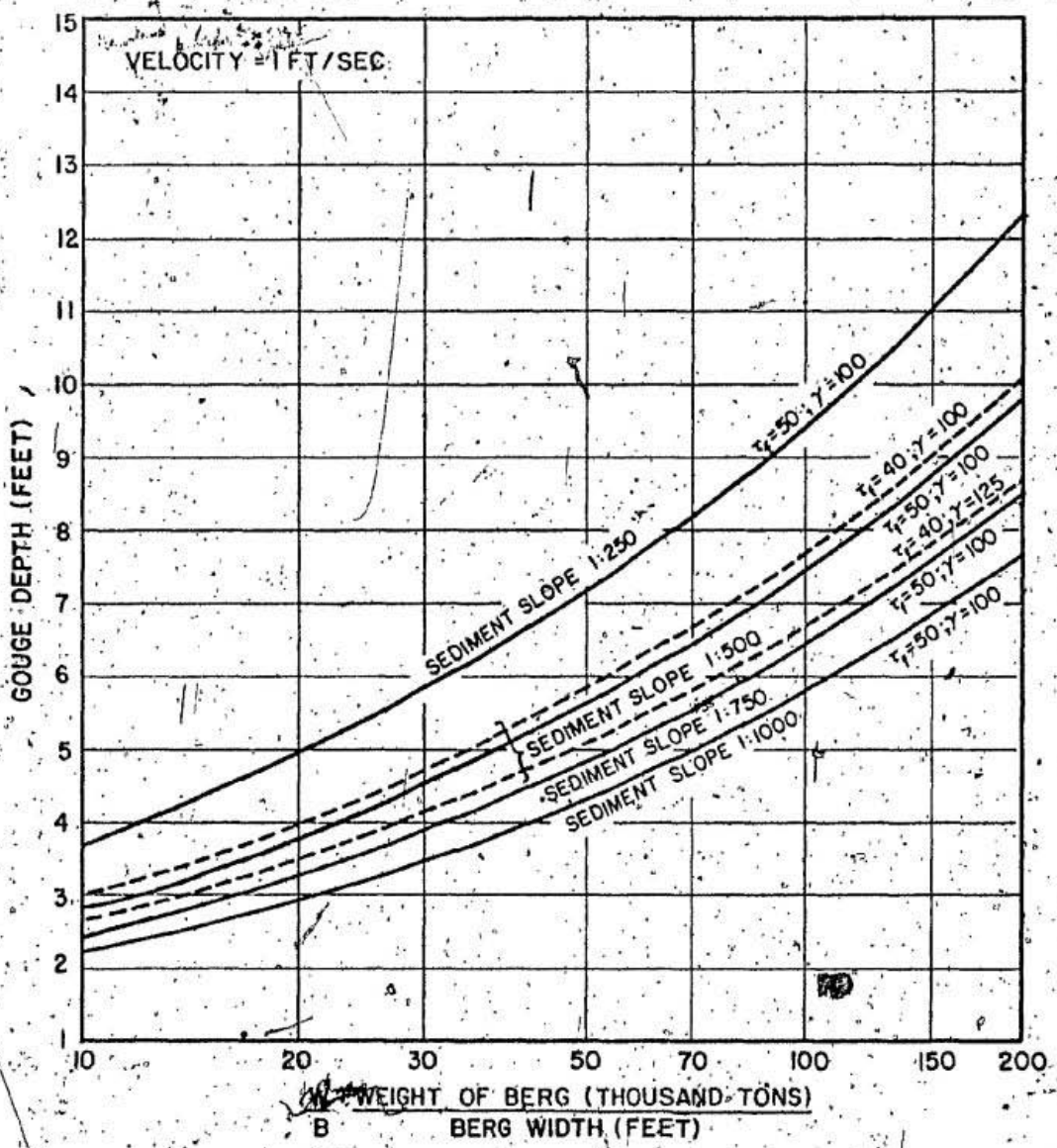

FIG. 26. - THEORETICAL ICEBERGS GOUGE DEPTHS

The approximation results in gouge lengths which are longer by about 1.2%. The error, if the effect of surcharge were neglected altogether, depends on the slope to which the displaced sediment settles. Even assuming this slope to be equal to the original slope of the continental shelf, the error would be about 10% for a 1:250 slope and about 5% for a 1:1000 slope.

ACCELERATION OF THE SHEARED WEDGE.

The effort required to accelerate the soil wedge in front of the moving iceberg was neglected in the previous section. In fact the soil wedge in front of the idealized berg is accelerated from rest to a certain velocity V_s (Fig. 27) which depends on the berg velocity V. If V_0 is the velocity of the berg at any instant of time,

$$V_s = \frac{V_o}{\cos \theta}$$

The weight of the soil gouged in time t, $= \frac{\gamma'}{g} B.d.V_o.t$

Acceleration $= \frac{V_s}{t}$

Acclerating force $= \frac{\gamma'}{g} Bd.V_o V_s = \frac{\gamma'}{g} Bd.\frac{V_o^2}{\cos \theta}$

Energy dissipated in soil acceleration

$$= \frac{\gamma'}{g} B.\frac{\tan \beta}{\cos \theta} \int \ell V_o^2 d\ell \qquad \ldots\ldots\ldots [32]$$

If the initial velocity of the iceberg is V,

$$V_o^2 = V - 2 f\ell$$

where f = the deceleration.

Assuming $\theta = 45^{\circ}$, equation [32] can be written as

$$\text{Energy} = \sqrt{2}\ \frac{\gamma'}{g}\ B \tan\beta \int (V^2 - 2f\ell)\ell d\ell$$

$$= \sqrt{2}\ \frac{\gamma'}{g}\ B \tan\beta \left[\frac{V^2\ell^2}{2} - \frac{2f\ell^3}{3}\right]_0^L$$

Since $f = \frac{V^2}{2L}$, energy dissipated $= \frac{\sqrt{2}}{6}\ \frac{\gamma'}{g}\ B.D.V^2.L$..... [33]

Since V is usually small, the work done in accelerating the soil is negligible compared with the initial kinetic energy of the iceberg and can be neglected.

DRIVING FORCE DUE TO OTHER ENVIRONMENTAL PARAMETERS

Wind, currents and ice all have the potential to feed energy into the system during the iceberg grounding process. In the free floating mode, forces due to these interact resulting in a steady state motion. The coupling of these different parameters with an iceberg is still not well understood. Icebergs are different from normal floating objects because of the presence of an envelope of melt water which always moves with the berg. The mode of transfer of forces to an iceberg through this envelope is still not well established.

Current drag: When an iceberg decelerates due to the sediment resistance there is a differential velocity between the berg and the propelling current which induces a fluid drag on the iceberg. Theoretically this may be conceived as causing a scour deeper than that computed from only the initial kinetic energy considerations.

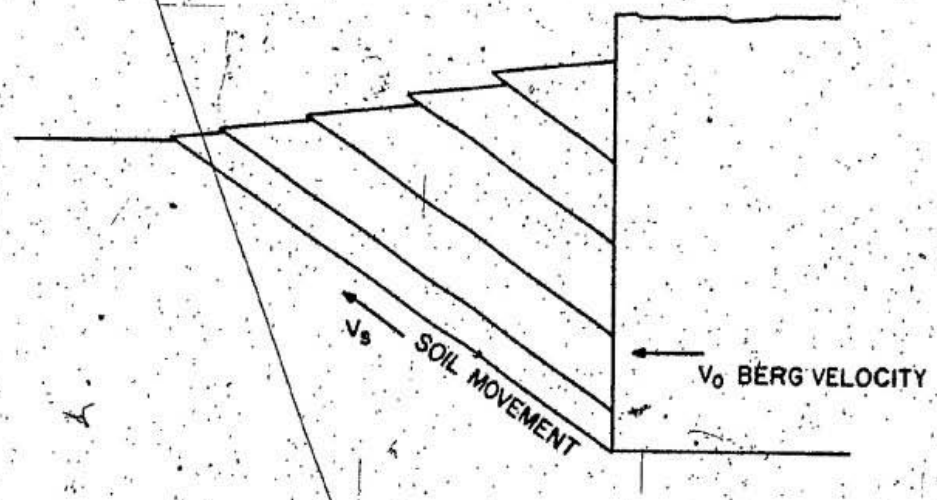

FIG. 27.- SOIL VELOCITY IN FRONT OF A MOVING ICEBERG (From Sohne[71])

The soil offers a passive resistance to the movement of an iceberg and when the berg finally comes to a stop due to dissipation of its initial kinetic energy, the fluid drag will cause further movement of the berg if this force is large enough to overcome the sediment resistance. An iceberg weighing 2 million tons would be approximately 300 ft wide and 750 ft long at the water surface with a total height of 400 ft. It is known from observations[3] that an iceberg is bilge shaped and a width of about 100 ft at the bottom is realistic in scour depth computations. In a slope of 1:500 this berg would gouge a depth of 3.8 ft if the sediment has a density of 100 lb/sft and a shear strength of 50 lb/sft. The soil resistance per unit width for a depth of 3.8 ft would be about 0.314 tons. The drag force F on the berg can be computed using equation[2],

$$F = \tfrac{1}{2} C_d \cdot \rho A V^2$$

but the evaluation of the coefficient C_d which depends primarily on the shape, is difficult. Budinger[20] estimated the range of C_d between 0.2 and 1.0 and used a value of 0.2 in his calculations. Assuming a value of 0.3 for C_d, and a current velocity of 1 ft/sec, the force per unit width on the soil would be about 0.14 tons. If, however, the drag force is greater in any particular situation, the corresponding depth at which the soil has an equal resistance will be the maximum scour depth.

Ice push: The interaction of sea ice with icebergs and the effect of ice push on icebergs is still to be established. The only recorded source is that of Milne[52] in which movement of icebergs independent of the ice fields is reported. Sea ice thrust appears

to be an important force in the grounding of ice islands in the Beaufort Sea. Kovacs and Mellor[43] computed the maximum ice thrust by considering the crushing strength of an ice sheet on an ice island. The strength of sea ice was taken as 400 lb/sq. in. and that of soil to be between 500 and 1200 lb/sft. Using a similar approach and assuming a 4 ft thick ice sheet with a conservative crushing strength of 200 lb/sq. in., the maximum ice thrust per foot width of the sheet can be calculated as 51,43 tons. In a weak soil of the type assumed in this investigation, this force would correspond to a gouge depth of about 75 feet. Gouges of this size have not been noticed in the literature surveyed. Kovacs and Mellor also considered the possibility of wind shear on ice sheets which in turn is transferred to an ice island as a thrust. The wind force on an ice sheet depends on its roughness, the presence of ridges, and the size of the sheet. Information on all these variables with particular reference to ice fields around an iceberg and the mutual interaction at the sea ice - iceberg surface is absent. However, if ice push is a force to be recognized, the theoretical expression for the gouge size is still valid. All the propelling forces can be grouped with the kinetic energy to constitute the push and the corresponding resistance of the soil to bring the berg to rest can be computed.

CHAPTER IV

EQUIPMENT DESIGN AND EXPERIMENTAL PROCEDURE

At the commencement of this research, theoretical analysis, field studies and laboratory modelling were all contemplated with a view to complement and prove the conclusions. During the cruise along the Labrador coast in 1972 it was planned to follow icebergs which were grounded or were in the process of grounding and scan the ocean floor for possible scour marks. These attempts were not rewarding as the bergs that were observed had grounded on rocky ledges. Water marks observed on the icebergs appeared to indicate that the bergs were raised during grounding and bergy bits were seen strewn all around. After the field trials to locate iceberg scour marks proved unsuccessful, it was decided to concentrate on the laboratory model where a model of the idealized berg could be towed into an artificially sedimented slope.

In the analytical model, it was assumed that the iceberg initially moves in a steady state with a velocity V, and gouges a scour length L, with a maximum depth D, in the process of moving into a slope. Fluid drag problems are usually modelled in the laboratory assuming the Froude number $\frac{V}{\sqrt{gl}}$ constant for the model and the prototype. If the linear scale of the model is λ_L

$$\lambda_L = \frac{L_p}{L_m}$$

where L is the length and suffixes p and m refer to the prototype and model, respectively.

Since $\left[\frac{V}{\sqrt{gL}}\right]_p = \left[\frac{V}{\sqrt{gL}}\right]_m$

$$\frac{V_p}{\sqrt{L_p}} = \frac{V_m}{\sqrt{L_m}}$$

The velocity scale $\lambda_V = \frac{V_p}{V_m} = \sqrt{\frac{L_p}{L_m}} = \sqrt{\lambda_L}$

The time scale $\lambda_T = \frac{T_p}{T_m} = \frac{L_p/V_p}{L_m/V_m} = \sqrt{\lambda_L}$

The force scale $\lambda_F = \frac{F_p}{F_m} = \frac{(\text{mass} \times \text{acceleration})_p}{(\text{mass} \times \text{acceleration})_m} = \frac{L_p^3}{L_m^3} = \lambda_L^3$

The stress scale $\lambda_\tau = \frac{F_p/A_p}{F_m/A_m} = \lambda_L$

If an iceberg is modelled to a scale of 1:100, the shear strength of the model sediment has to be scaled down by 100. Scaling an ocean sediment with a shear strength of 50 lb/sft to 0.5 lb/sft does not seem to be easily feasible. The wet density and the particle size of the soil are also not easily scalable according to the laws of similitude. A verification of equation [31] in its exact form is not practicable in a laboratory model unless the soil property is also scaled.

An alternative is to use a sediment whose properties resemble the actual ocean floor deposit and study its interaction with a model iceberg. Models could be towed at constant speeds into a slope of such a sediment and the effect of variables such as speed, shape and size

could be studied. These experiments could be expected to provide information on the pressure distribution, sediment resistance and the pattern of soil movement which could be then extrapolated to the actual gouging.

OBJECTIVES OF THE LABORATORY EXPERIMENTS

The aims of laboratory experiments in the light of the suggested analytical model can, therefore, be defined as:

1. To measure the pressure and its variation on the different faces of a blocky berg while it scours into a sediment of low shear strength and to detetmine the predominance of these pressures,

2. To measure the total force on this model during gouging and compare the measurements with the computed values,

3. To observe the soil movement in front of the berg in order to decide the type of soil failure and

4. To observe the gouge shape and type of soil flow around the model.

EXPERIMENTAL AND DESIGN REQUIREMENTS

The following facilities were considered necessary for laboratory modelling.

1. A sediment slope which could be easily formed with similar properties for each test,

2. A mode of towing bodies of different shapes into the slope,

3. Means of varying the towing speed within the range of normal iceberg drift velocites,

4. Facility to continuously monitor and record the pressures and total force on the model, and

5. Suitable provision to observe and record the soil movement around the model berg.

The towing tank: A towing tank of steel 12'-0" long, 2'6" wide and 2' 3" deep (all dimensions internal) was fabricated incorporating most of the above requirements. A substantial portion of this research had to be devoted to constructing, instrumenting and proving the test system. Preliminary qualitative tests were conducted in a 18" wide by 24" high by 32 ft long hydraulic flume before building the separate test tank.

Fig. 28 shows a plan view and an elevation of the facility. One long side of the tank was of 1/2" thick clear plate glass and the other three sides and bottom were of 1/4" mild steel plate. The entire weight of the tank was carried by three 5" by 3" I sections through channels 3" by 1½", spaced 2' 6" intervals. To reduce the bending movements and deflections the beams overhanged their supports by 18 inches. One of the supports was a hinge and another was a modified 8 Ton hydraulic jack which facilitated the tilting of the tank about the hinge. Two intermediate portal type supports on the long sides of the tank were added after the initial test, to prevent excessive deflection of the glass plate. All joints were bolted for easy dismantling if there was a need to change the soil sample and also to facilitate easy handling while moving.

The top edges of the tank supported two guide tracks along their length to carry a moving trolley. The trolley (or carriage) was

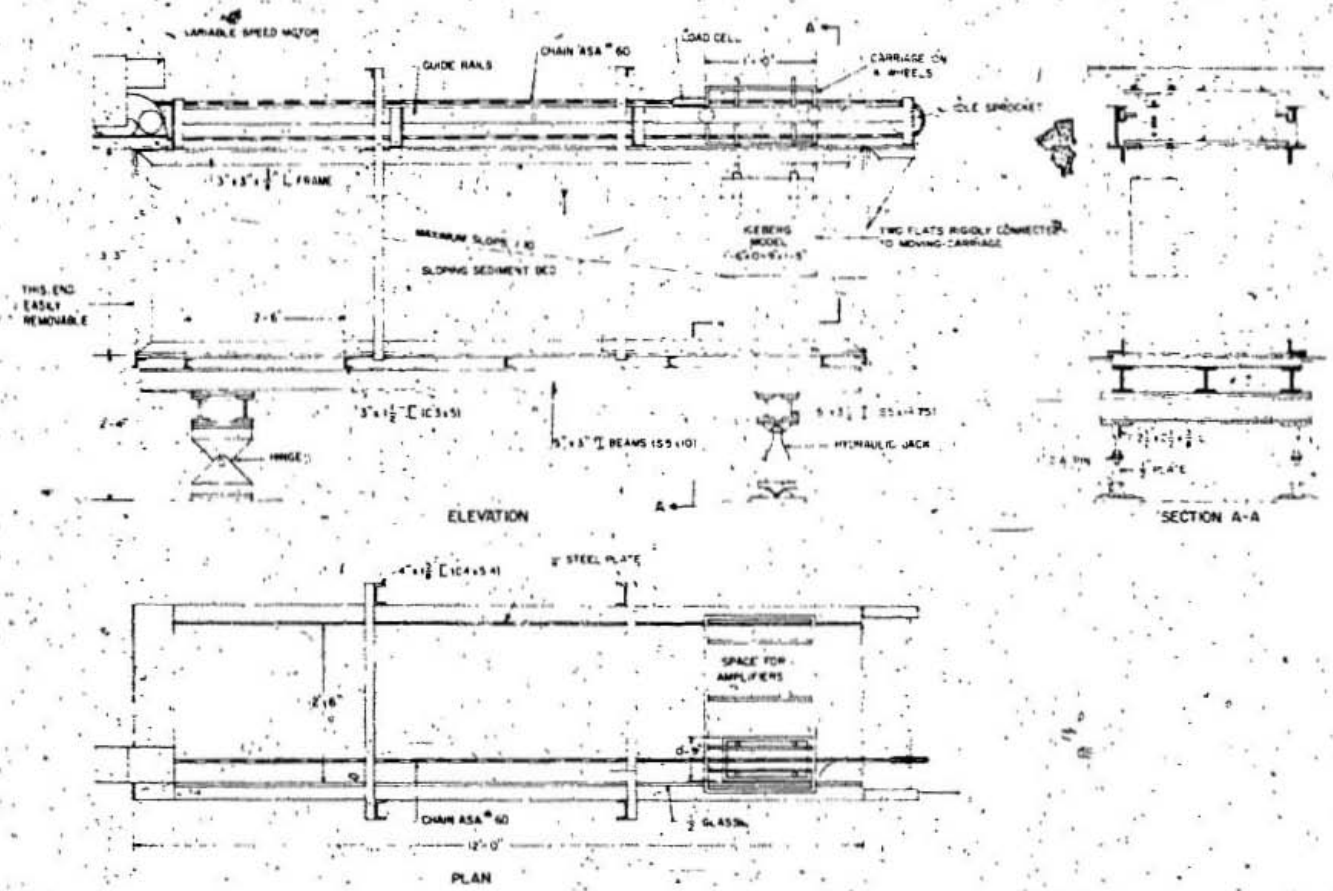

FIG. 28.- PLAN VIEW AND ELEVATION OF THE TEST TANK

made out of 1" by 1" angles and supported on 4 wheels (Fig. 29). The iceberg model was supported from the trolley through 5/8" steel bars and also pushed from behind by a vertical frame made of 1½" by 3/8" flat bars, rigidly fixed to the trolley. This ensured that the model was held rigid while being pushed into the slope. The carriage was pulled by an ASA chain no. 60. A load cell (Fig. 29) attached at the junction between the chain and the carriage registered the total pull on the model. A variable speed 1.5 H.P. U.S.Vari-speed motor with a speed range of 11 to 92 R.P.M. was used for driving the chain. The carriage speeds could be varied from 0.2 to 2.2 feet per second. Limit switches at the two ends of the tank prevented the carriage from driving through.

PREPARATION OF THE SEDIMENT SLOPE

The properties of the soil used will be given in Chapter V. It was felt that this soil when mixed and settled in water, with the tank in a tilted position, would result in a sloping sediment sample of low strengths. The idea of tilting the tank to form the slopes was evolved after trials with a small plexiglas tub. During the course of the fabrication and trial runs, it was noted in the literature that Doyle[30] used a similar tank for studies of wave effects on continental slopes. Doyle lowered the forward end to form the slope and had plexiglas on one side.

To prepare the sediment slope, the tank was first tilted to the required slope, the soil was mixed thoroughly into a thick slurry using steel rakes and allowed to settle for 48 hours. Agitation with

compressed air jets was adopted periodically whenever it was felt that the bottom layers were consolidating. When this type of mixing was done the time for settlement had to be at least 96 to 144 hours. This was mainly because of the use of more water during air jetting which resulted in a thinner slurry and greater time for settling to the required density and strengths. Air agitated sediment was too weak to retain the slope after 48 hours. Fig. 30 shows the tank in the tilted position with the settled soil. A few hours before every experiment, the tank was righted to the horizontal position which resulted in a sloping sediment bed (Fig. 31).

ICEBERG MODELS

The iceberg model was 9" wide by 18" long by 17" deep and made out of ¼" thick plexiglas. Most of the experiments were conducted with the idealized shape (Fig. 32). Limited observations were made on two other shapes of the same overall dimensions (Fig. 33,34).

INSTRUMENTATION

The selection of a suitable pressure measuring device involved considerable time and effort. One of the experimental objectives was to measure the pressure on the different faces of the model. On a soil slope of 1:10, the maximum expected experimental gouge depth was about 9 inches. It was essential that the pressure transducers be small and have a good degree of resolution. "Pitran pressure transistors" had a diameter of only 0.2 inches and different varieties of these are available for various pressure ranges starting from 0.07 psi. But on

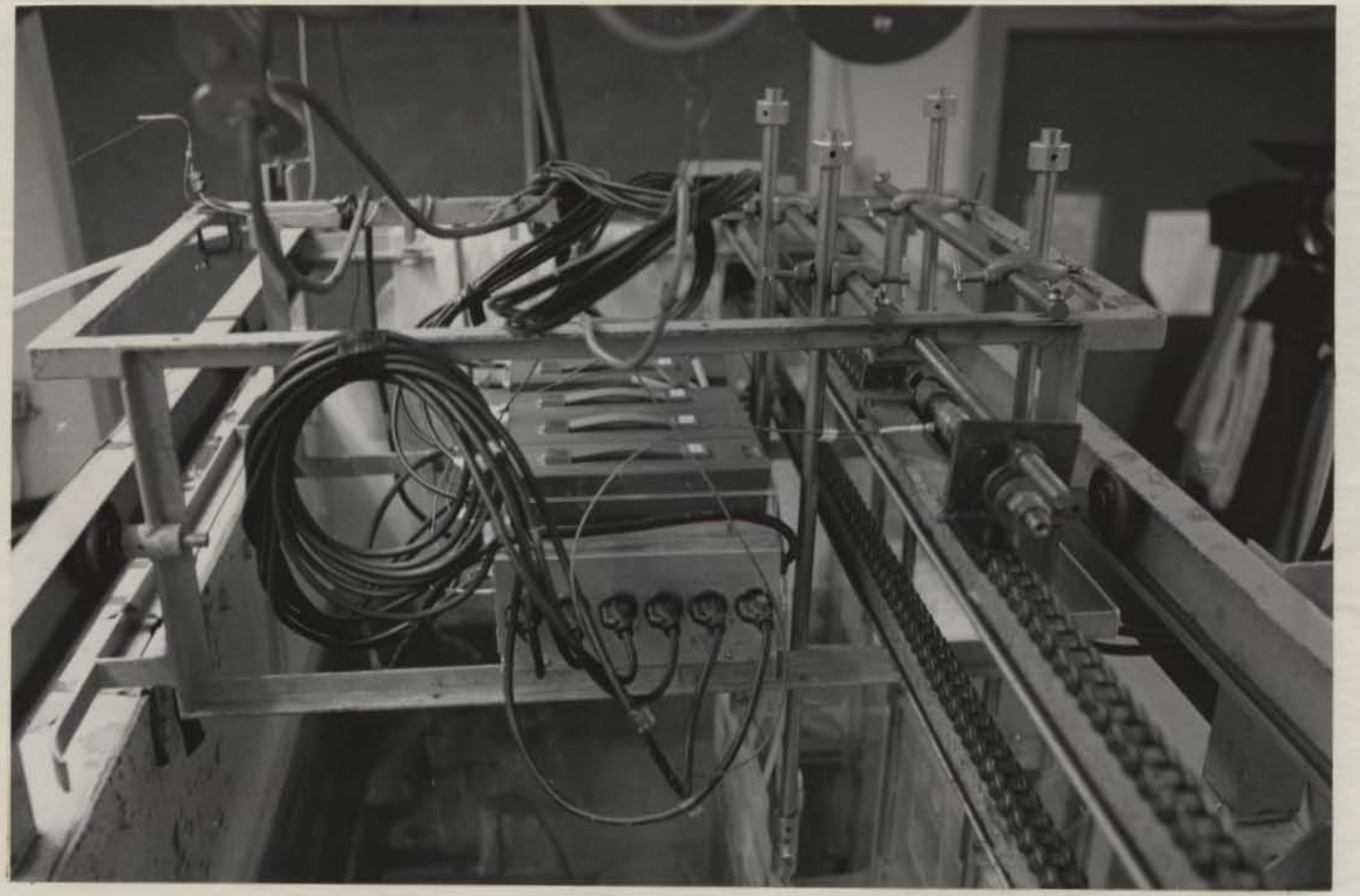

FIG. 29.- PHOTOGRAPH OF THE CARRIAGE ON TOP OF THE TEST TANK

This photograph also shows the guide rails, the iceberg model, load link, chain drive and amplifiers.

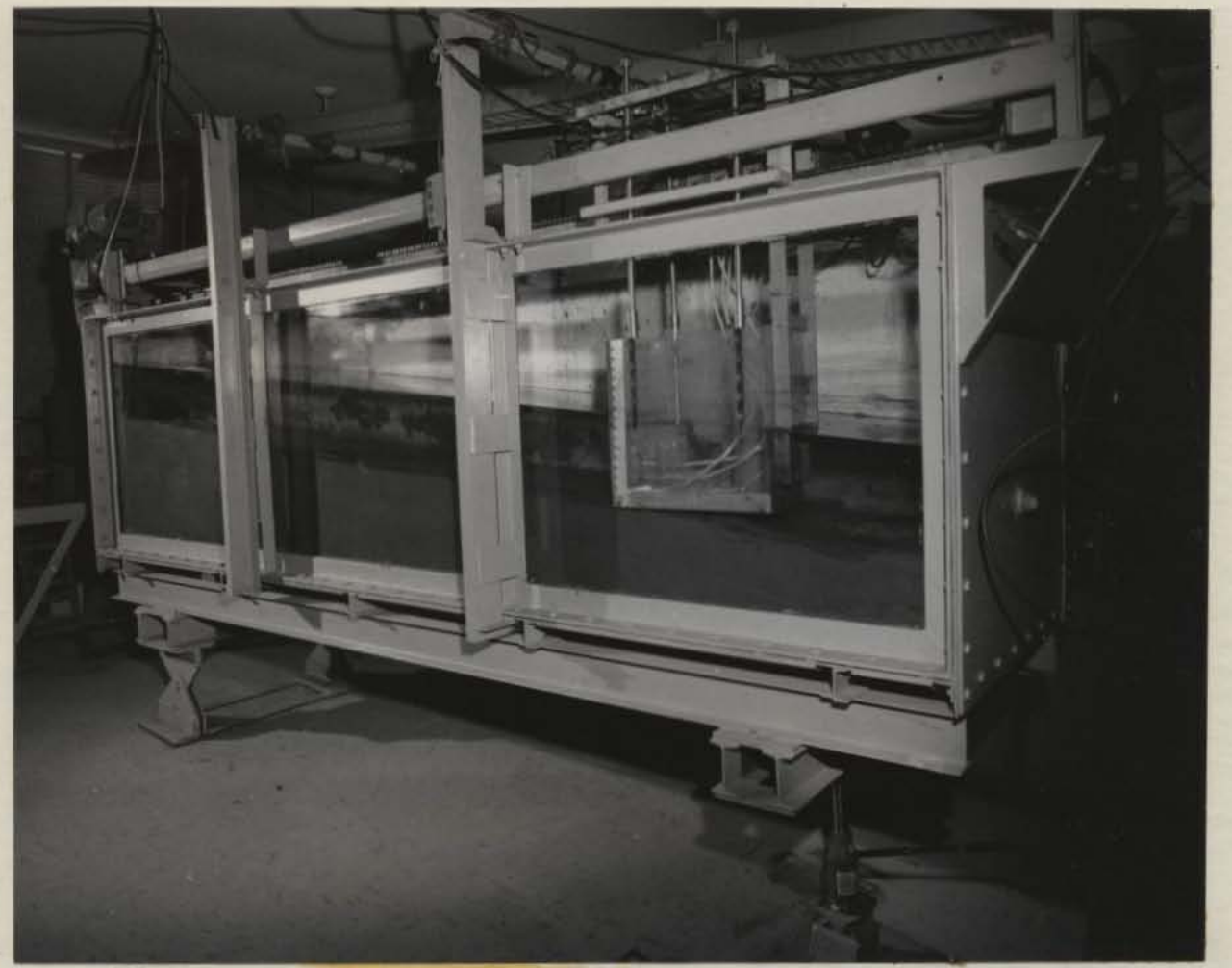

FIG. 30.- PHOTOGRAPH OF THE TEST TANK IN THE TILTED POSITION

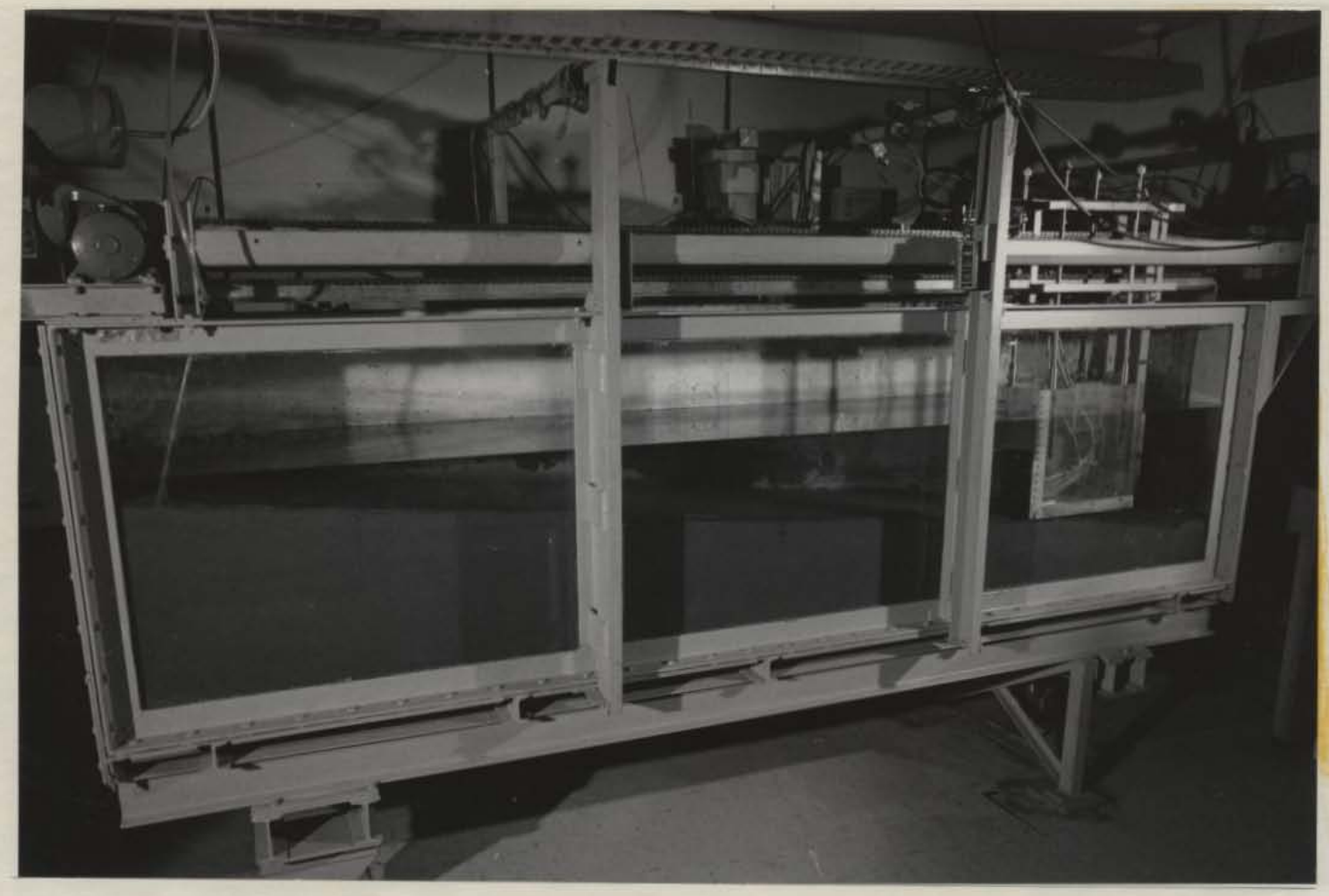

FIG. 31.- PHOTOGRAPH OF THE TEST TANK AFTER RIGHTING

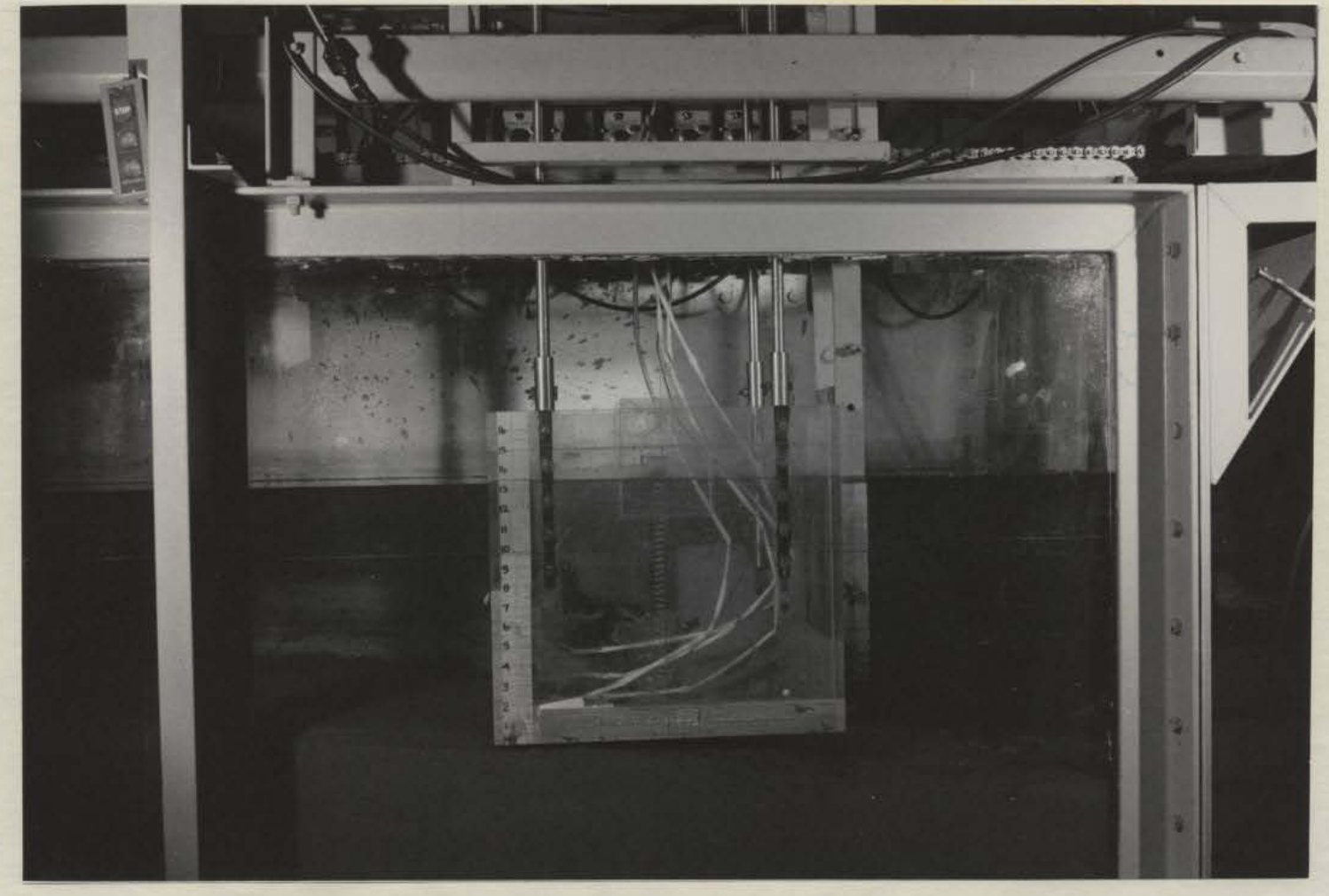

FIG. 32.- PHOTOGRAPH OF THE IDEALIZED ICEBERG MODEL

The initial position of the model toe close to the soil slope can be seen

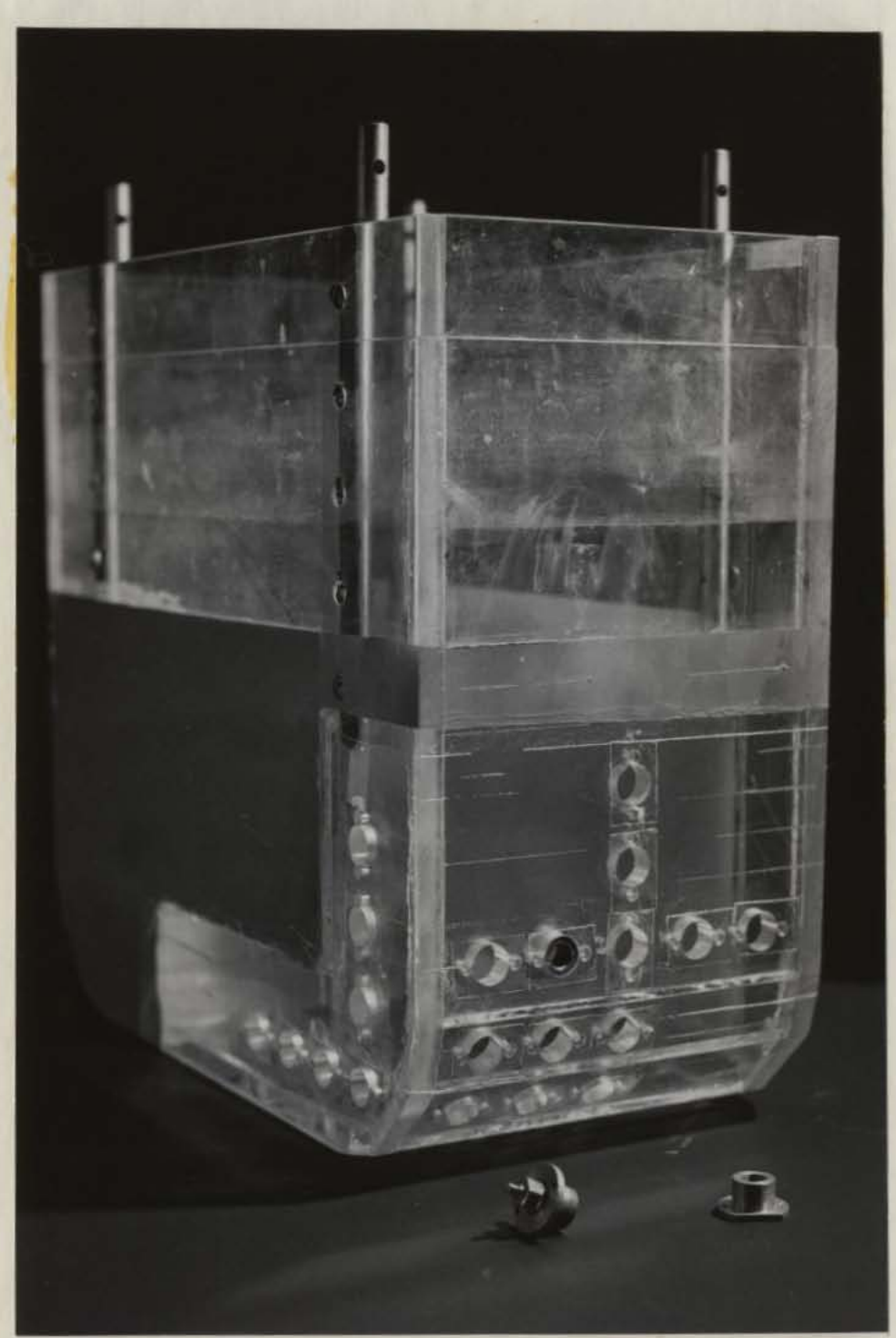

FIG. 33.- PHOTOGRAPH OF THE MODEL M_2 WITH A ROUNDED TOE

The brass holders and a pressure transducer can be seen in the foreground

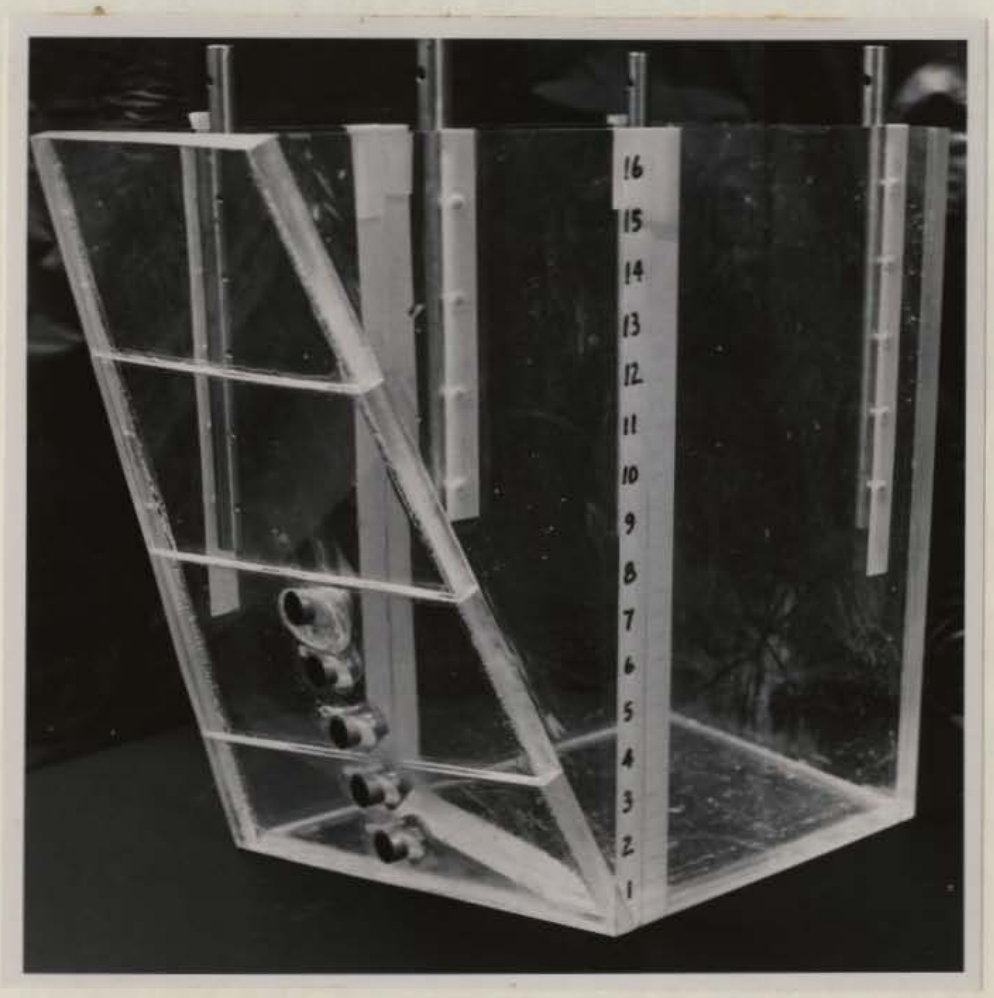

FIG. 34.- PHOTOGRAPH OF THE MODEL M3 WITH A TWISTED AND INCLINED FRONT FACE.

actual use in the iceberg model, it was found that these transistors were very fragile and were damaged either during mounting or due to abrasion during testing in the tank. Attempts to put a membrance in front of the gouge were not successful. While these transducers have been used successfully in fluid mechanics and bio-medical engineering, they could not be used in this case.

After considerable further search and trials of different alternatives to keep the cost low, it was decided to use 'Kistler quartz piezo-electric transducers'. These were 0.5 inch in diameter and slightly bigger but has an overload capacity of 10 times the rated range (1000%) of 30 psi with a resolution of 0.005 psi. Because these transducers were piezo-electric, the initial electric charge could be grounded before starting the experiment and the increase in the sediment pressure could be recorded as the scouring progressed. Each of these gauges had to be used in combination with a charge amplifier which made the instrumentation system expensive and put a restraint on the number of tranaducers that could be used. It would be ideal to mount transducers on all the faces of the model and measure their relative influence under identical experimental conditions. However, as this was an expensive proposition and amounted to $1100 per gauge (transducer and amplifier), it was decided to observe separately the pressures on each face of the model with uniform simulation of the experimental conditions. Brass holders were mounted at different points on the model and the transducers were screwed in until the face was flush with the plexiglas sheet of the model. Details of the specification, calibration and mounting are given in Appendix D. Even with these piezo-electric transducers, initial results were

frustratingly non-uniform. A detailed examination of the system revealed that even a small temperature difference between the water and the soil caused the signal drifting. This problem was subsequently corrected by temperature measurements allowing it to stabilize before running the experiments. The total pull was measured by a Kistler Quartz force link type 932 - A (Fig. 29) in combination with a charge amplifier. The problem of temperature stability for the force link did not arise as it was at a uniform air temperature throughout the experiments. The charge amplifiers were mounted on the carriage to prevent leakage of charge due to long leads.

A slider was attached to the carriage and moved on a resistance wire having one volt D.C. potential difference across and stretched between the two ends of the tank. The variable speed motor was calibrated by recording the voltage variation at the slider for different speed settings and also measuring the corresponding distances travelled by the carriage. The voltage change which represents the distance travelled was plotted on a x - y plotter, with time along the abscissa and voltage on the ordinate. The calibration curve as shown in Fig. 35 was then obtained.

RECORDING SYSTEM

Output from the charge amplifier was fed to a 8 channel 'Lyrec' instrumentation recorder model TR 61-3. This had seven F.M. channels and one channel for direct recording. A time-mark generator, 'Fairchild' type 781 was used to generate signals at 1 second intervals to synchronize the different signal traces at the time of replay. The

voltage at the slider, pull from the load link and output of the pressure transducers were recorded on the F.M. channels. Time pulses at intervals of one second were recorded on the direct recording channel. The exact experimental procedure will be described in a succeeding section of this chapter. Recorded signals were played back and plotted one channel at a time on a Hewlett Packard X - Y plotter model 7001-A. The instrumentation system is shown in Fig. 36 with a schematic diagram in Fig. 37. An alternative recording system used during the trial runs with the 'Pitran transistors' is also shown in the diagram.

DETERMINATION OF SOIL PROPERTIES

The sediment slope was formed by settling a soil-water slurry as described in an earlier context. Because of the very low strength and loose state of the sediment it was not possible to take out any undisturbed sample for strength determination. With soils of this type, in-situ strength determination such as vane shear tests are best suited. A laboratory vane shear equipment model WF 2350 manufactured by Wykeham Farrance Engineering Ltd. was modified to facilitate a 24" vertical movement of the vane. The modified vane shear apparatus and the vanes used are shown in Fig. 38. The normal laboratory vanes were 1/2 in. by 1/2 in., but for the low strength soils of the type used here, a special vane 2" dia. by 1" ht. was fabricated out of 0.02" stainless steel. To facilitate a direct reading of the shear strength from the angles of twist at soil failure, the vane was calibrated (Fig. 39) in combination with the standard spring no. 2,

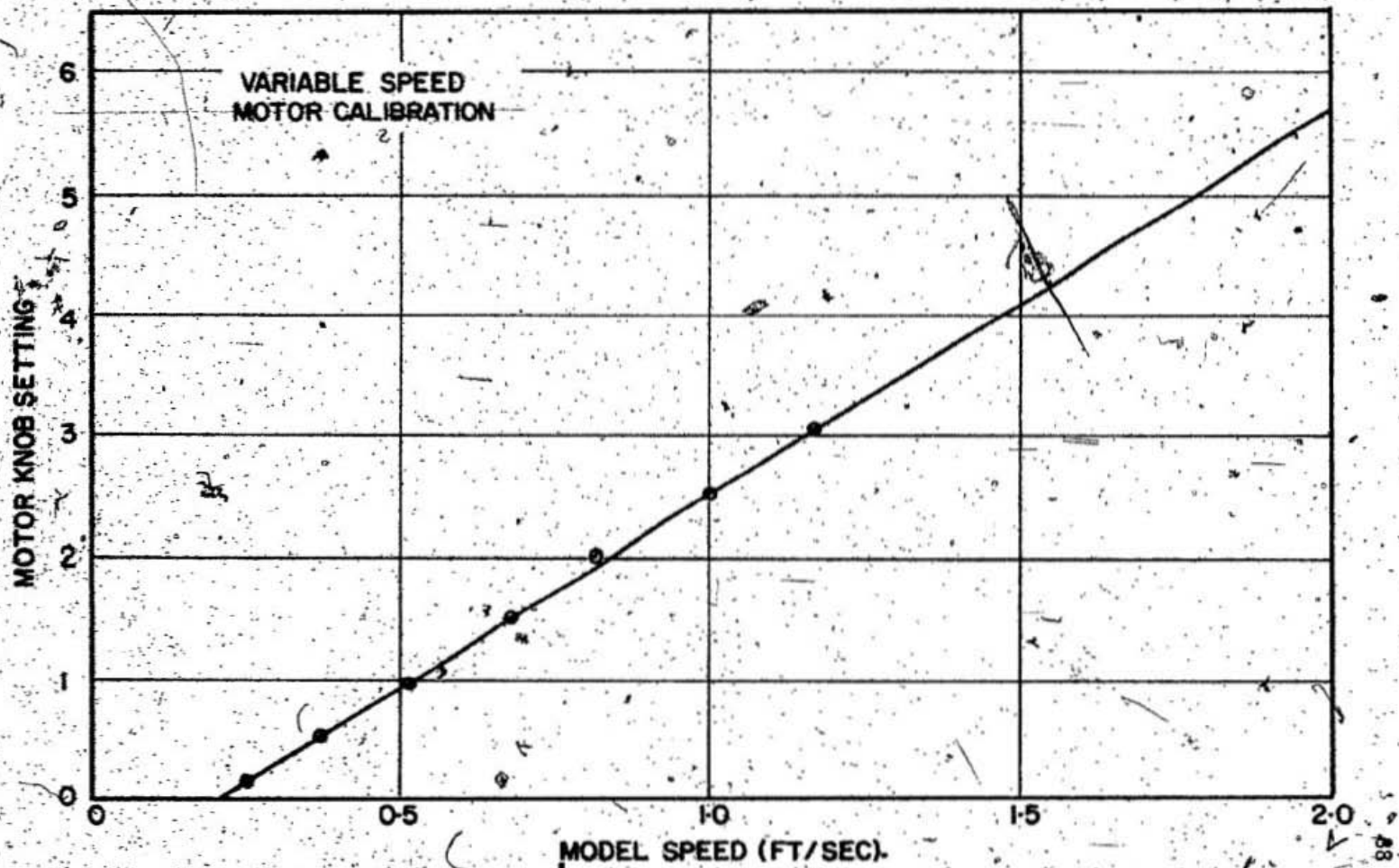

FIG. 35.- CALIBRATION CHART FOR THE VARIABLE SPEED MOTOR

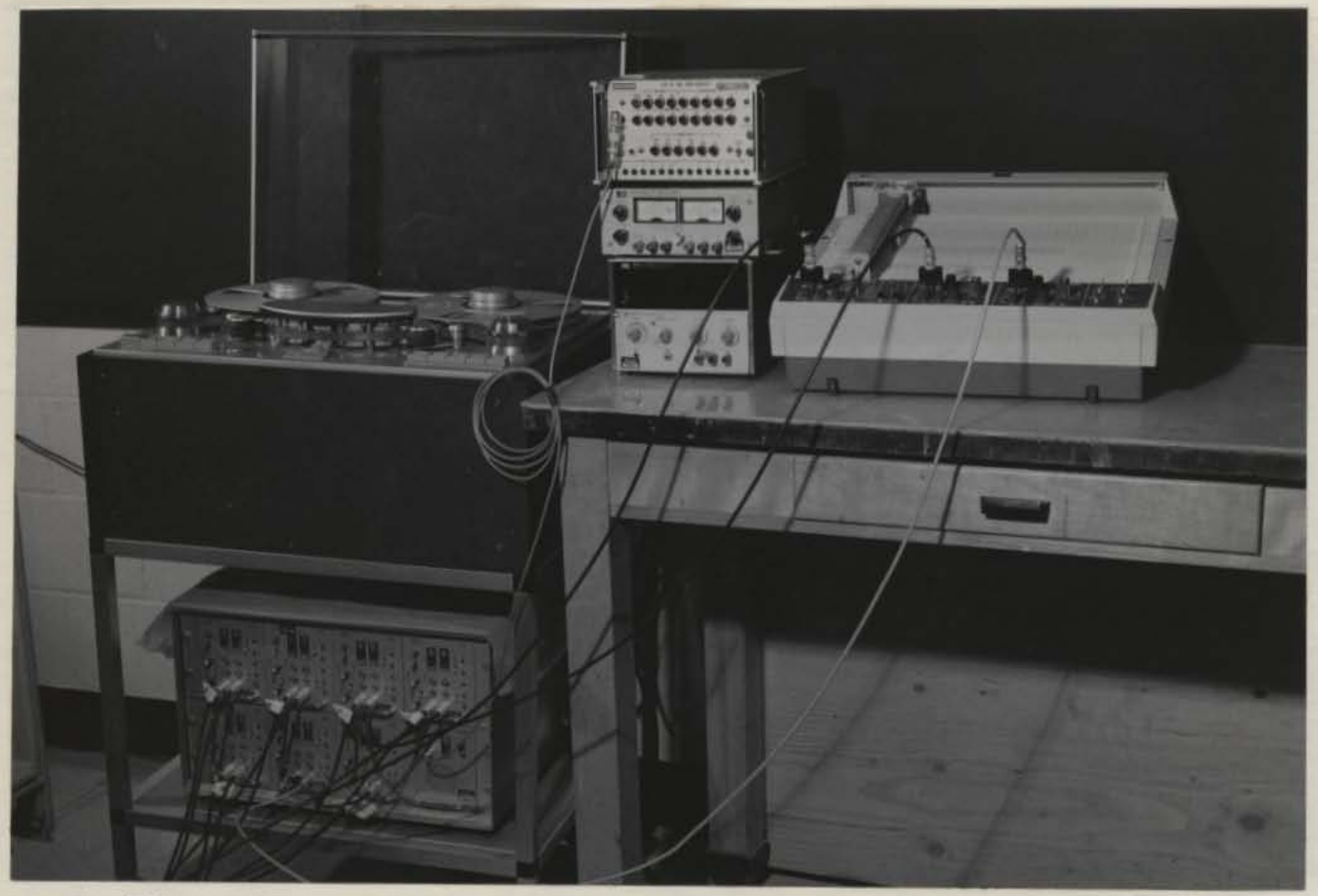

FIG. 36.- PHOTOGRAPH OF THE RECORDING SYSTEM

The tape recorder is seen on the far left, the digital voltmeter, D.C. power supply and the time mark generator are in the middle one above the other in that order and the X-Y plotter is to the far right

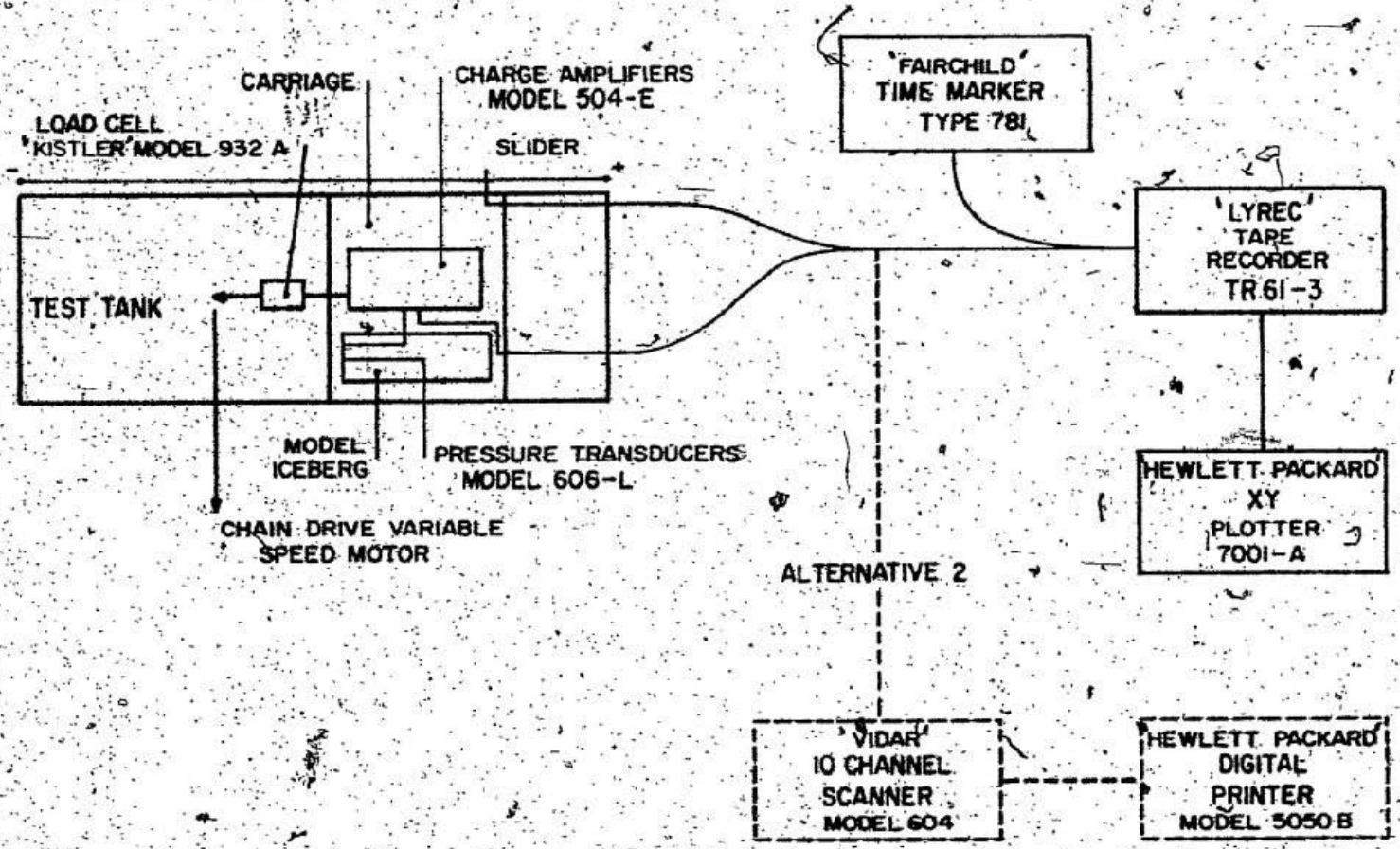

FIG. 37.- SCHEMATIC OF THE INSTRUMENTATION

Alternative 2 was used during the initial stages of the project

FIG. 38.- PHOTOGRAPH OF THE MODIFIED VANE SHEAR APPARATUS

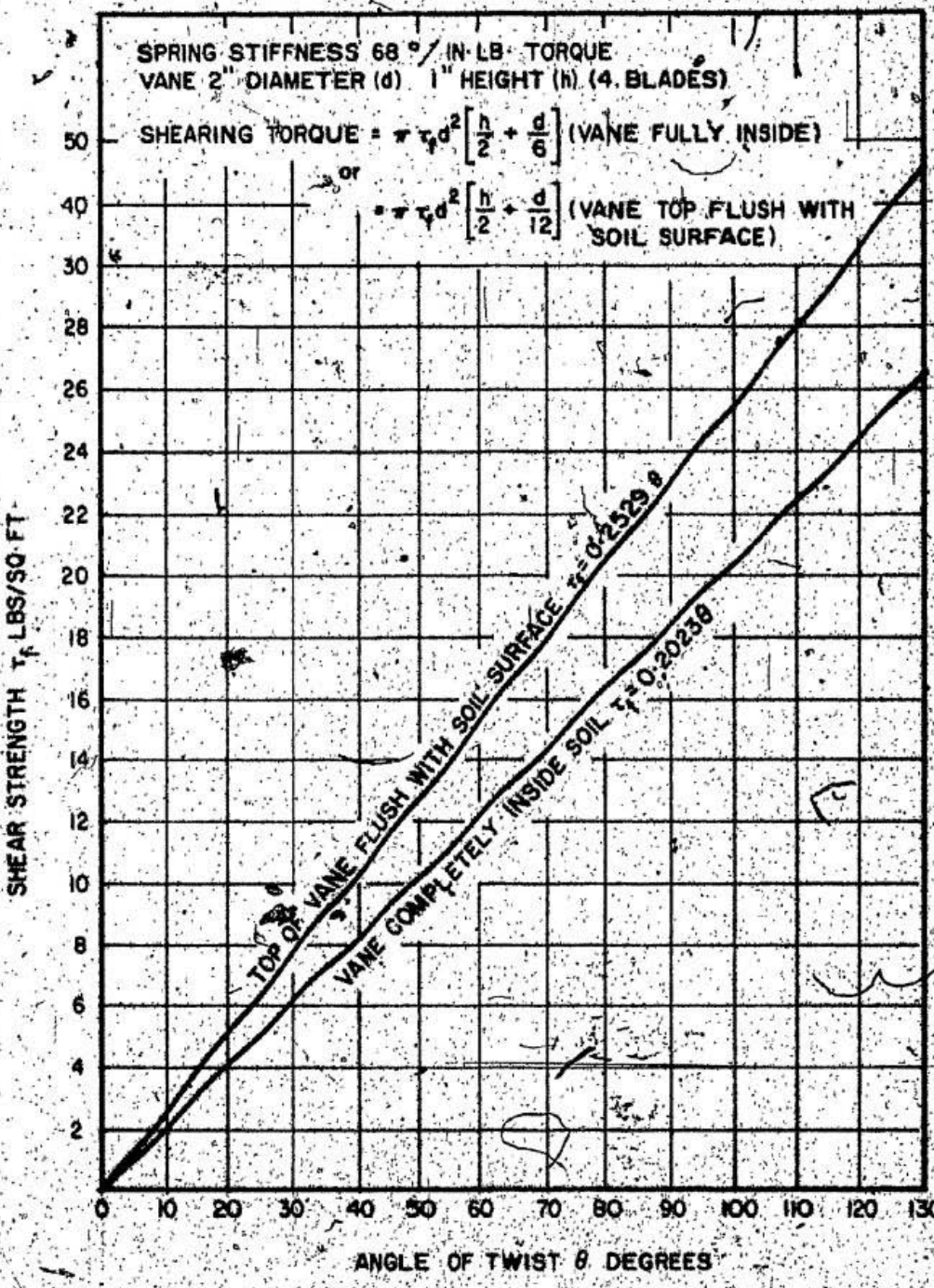

FIG. 39. – CALIBRATION CHART FOR THE MODIFIED VANE SHEAR APPARATUS

supplied by the manufacturers.

Sampling of the soil even for the bulk density determinations had to be done with great care. Aluminium moisture cups 2.5 inch diameter were converted into thin-walled tubes 1.75 inch long, by cutting out the bottom. These tubes were pushed into the soil. While the tube was still inside the soil, the bottom was carefully covered by sliding a square plate across. The tube with the plate was carefully taken out, the top levelled and the weights determined. Great caution had to be exercised to prevent possible compression of the soil into the tube.

QUALITATIVE OBSERVATIONS

The test tank was intended to permit observation of the soil movement through the glass side, but in practice only very small movements could be discerned by the naked eye during the experiments. At the conclusion of only five tests out of a total of twenty-eight, failure modes were seen. Attempts to study the soil movement using neutrally buoyant beads were unsuccessful as the beads were obscured by a coating of the fine soil. Placing coloured marks with a dye and soil of contrasting colour was also unsucceessful.

A smaller glass tank 24" by 8" by 8" was fabricated (Fig. 40) with a view to tow 2" wide models of different shapes in this tank. A 1/8 H.P. variable speed D.C. motor was used to push a carriage on guide tracks. Models of different shapes were supported from this carriage. One side of this tank was constructed completely of fused quartz glass sheets. Willemite which is a fluorescent material was

mixed with the soil in a powdered form (passing 200 sieve). The soil movement was clearly seen when viewed in ultra-voilet light through the quartz glass. However, photography with ultra-voilet - light was not successful inspite of trials with different types of filters. Without spending too much further time on trials in this direction, it was decided to introduce reference bands using a clay of contrasting colour. Series of photographs were taken of the entire experiment at an interval of one second between exposures. Failure surfaces were seen at the end of all the experiments except one out of a total of six.

Study of the soil movement using the fluorescent material is still a desirable technique deserving further exploration under a separate study.

EXPERIMENTAL PROCEDURE

The period allowed for the soil to settle was about 2 days, but the preparation such as tilting the tank, draining out water, mixing the soil and again letting in water took additional time and only two experiments per week could be performed, while the duration of the actual experiment was less than 30 seconds. Even a minor lapse resulted in a repetition of the entire series of operations and hence, an elaborate check list was verified before commencing each experiment.

The test tank was first tilted to the required slope (normally 1:10) and the water was drained till only 2" remained on top of the soil. Using steel rakes, the sample was thoroughly worked till it became a uniform slurry. This slurry was allowed

to settle for about 12 hours till the soil reached a previously marked level. Water from the laboratory faucet was then allowed to flow into the tank in a very fine spray till the water level reached about 12" above the sediment bed, enough to keep the entire slope submerged when the tank was righted. It was found by trial that a period of 24 hours had to elapse before the soil-water temperatures equalized to enable the transducer signal stability. This also allowed the sediment to gain in shear strength. At the end of this period, a cradle was lowered into the tank with the modified vane shear apparatus mounted on it. The cradle could be moved along the tank to different positions and shear strength was verified at different points along the path of the model berg. Soil and water temperatures were also checked at different points. The charge amplifiers were allowed to warm up for about 1/2 hour and the transducers were checked for stability. The tank was then righted to the horizontal position slowly, avoiding any collapse of slope due to wave action. The check list was verified and the experiment was run and the signals recorded on the tape recorder. Recorded signals were played back for analysis.

A description of the experiment types and the results are presented in the following chapter.

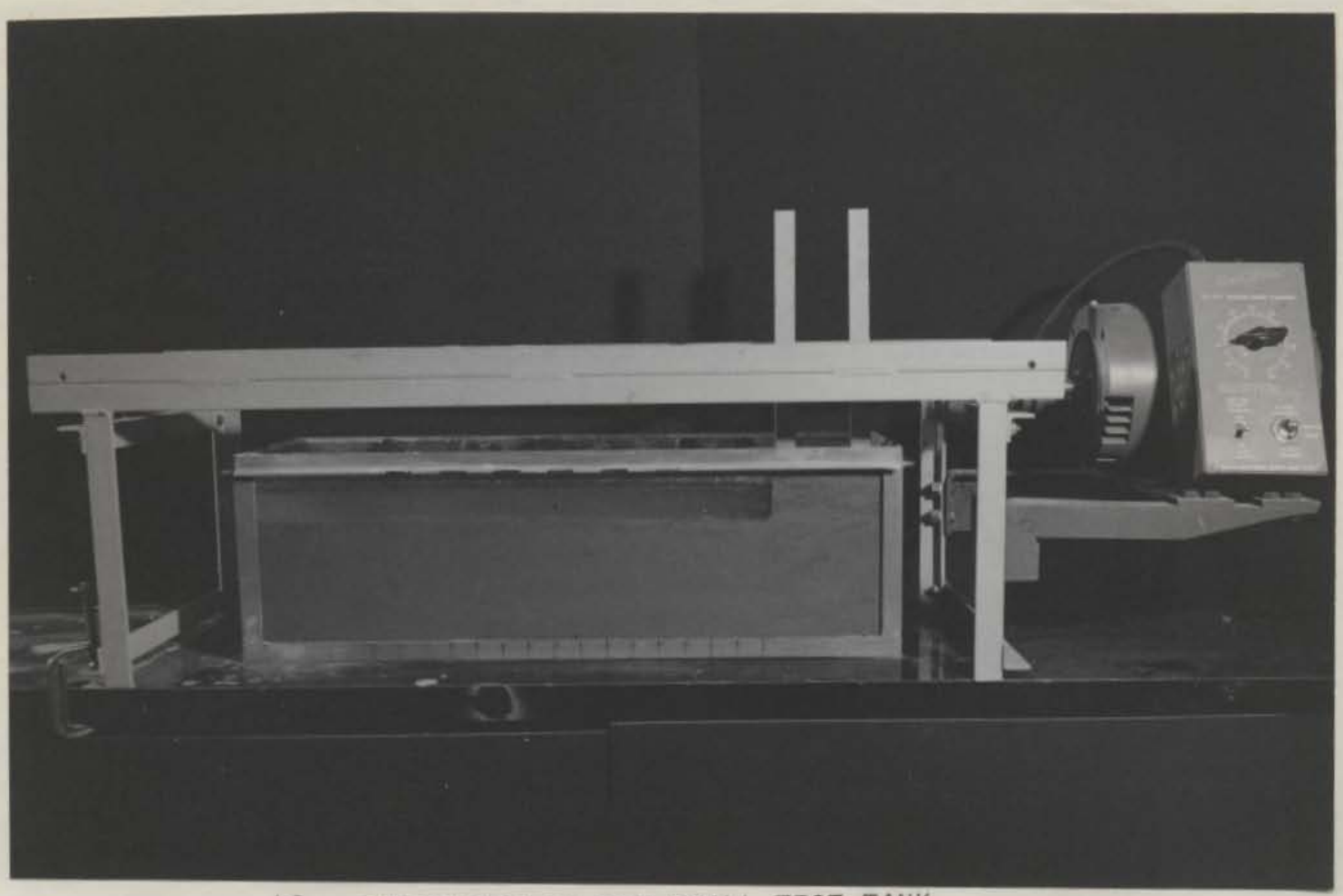

FIG. 40.- PHOTOGRAPH OF THE SMALL TEST TANK

The motor is on the far right. The carriage is hidden behind the guide rails

CHAPTER V

EXPERIMENTAL RESULTS

The experimental programme can be divided into three major areas.

1. Development of a method of preparing a uniform sediment bed with similar low strength characteristics for each experiment.

2. Quantitative tests carried out on a laboratory model similar to that used in the theoretical analysis and measurement of the total force required to push the model into the sediment and the soil pressures exerted on the model, and

3. Qualitative tests - observation of the type of soil failure and confirmation of the gouge track shape.

These observations were carried out in two tanks.

a) In the large tank as part of the quantitative tests

b) In a small tank where shapes and soil could be interchanged much more easily and where it was possible to devise techniques to study soil movement during the test.

PREPARATION OF SEDIMENT BED

Soil: The soil used in all the experiments of this investigation was modelling clay. The physical and classification properties of this soil are shown in Table VIII. The grain size distribution curve is shown in Fig. 41.

The settlement characteristic of the soil was observed

TABLE VIII

PHYSICAL AND CLASSIFICATION PROPERTIES OF THE SOIL SAMPLE

Colour	Brown
Liquid Limit	37.5%
Plastic Limit	19.48%
Plasticity Index	18.02
Clay content (less than 2 microns)	40%
Silt	46%
Sand	14%
Specific Gravity of Solids	2.798
Wet Density	108.35 lb/ft
Insitu moisture	33.49%
Void ratio	1.395
Clay minerals	Predominantly Illite and Chlorite Traces of Quartz, Feldspar and Kaolinite

during the consolidation of the slurry and a settlement curve as shown in Fig. 42 was drawn. The consolidation was 88% after 48 hours, and it took nearly 7 days for the settlement curve to become asymptotic.

Strength Tests: A summary of the shear tests with the modified vane shear apparatus is shown in Fig. 43. These results cover the tests conducted during the entire investigation, including those done during the trial runs and show the range of variability of the soil

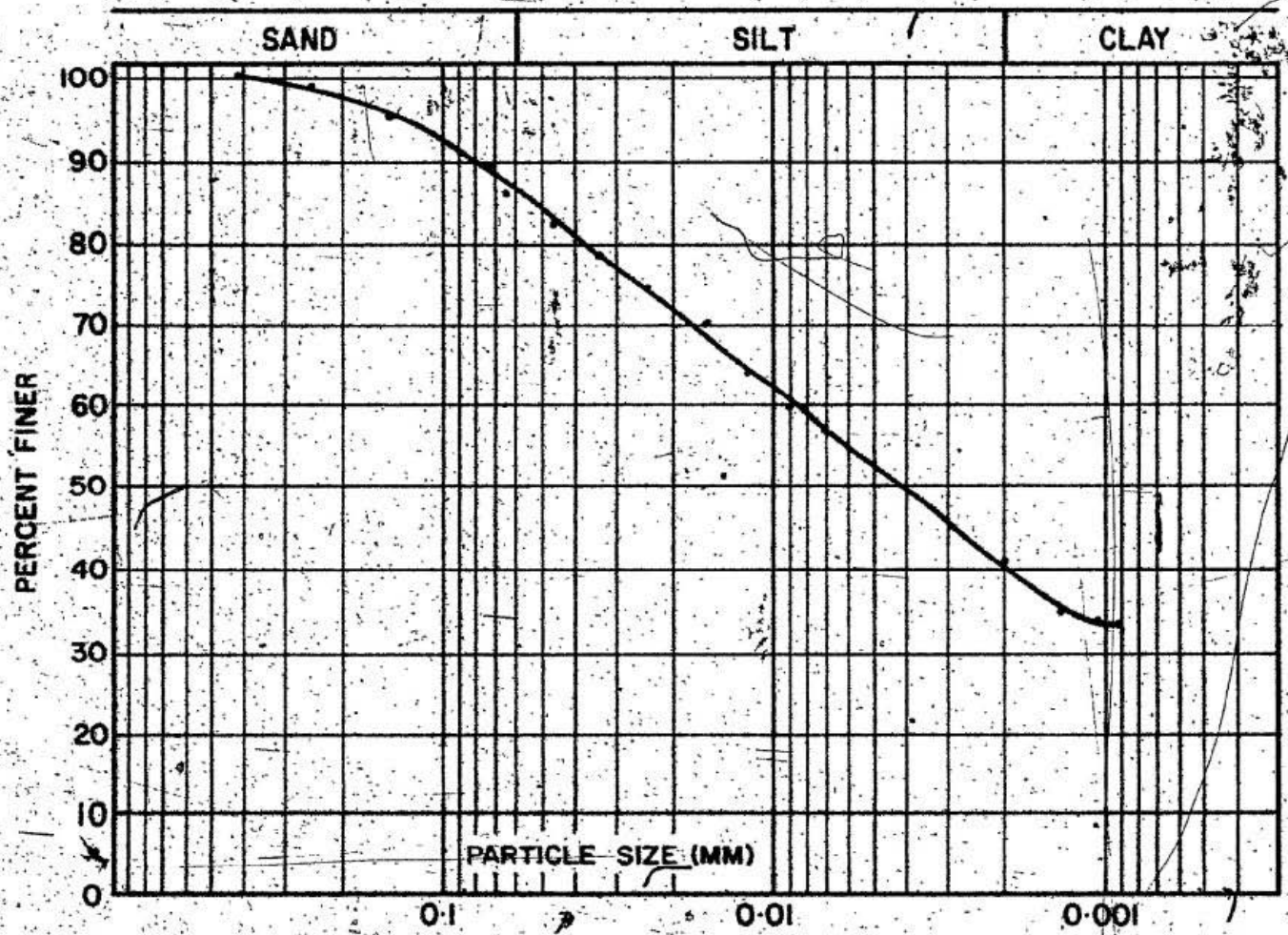

FIG. 41.- GRAIN SOIL DISTRIBUTION CURVE OF THE SOIL SAMPLE

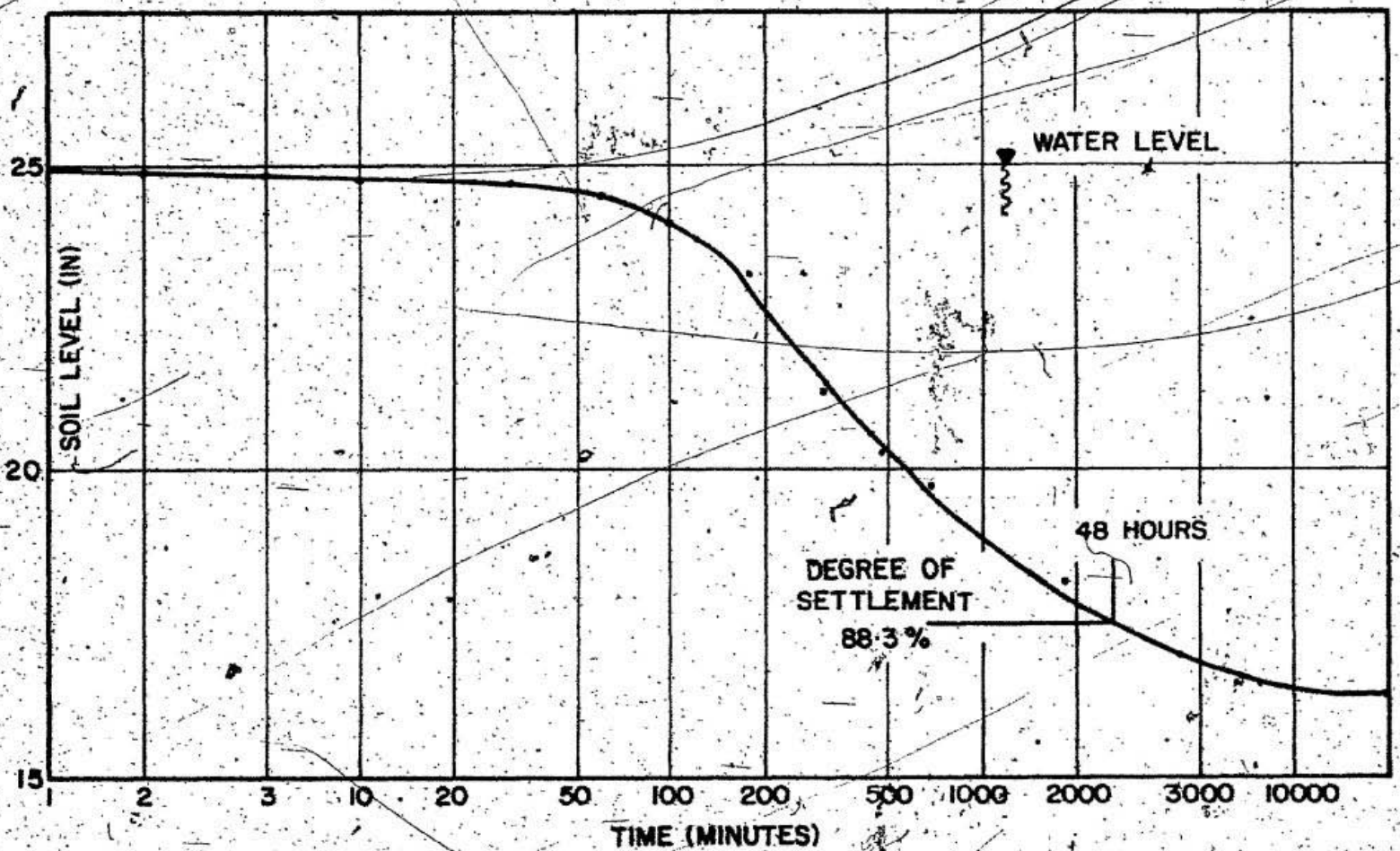

FIG. 42.- VARIATION OF SEDIMENT LEVEL WHILE SETTLING
Time is reckoned from the instant the slurry starts to settle after the stirring is stopped

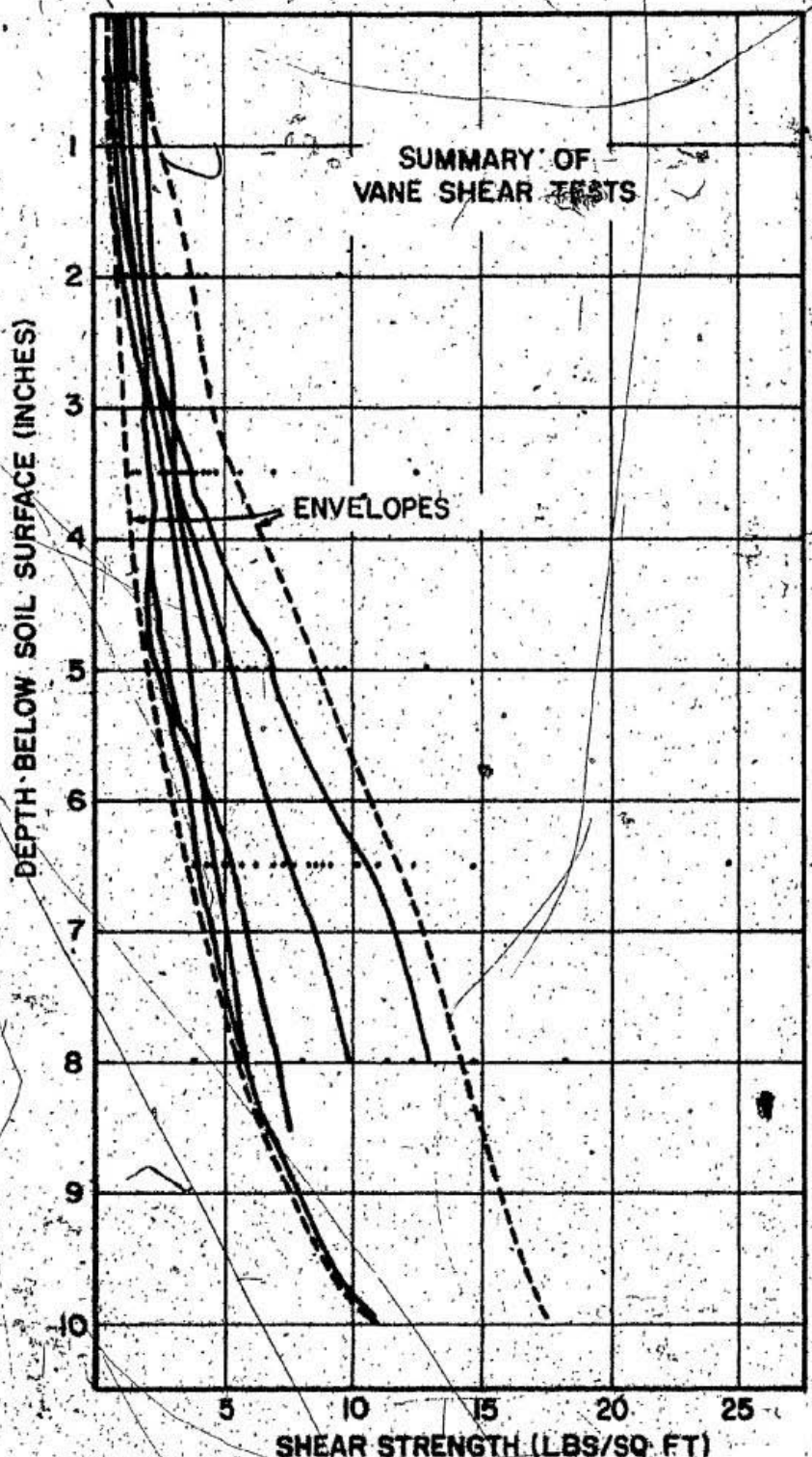

FIG. 43.- SUMMARY OF VANE SHEAR TESTS

strength. The profiles falling within the envelope are realistic of such sedimented deposits and similar to those obtained by Doyle[30]. Individual profiles were used to find the average shear strength in the computation (Fig. 44).

QUANTITATIVE TESTS

Plexiglas models made out of ½" thick sheets were used in all the tests to approximate to the low coefficient of friction between iceberg and soil. The rigidity of this model relative to the soil pressure was of primary concern. To check this, a strain gauge was mounted on the front face of the model and it was towed into a 1:10 soil slope. The strain at the end of the experiment was measured as 12 micro inches/inch when the model was subjected to a maximum thrust. This represents a negligible deflection of 108 micro inches at the centre of the front face of the model, confirming it to be rigid compared to the soil.

The regular quantitative tests were three types. In the first series, the model was towed through a level sediment deposit and the pressure on the front and the total pull were recorded. A set of raw data as obtained from the plotter is shown in Fig. 45. This experiment was to verify the behaviour of the soil of very low strength in reference to experiments with blades in subaerial soils reported in the literature. The results obtained were similar to those obtained for blades by Nelson[57] and Siemens[67].

In the second type of experiments, the model was towed into a slope of 1:10 at six different model speeds. The variable speed motor

was set at 0.5, 1.0, 1.5, 2.0, 2.5 and 3.0 settings. The corresponding speeds were read from the calibration chart of the motor. The different motor settings of the motor were chosen as reference from consideration of easy repeatability of the settings. The lowest and highest carriage speed were respectively, 0.38 and 1.16 ft/sec. The pressures on the front face and the total pull on the model were recorded. Typical raw data for this experiment are shown in Fig. 46. The pressure transducer was at a height of 1 1/8 inch from the bottom. If the soil slope is drawn to scale the position of the model at any instant can be located (Fig. 47) and the variation of the pressure on the front face can be represented as shown. The measured pulls on the model for the different speeds compiled from the recorded data are shown in Fig. 48.

In the same series of experiments at a motor setting of 3, pressures on the side of the model and front face were compared to determine their relative magnitudes (Fig. 49) by conducting a test in which one transducer was placed on the front and the others on the side. Similar comparison was made of the pressure on the bottom of the model and results were obtained as in Fig. 50. A change in the slope of the soil to 1:20 showed the gouging process to be similar except that the gouge depth and the corresponding resistance to the model were less. It was, therefore, concluded that the effect of the variation of the slope need not be examined in further detail.

Pressure transducers were mounted on a frame, which was fixed to the base of the tank inside the soil at a level below the expected scour depth, to understand qualitatively the pressures outside the model when it was pulled into the slope.

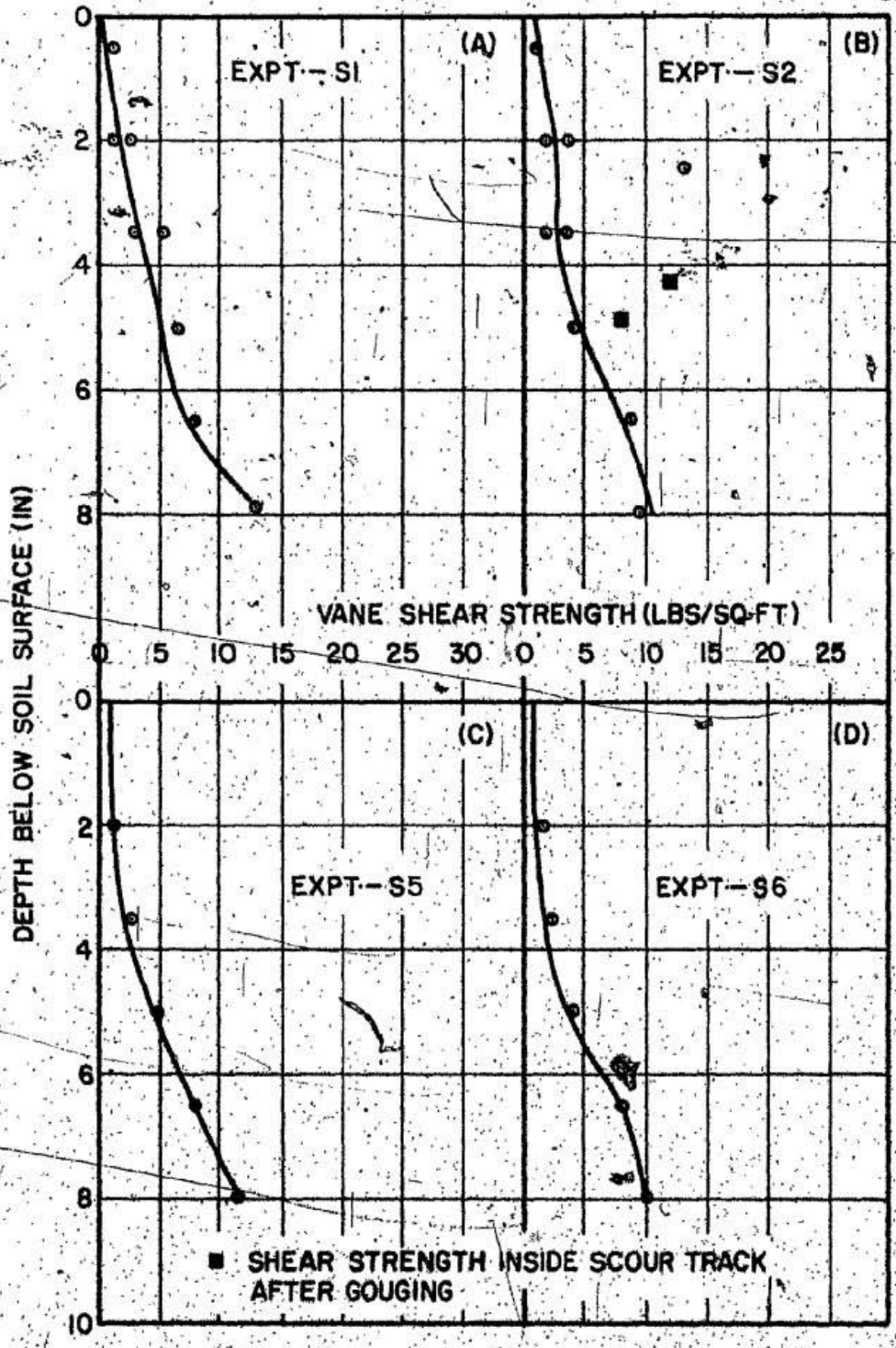

FIG. 44.- INDIVIDUAL SHEAR STRENGTH PROFILES

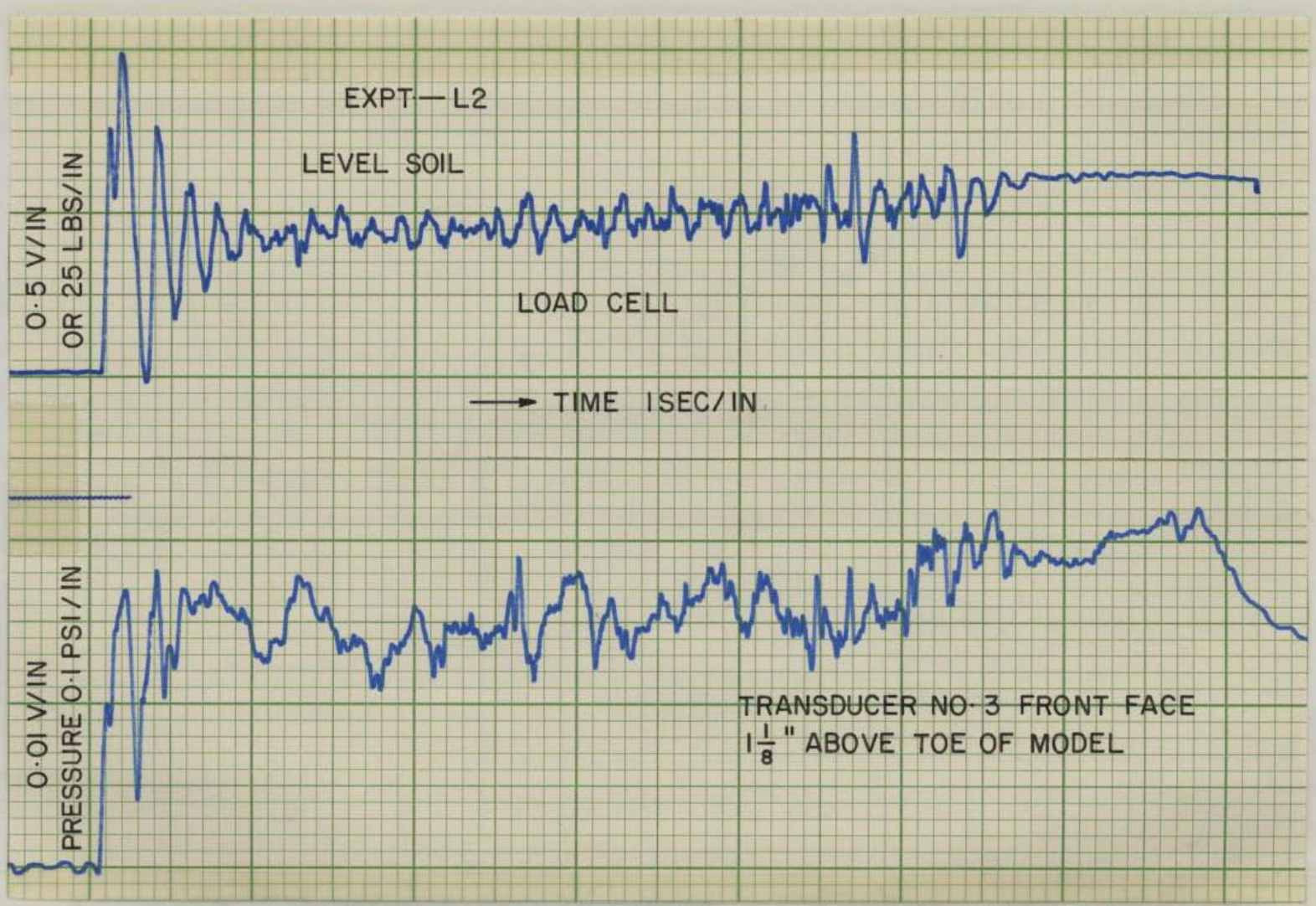

FIG. 45.- RAW DATA OF TOTAL PULL AND PRESSURE FROM THE EXPERIMENT IN A LEVEL SOIL SURFACE

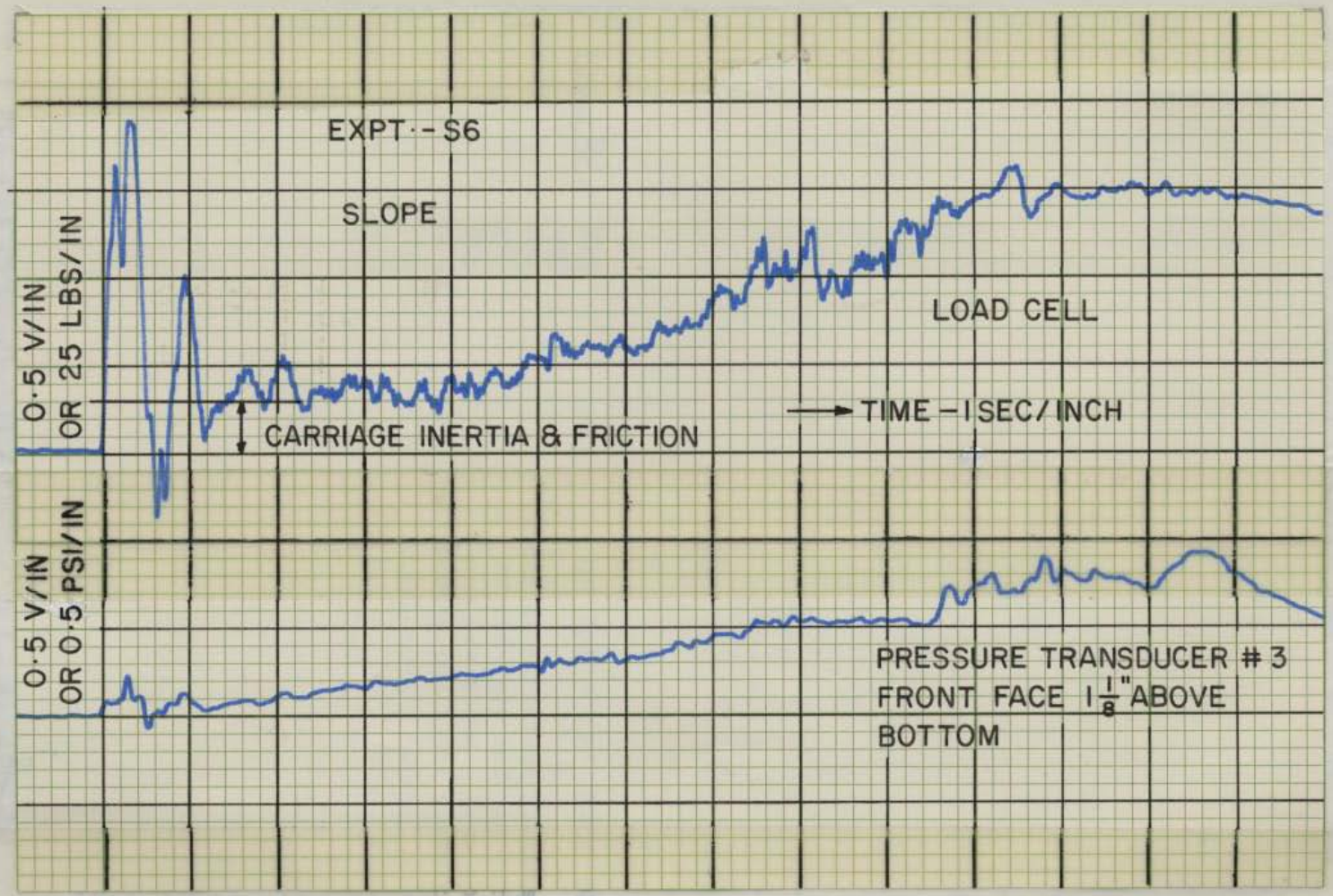

FIG. 46.-TYPICAL RAW DATA OF THE TOTAL FORCE AND PRESSURE FROM A TEST IN A SLOPE

(TO FACE PAGE 108)

FIG. 47.- PRESSURE VARIATION ON THE FRONT FACE OF THE MODEL
The location of the model at different instants of time after the commencement of the test and the corresponding pressure distributions are shown. Note the effect of surcharge as indicated by the point where the pressure is zero

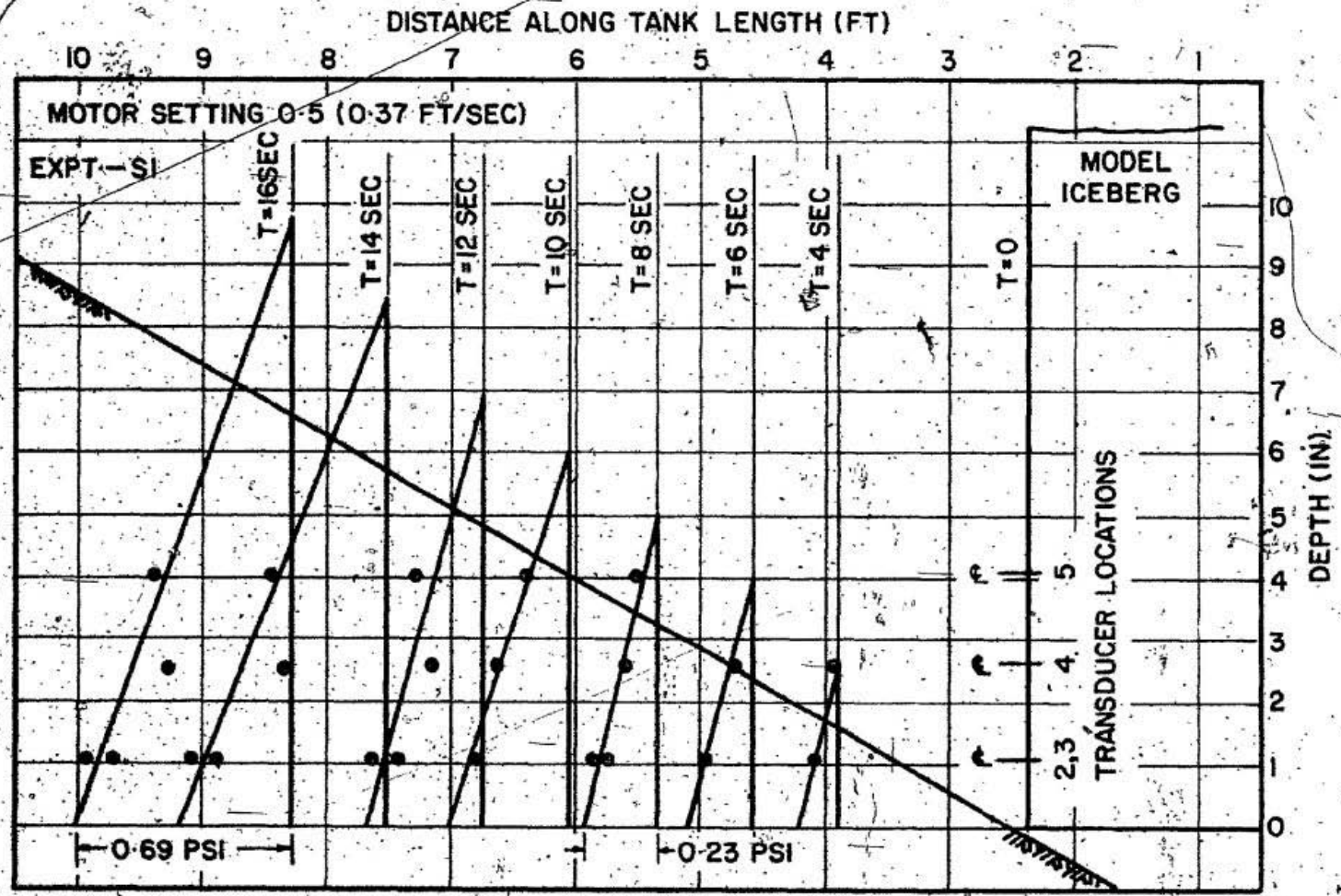
DISTANCE ALONG TANK LENGTH (FT)
10
9
8
7
6
5
4
3
2
1
MOTOR SETTING 0·5 (0·37 FT/SEC)
EXPT—SI
T=16SEC
T=14 SEC
T=12 SEC
T=10 SEC
T=8 SEC
T=6 SEC
T=4 SEC
T=0
MODEL ICEBERG
TRANSDUCER LOCATIONS
2,3
4
5
DEPTH (IN.)
0·69 PSI
0·23 PSI

FIG. 47

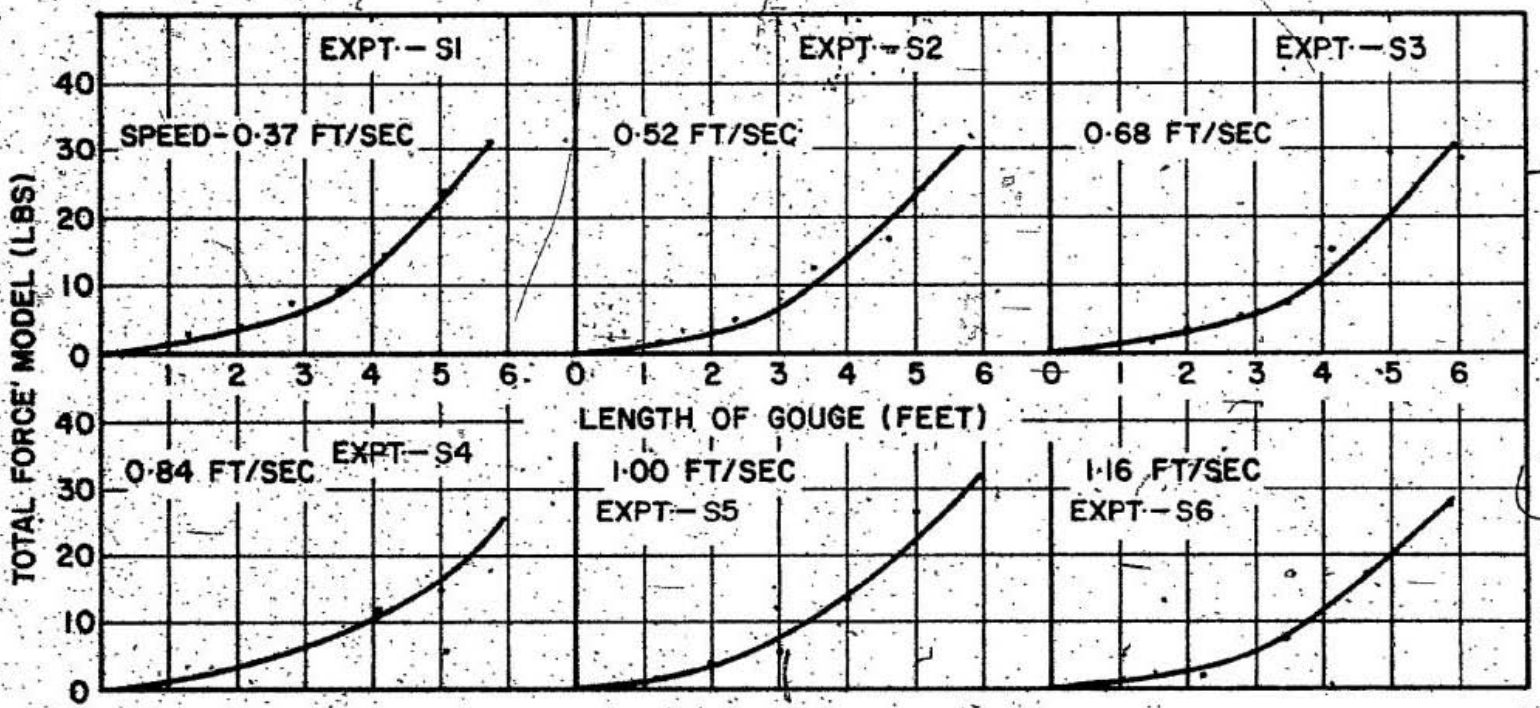

FIG. 48.- VARIATION OF THE TOTAL PULL ON THE MODEL AT SIX DIFFERENT SPEEDS

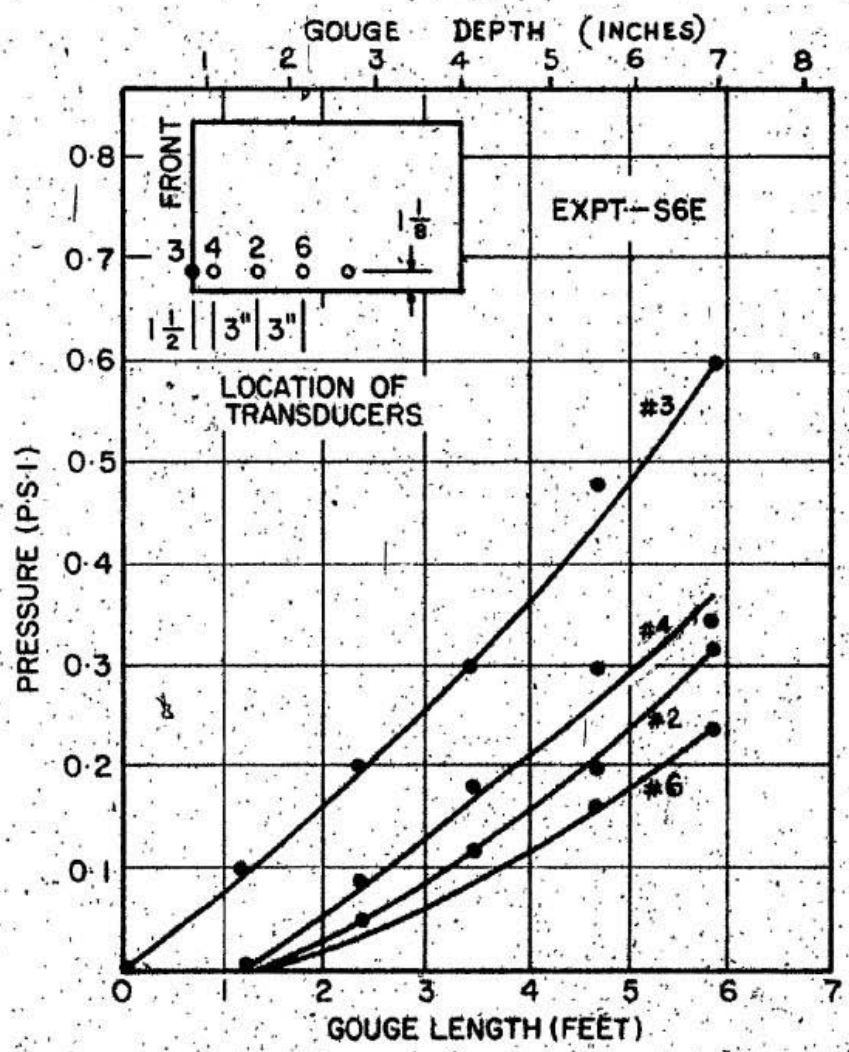

FIG. 49.- COMPARISON OF THE PRESSURES ON THE SIDES AND FRONT OF THE MODEL

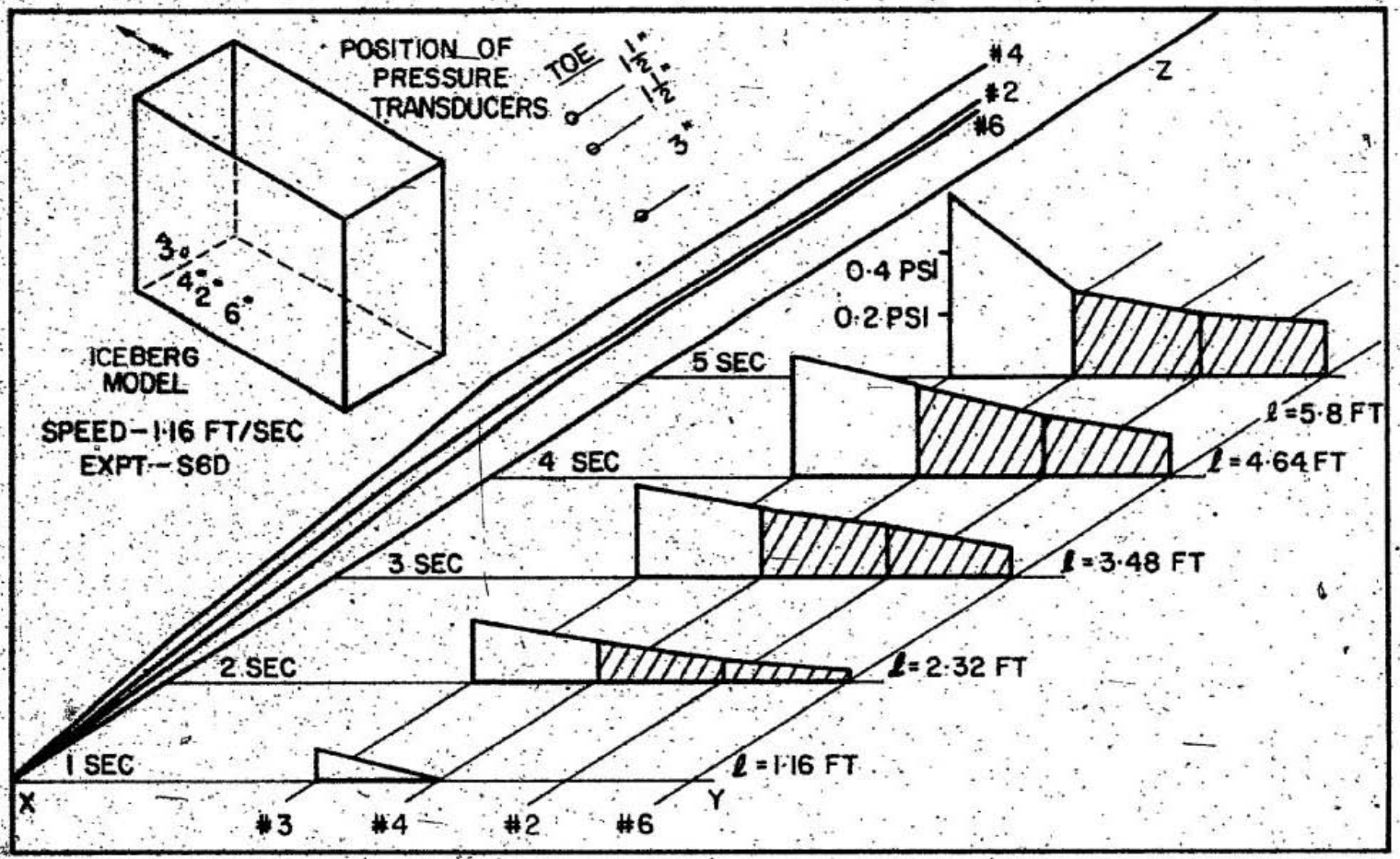

FIG. 50.- COMPARISON OF THE PRESSURES ON THE BASE AND FRONT OF THE MODEL

(TO FACE PAGE 113)

FIG. 51.- RESULTS OF THE EXPERIMENT WITH PRESSURE TRANSDUCERS INSIDE THE SOIL

This figure shows the influence lines of the pressures at A and B when the model moves along the tank

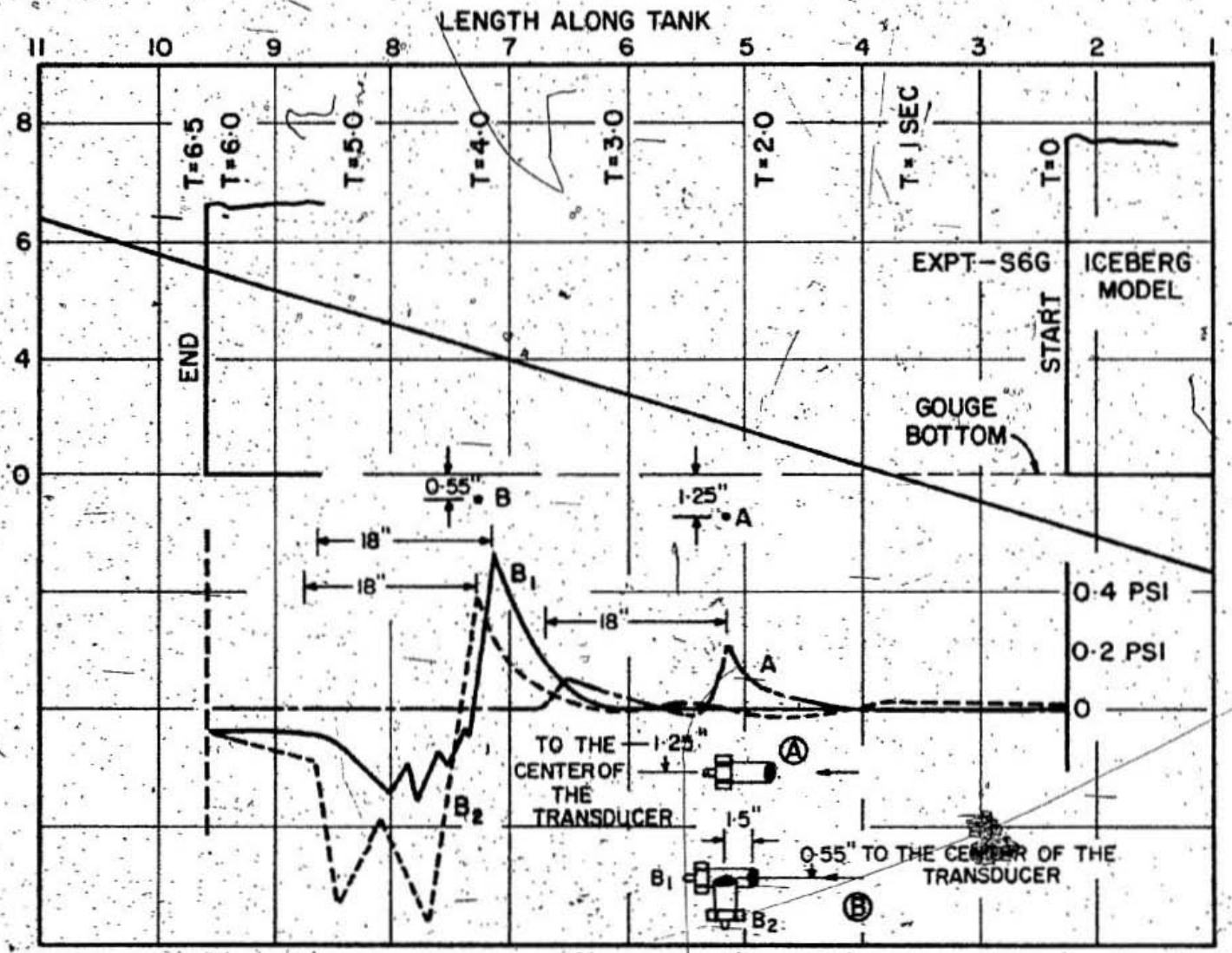
LENGTH ALONG TANK
11
10
9
8
7
6
5
4
3
2
1
8
6
4
0
T=6·5
T=6·0
T=5·0
T=4·0
T=3·0
T=2·0
T=1 SEC
T=0
END
START
EXPT—S6G
ICEBERG MODEL
GOUGE
BOTTOM
0·55"
B
1·25"
A
18"
18"
18"
B1
B2
A
0·4 PSI
0·2 PSI
0
TO THE CENTER OF THE TRANSDUCER
1·25"
1·5"
0·55" TO THE CENTER OF THE TRANSDUCER
B1
B2
Ⓐ
Ⓑ

One set of results obtained from these tests is shown in Fig. 51. The pressure inside the soil gradually increased as the model came closer to the location of the transducers, reached a maximum when the toe of the model was just above the transducer and then dropped suddenly as soon as the toe crossed. When the model moved away from the transducer location, the pressure increased again. This type of tests was limited to a total of only three, though it would have been desirable to repeat them. In the trials of these experiments two transducers placed inside the soil did not function due to the entry of moisture at the cable junction. There was a further possibility that the leads connecting the transducers and the amplifiers would foul the moving model and drown the amplifiers. After weighing the constraint of time and the cost of the equipment it was felt prudent to limit this type of experiment. In another experiment of this type, a pressure transducer was placed in the soil at a distance of 7.8 feet in front of the model, facing it just above the level of the bottom edge. This transducer sensed an increase in pressure when the model was still 5 feet away. The pressure gradually increased to a maximum of 0.25 p.s.i. when the model finally stopped at a distance of 0.34 feet in front of the transducer.

QUALITATIVE OBSERVATIONS

Main Tank: At the end of each experiment in the main tank, the soil in front of the model was observed closely to find the failure pattern in the soil . Out of a total of 28 experiments, the failure

pattern in the soil was noticed only in five (Figs. 52-56). These were in the form of a very fine and short lines and a failure surface which could be imagined to be a continuation of these lines appeared to start at angles between 25° and 29° with the horizontal at the toe and meet the sediment/water interface at 43° to 45°. After completion of the observations in front of the model, the tank was tilted, the water was drained and the soil surface was profiled by measuring the depths of the soil surface from the top of the tank. A computer plot of the contours and the cross section profiles are shown in Figs. 57 to 60. The surcharged soil in front of the model was fan shaped as shown in Fig. 61 and 62. There was flow of slurry not only into the scour track but to the side of the tank and this side wall effect can be noticed in Fig. 60.

Small Tank: Experiments in the small tank were for the purpose of understanding the soil movement in front and below the model. The soil in these tests was level. In the first set of experiments, models of five shapes were tested with vertical coloured bands in the soil and the experiment was photographed at 1 second intervals. These experiments clearly showed a movement in the soil far ahead of the model, but the vertical movement of the soil near the model could not be clearly seen. In the second type of experiment, horizontal lines were laid. Preparing this required great care. Slurries of two different colours were poured through a funnel taking care not to disturb the layer below while laying the one above. The position of the model in this type of test at the commencement, middle and end of the experiment are shown

in Figs. 63 to 65 for clay and in Figs. 66 to 68 for sand. Preparation of the sand sample which contained 94% sand size (0.06 to 2.0 mm) particles with an effective size of 0.13 mm and uniformity coefficient of 3.85, was relatively easy and was laid dry. The entire sequence of photographs were analyzed by laying on them an overlay of the first position of the model and drawing the planes along which shearing of the soil appeared to occur (Figs. 69,70). In addition to the compression of the soil in front, the experiment with the clay soil showed that there was a compression of the soil below the toe of the model as seen from the last coloured band.

In the experiments conducted on four other shapes (Fig. 71) failure patterns were noticed at the end of three experiments and these are shown in Figs. 72 to 74.

An analysis of these results and discussion follow in the next chapter.

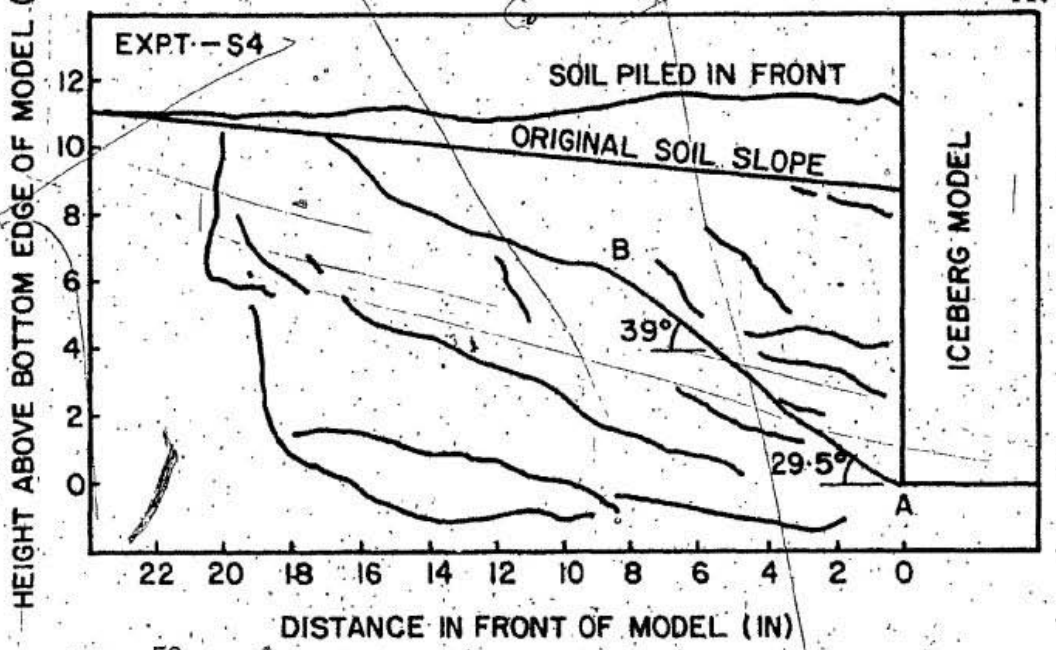

FIG. 52.- OBSERVED PATTERN OF SOIL FAILURE - IDEALIZED SHAPE - TEST S4
The lines observed were very faint. The continuous line AB was drawn by noting a slight difference in the colour of the sediment above and below the line

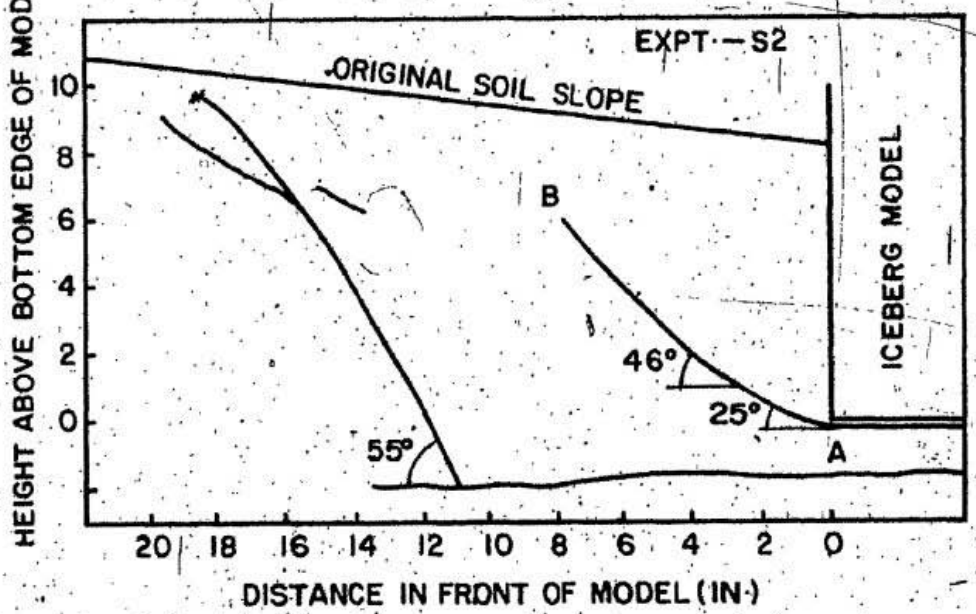

FIG. 53.- OBSERVED PATTERN OF SOIL FAILURE - IDEALIZED SHAPE - TEST S2

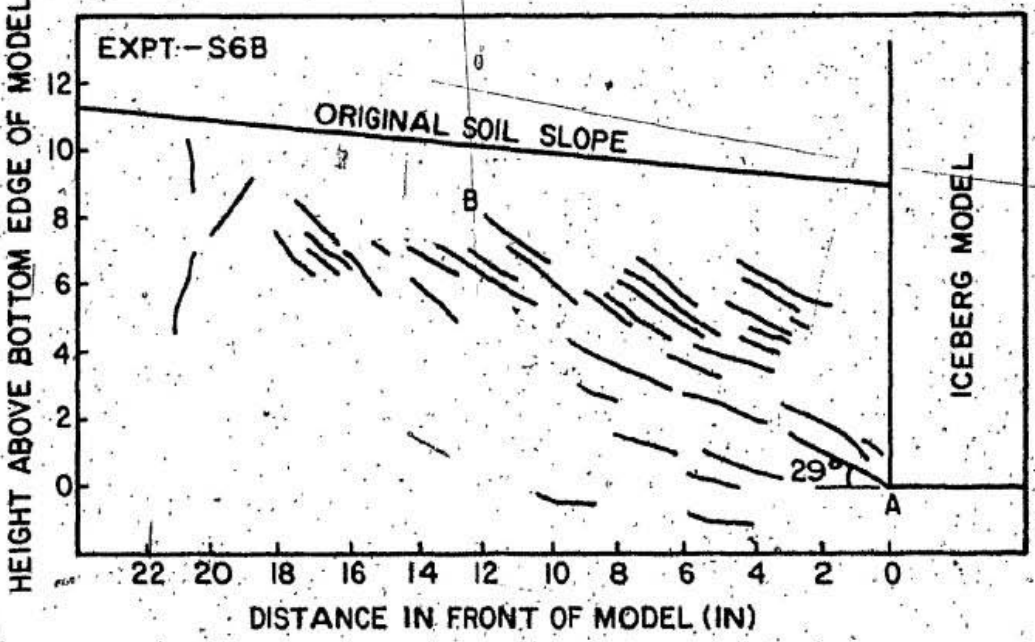

FIG. 54.- OBSERVED PATTERN OF SOIL FAILURE - IDEALIZED SHAPE - TEST S6B

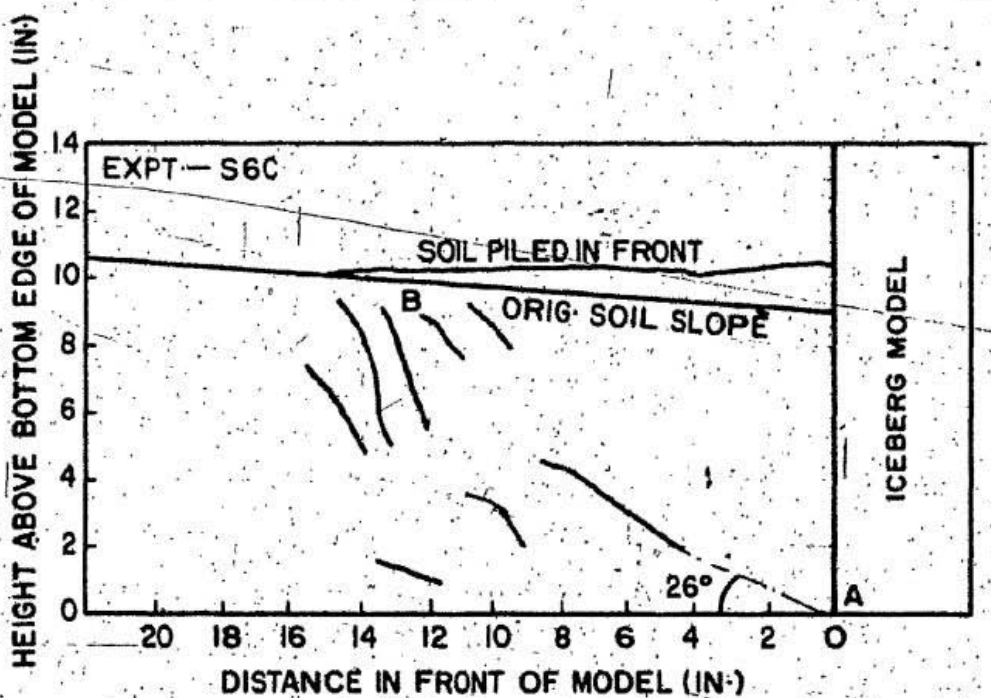

FIG. 55.- OBSERVED PATTERN OF SOIL FAILURE - IDEALIZED SHAPE - TEST S6C

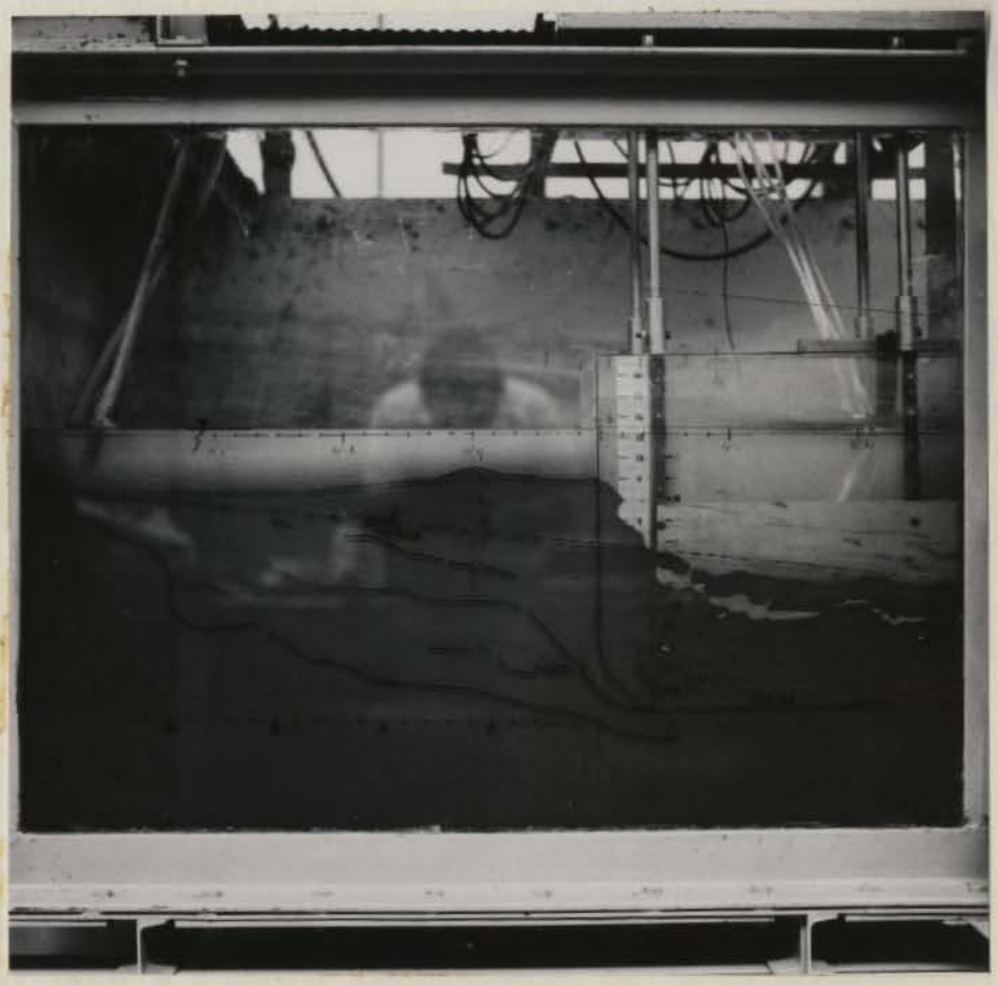

FIG. 56.- OBSERVED PATTERN OF SOIL FAILURE IN FRONT OF MODEL M2

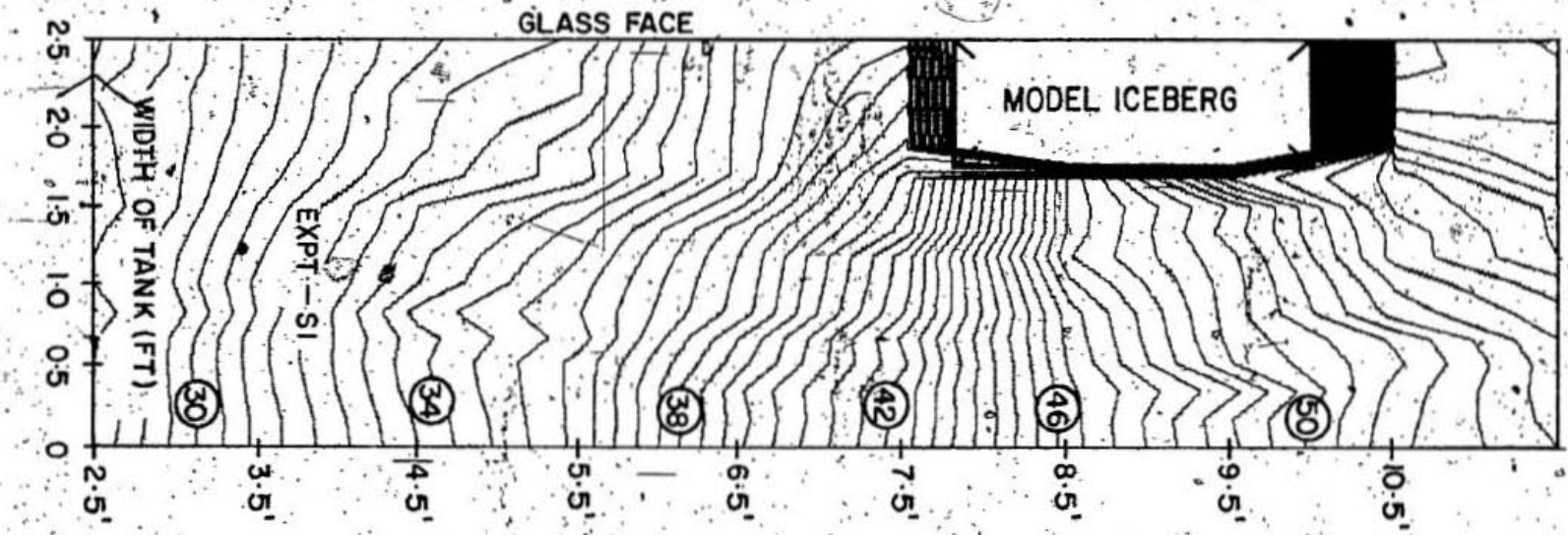

FIG. 57.- CONTOUR OF THE SEDIMENT SURFACE AFTER THE EXPERIMENT

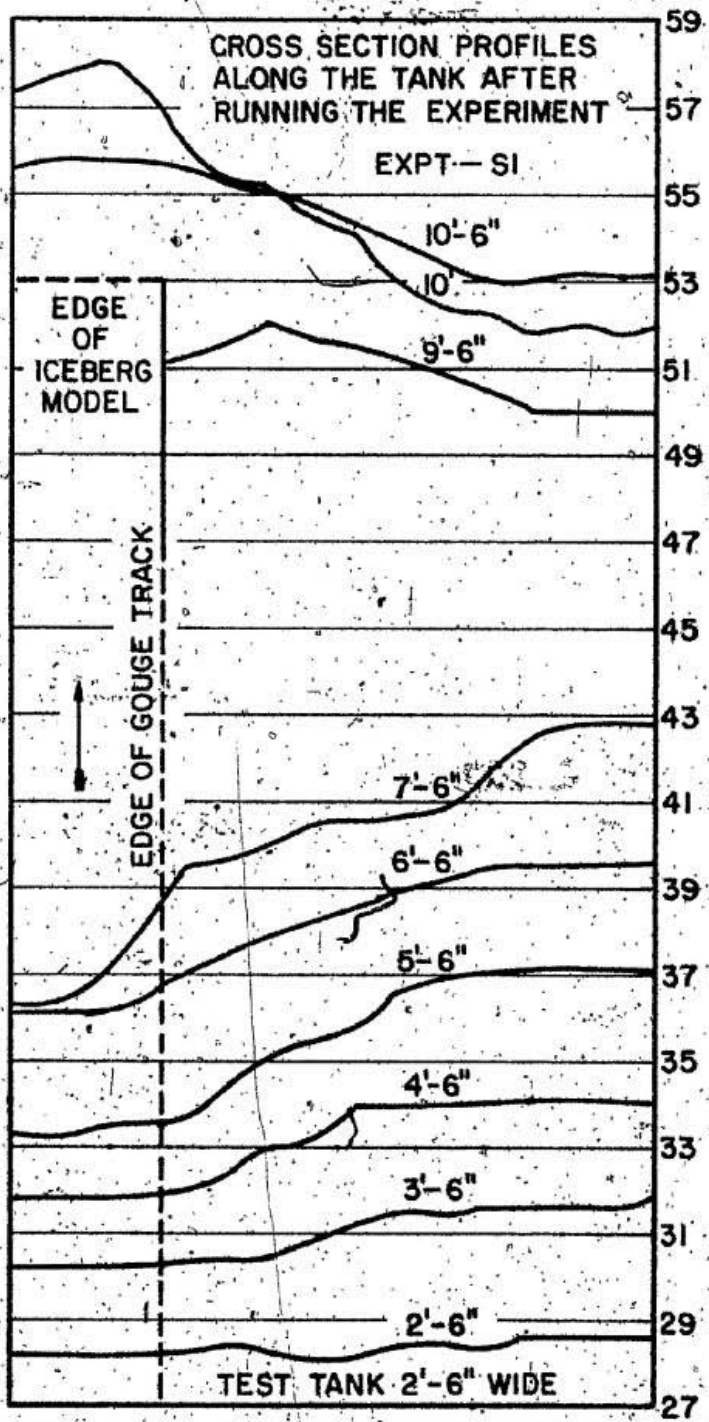

FIG. 58.- CROSS PROFILES AFTER SCOURING - EXPERIMENT S1

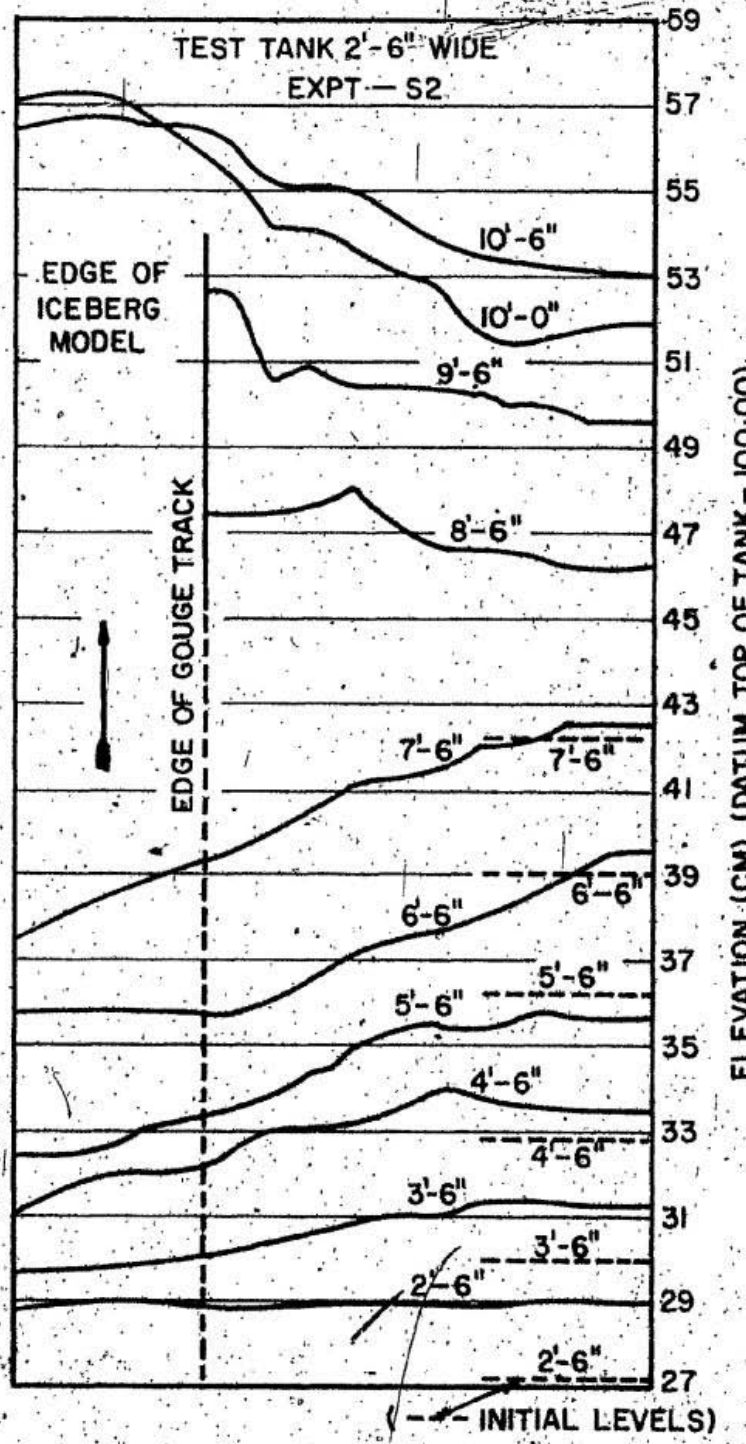

FIG. 59.- CROSS PROFILES AFTER SCOURING - EXPERIMENT S2

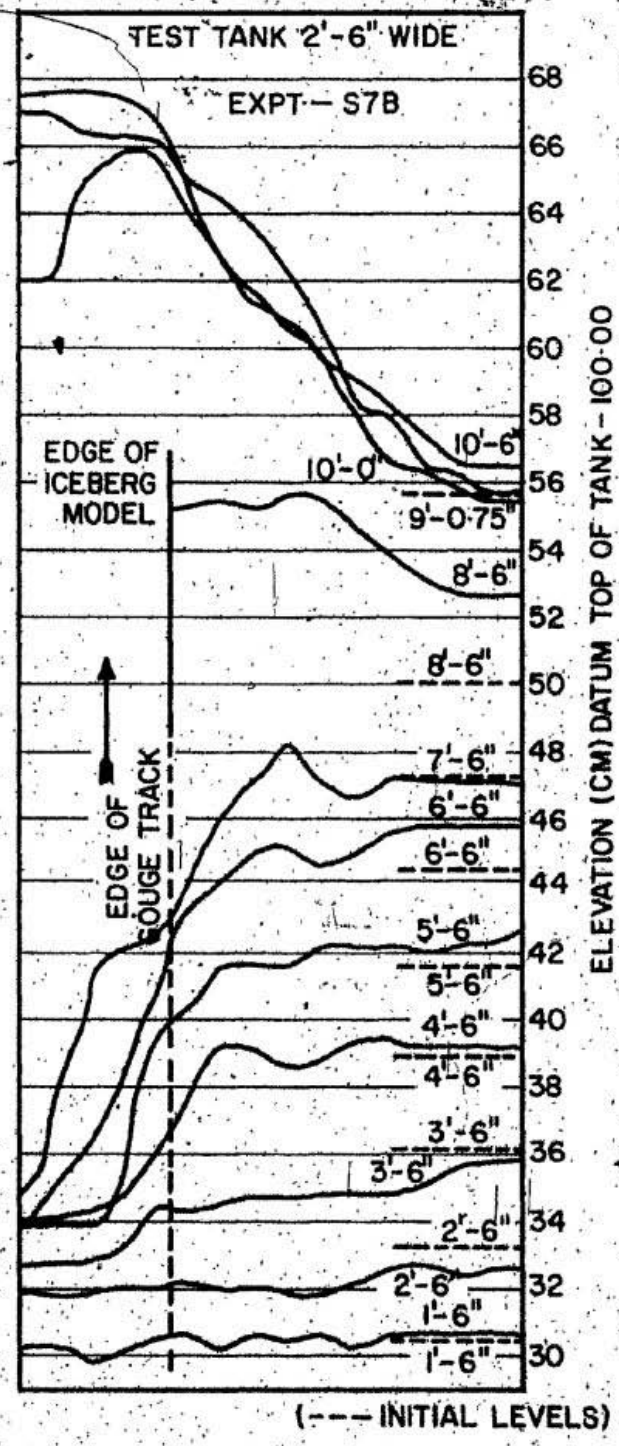

FIG. 60.- CROSS PROFILES AFTER SCOURING - EXPERIMENT S7B

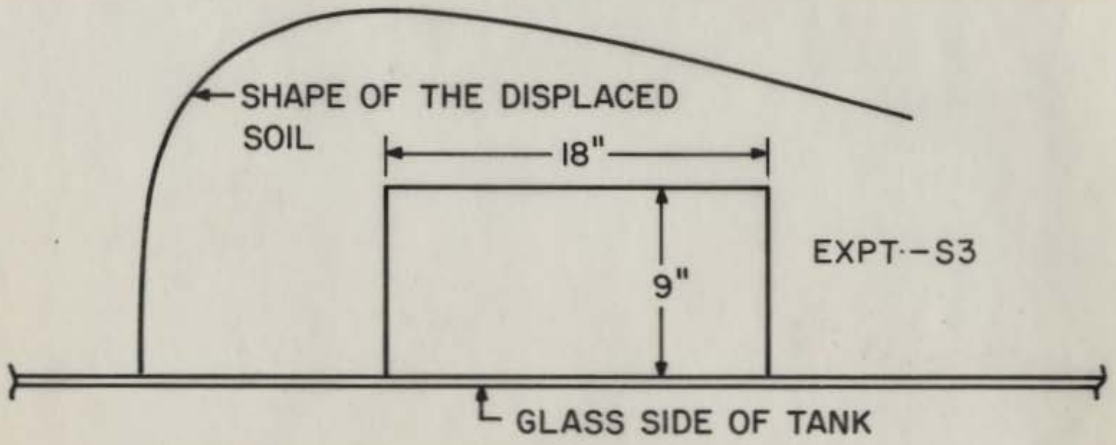

FIG. 61.- PLAN VIEW OF THE SHAPE OF SOIL FLOW

FIG. 62.- PHOTOGRAPH OF THE SOIL FLOW AROUND A LABORATORY GOUGE TRACK

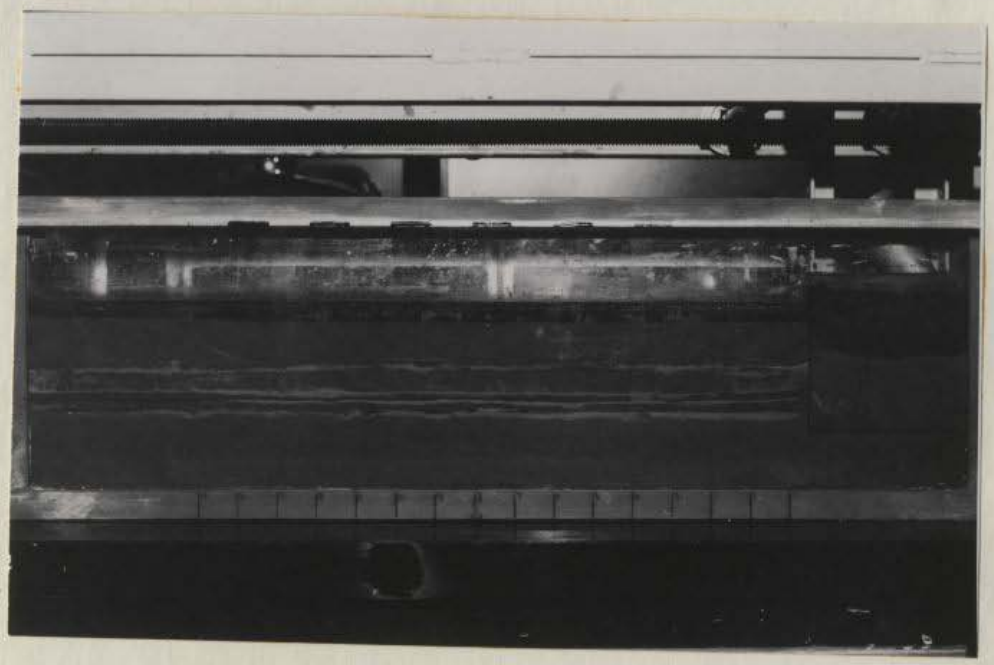

FIG. 63.- PHOTOGRAPH OF THE SMALL MODEL AT THE START OF THE TEST IN CLAY
Note the position of the coloured line nearest the toe

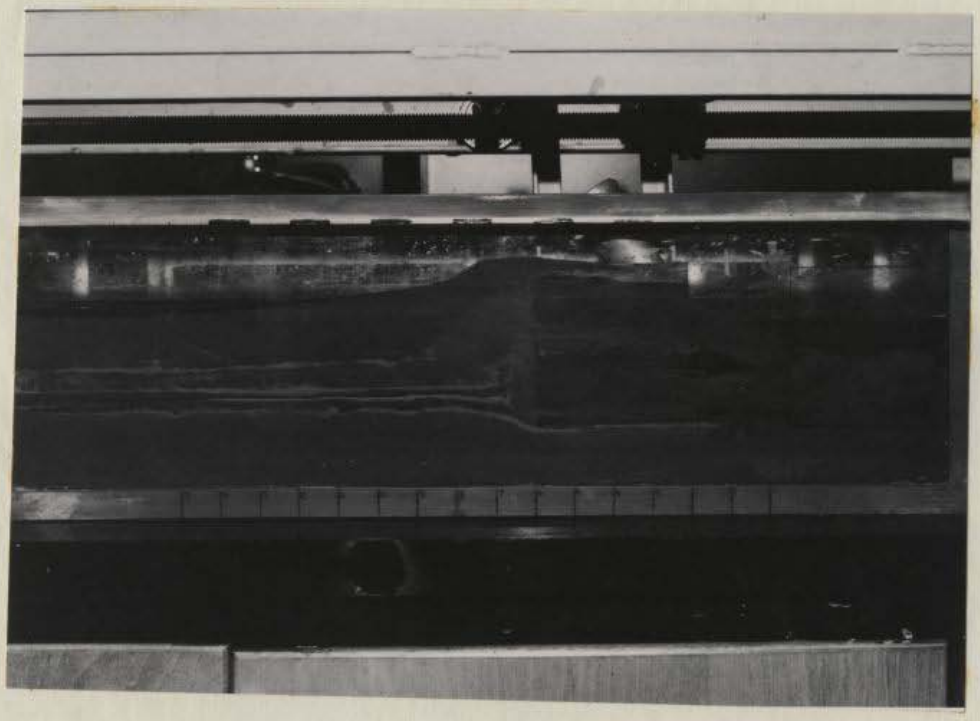

FIG. 64.- PHOTOGRAPH OF THE SMALL MODEL DURING THE TEST IN CLAY
Note the compression of the soil as seen by the lowering of the last coloured line

FIG. 65.- PHOTOGRAPH OF THE SMALL MODEL AT THE END OF THE TEST IN CLAY

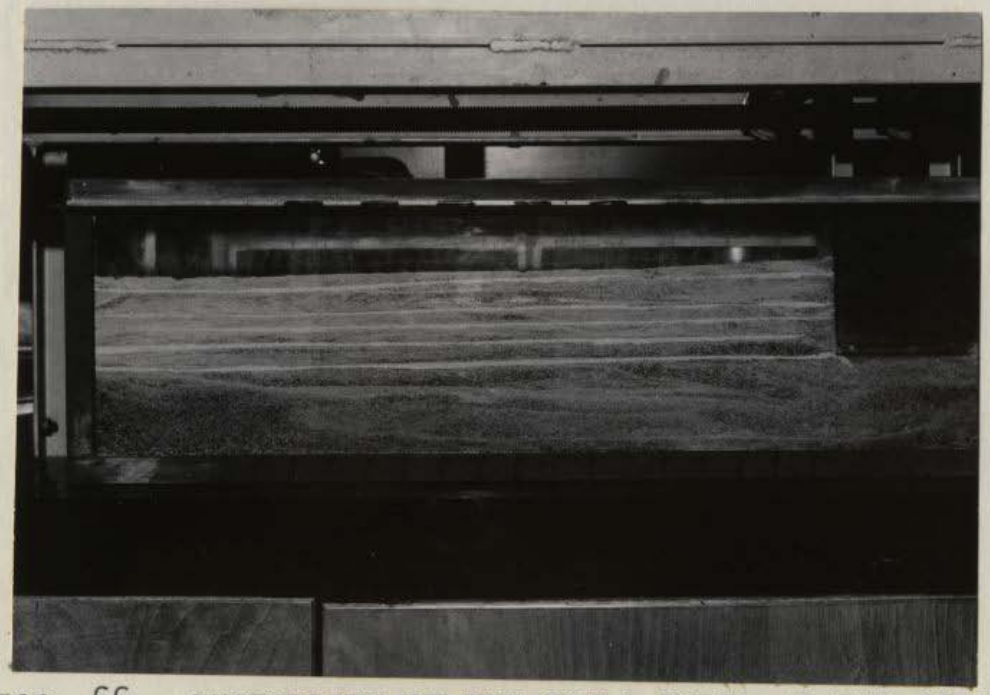

FIG. 66.- PHOTOGRAPH OF THE SMALL MODEL AT THE START OF THE TEST IN SAND

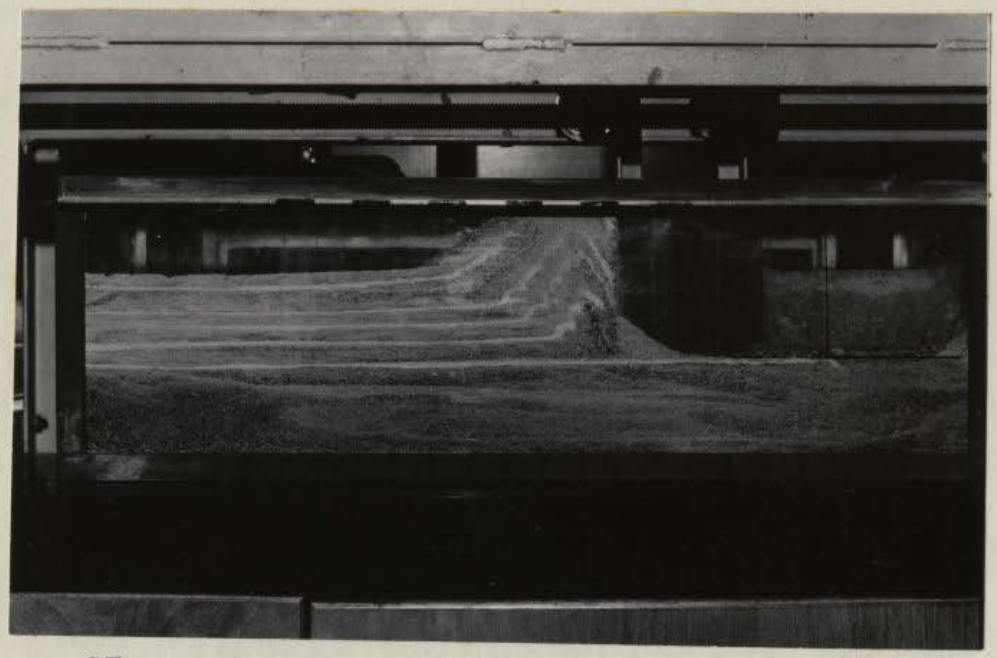

FIG. 67.- PHOTOGRAPH OF THE SMALL MODEL DURING THE TEST IN SAND

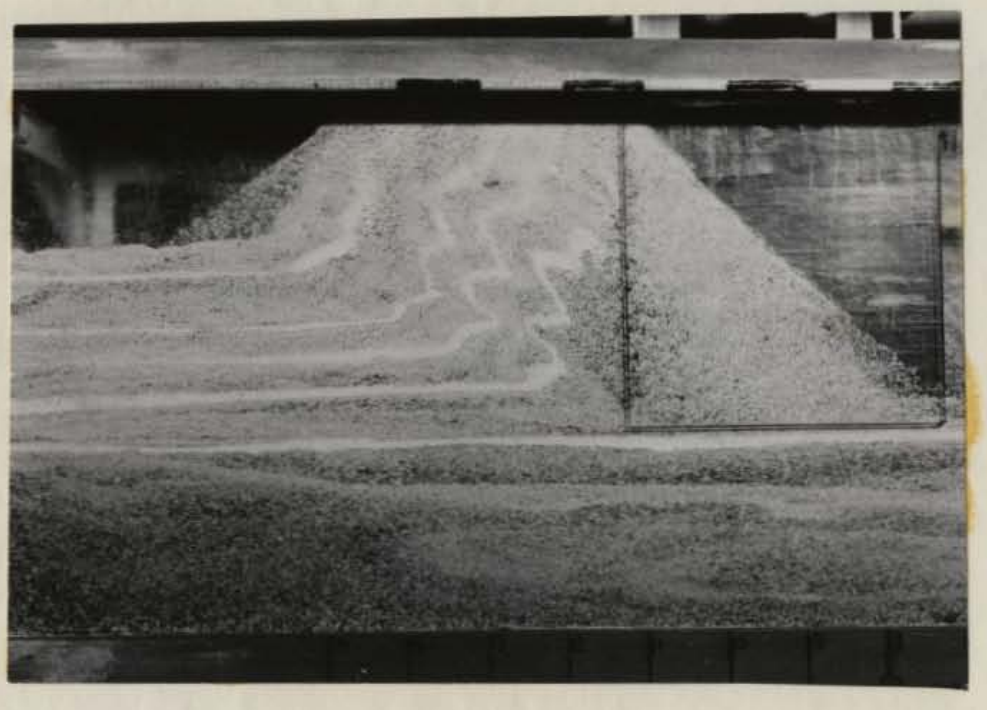

FIG. 68.- PHOTOGRAPH OF THE SMALL MODEL AT THE END OF THE TEST IN SAND

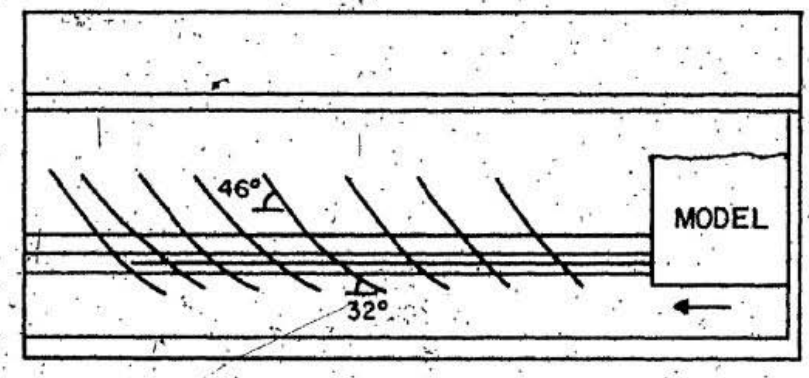

OVERLAY-CLAY SAMPLE

FIG. 69.- ANALYSIS OF THE SMALL MODEL TEST IN CLAY

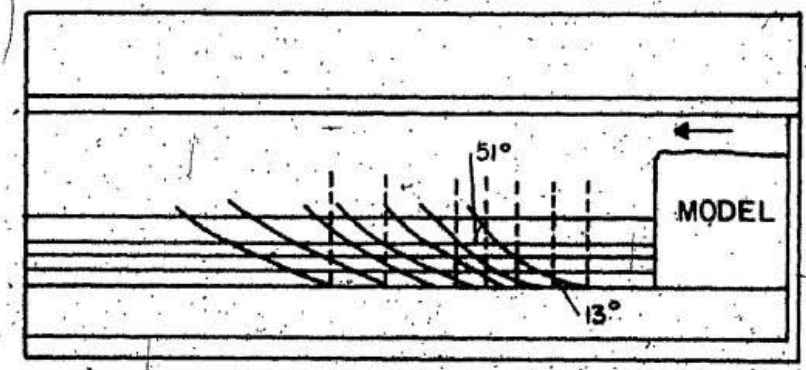

OVERLAY-SAND SAMPLE

FIG. 70.- ANALYSIS OF THE SMALL MODEL TEST IN SAND

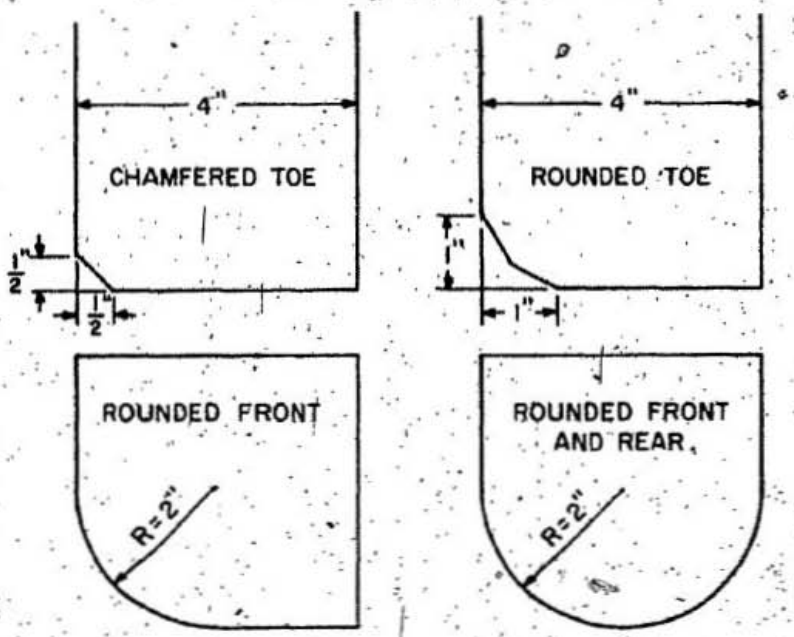

FIG. 71.- SIDE ELEVATION OF THE 2" WIDE NON-PRISMATIC MODELS

FIG. 72.- PHOTOGRAPHS SHOWING THE SOIL FAILURE IN FRONT OF THE 2" WIDE MODEL WITH CHAMFERED TOE

FIG. 73.- PHOTOGRAPH SHOWING THE SOIL FAILURE IN FRONT OF THE 2" WIDE MODEL WITH ROUNDED TOE

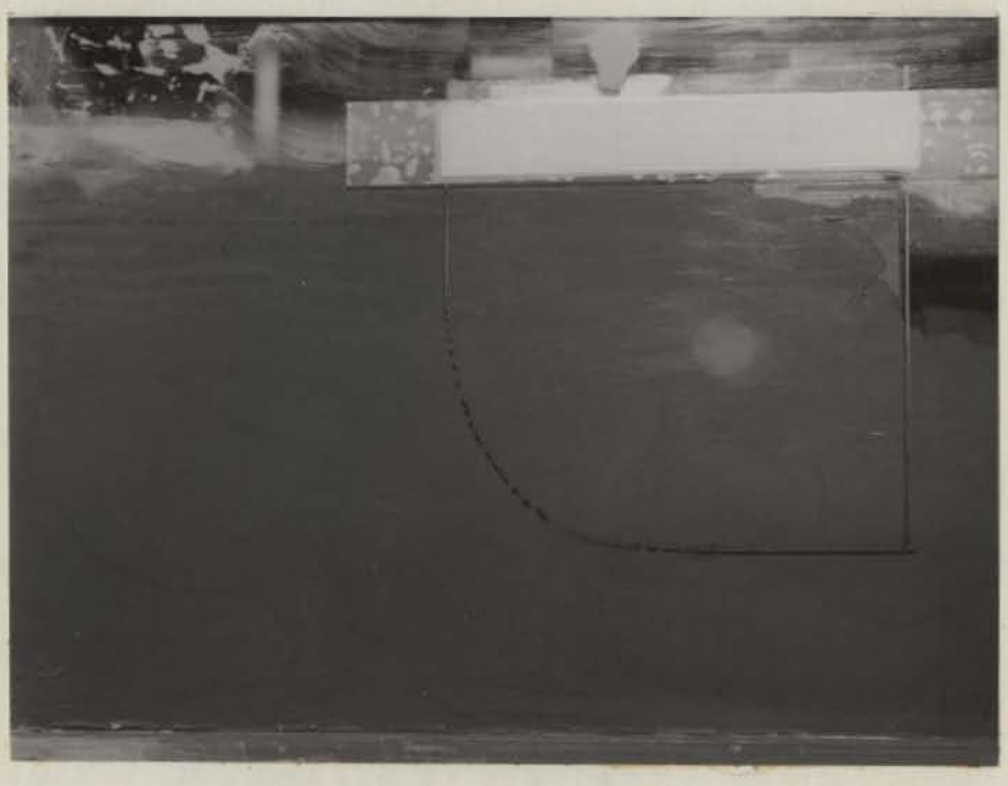

FIG. 74.- PHOTOGRAPH SHOWING THE SOIL FAILURE IN FRONT OF THE MODEL WITH A ROUNDED FRONT

CHAPTER VI

DISCUSSION OF RESULTS

As has been stated in the previous chapter the experiments included both quantitative and qualitative tests and utilized two different tanks, a large one for both types of tests and a very small one used for qualitative work. The aim of these experiments was primarily to verify some of the concepts proposed in the analytical model. In discussing the results to obtain a conclusion, tests that confirm a similar observation will be grouped together and thus, there will be some inevitable leaping from qualitative to quantitative tests and the work in large or small tanks during the discussion. It is hoped that this will not lead to any ambiguity or confusion.

SCOUR PROFILES

The aim of the measurement of the scour profile was to compare the shape of the gouge with that reported from field observations. Gouge tracks on the ocean floor have been observed to have raised shoulders on either side. Measurements in the laboratory identified the scour clearly but the sides slipped as soon as the model moved forward resulting in a diverging ridge (note Fig. 60). This can be expected in a weak soil of the type used in the experiment. A similar process in the ocean would result in a gouge track which will have part of the depth filled by the scoured material and thus, the gouge bottom will not be horizontal. Gouge

depths observed in such soils by side scan sonar will not therefore, represent the maximum depth. If tracks were observed in soils of low strength with diverging ridges, they can be interpreted as iceberg scour marks. This can be distinguished from submarine slumps which would diverge down the slope.

SOIL MOVEMENT IN FRONT OF THE MODEL

Results of these tests showed that the frontal resistance to the model predominated. Soil movement occurred far aheard of the model and this was observed both in the big tank and the small tank. The failure of the soil in front of the model as observed in the big tank was local. However, the failure surface appeared to start at flat angles from the toe of the model. The skin friction at the face needs a closer examination before attributing the flat angles to the low strength of the soil.

Friction between the soil and model: An iceberg surface is continuously lubricated by the melt water which forms an envelope all round. In an interaction with the soil the iceberg-soil interface can be considered a frictionless surface.

No simple method could be devised to verify the friction between the soil and plexiglas surface though such measurements are conclusive and desirable. Meyerhof[51] concluded that the skin friction can be better expressed as ratios of the soil structure adhesion to the soil cohesion $\frac{c_a}{c}$ and the ratio of the angle of skin friction to the angle of soil internal friction $(\frac{\delta}{\phi})$. For smooth steel against cohesive soils these values were given as $\frac{c_a}{c}$ = 0.1 to 0.3 and

$\frac{\delta}{\phi}$ = 0.4 to 0.6.

In a cohesive soil with a cohesion of 1.8 lb/sq.in. and an angle of internal friction of 2.5° to 4°, Witney[86] measured the adhesion between glass and soil as 0.2 lb/sq.in. For a medium sand with a density of 106 lb/cft and an angle of internal friction of 34°, Nelson[57] measured the angle of friction between a glass surface and the soil as 9°. For a soil with a cohesive strength of 1.9 lb/sq.in. and a coefficient of friction 0.203, for a steel blade, Wisener and Luth[84] measured the adhesion as 0.42 lb/sq.in.

The outcrop of the passive failure surface appeared to intersect the ground at an angle of 39°. This suggests[40a] that the soil would have a true angle of friction of 12°.

The effect of friction between the model and the soil is a factor which would influence the failure pattern and the passive pressures. The slight curvature of the failure surfaces at the toe of the model indicates the presence of friction although of small magnitude. As discussed earlier, the soil adhesion and friction would depend on the soil strength. The soil used in these experiments had a low shear strength in the range of 0.007 to 0.125 psi. It was thus deduced that the effect of wall friction would be small.

Types of shear failure in soils: Shear failures in soils are classified as general shear, punching shear and local shear failure[80] (Fig. 75). A general shear failure is characterized by a well-defined failure plane extending to the soil surface. The strain in the soil is preceeded by a plastic flow. In punching shear the soil outside the stressed area remains relatively unaffected and the structure punches through the soil. In the local shear failure, plastic

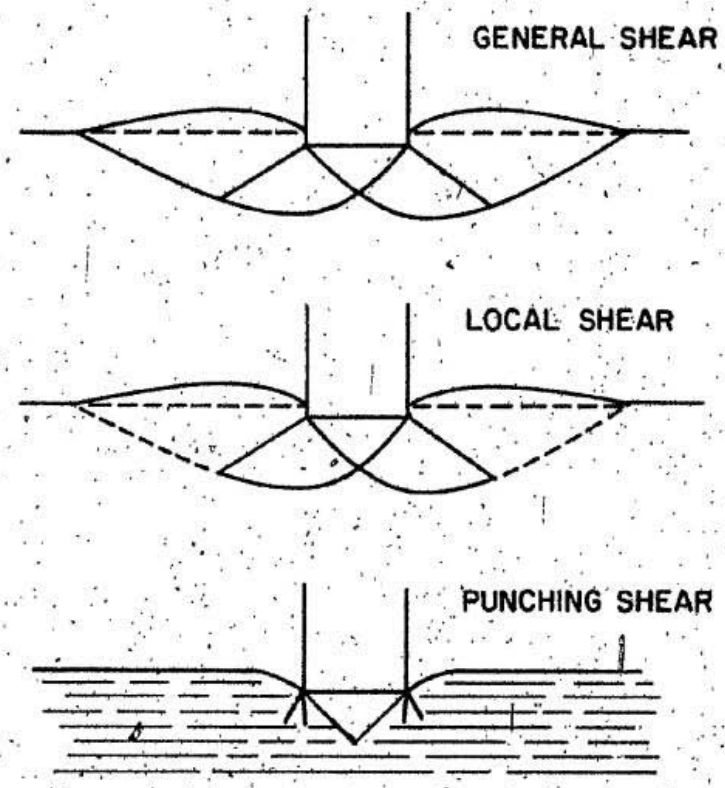

FIG. 75.- MODES OF SOIL SHEAR FAILURE IN FOUNDATIONS
(From Vesic[80])

yielding of the soil is preceeded by large strains. The failure surfaces start at the edge of the structure but end within the soil mass. The soil compression normal to the loading of the structure is significant. Local shear is a transitional mode between punching shear and general shear failures. The relative compressibility of the soil, the geometry of the structure and the loading conditions generally influence the type of the shear failure.

It was not possible to clearly distinguish any soil movement during the experiments in the big tank, while the model was moving. Movement of the soil below the maximum gouge level and extending far ahead of the conventional zone of shear was noticed at the end of the experiments. The failure appeared to start at very flat angles at the toe, but appeared to meet the surface at steeper angles of almost 45°. From these patterns it is concluded that the failure of the soil in front of the model was highly local, almost amounting to a punching shear.

In the experiments with clay soil in the small tank, soil movement was seen in front of the soil both in the horizontal and vertical directions. The plane of shear failure appeared to start at 31° at the toe and quickly became steep and met the surface at 46.5°. The failure wedge in front appeared to be in conformity with the assumption of a Coulomb wedge, inspite of the failure being local. However, movement of the soil outside this zone was seen. This was particularly noticed at the toe of the model, where the last horizontal coloured mark which was originally at a slightly higher level than the toe could be seen being progressively compressed and pushed down.

In the experiments with sand, again in the small tank, analysis of the photographs by the overlay method showed a curve for the frontal wedge at the toe which is common in walls with significant soil-wall friction. This test established that the accepted difference in behaviour in loose dry sand and wet clay still applied.

Transducers placed inside the soil below the level of the model during the quantitative tests in the large tank, registered an increase in pressure as the model approached closer, reaching a peak when the leading edge was just above the transducers. This effect was clearly due to a compression of the soil which extended below the level of the scour. It is most probable that the push from the model was transmitted to the soil ahead through the inclined face of the shear plane of the frontal wedge (Fig. 76) resulting in the compression of the soil ahead as well as below the model. The transducer placed inside the soil ahead of the model recorded pressure increase when the model was 5 feet away. A soil front of this magnitude was in motion in front of the moving model.

Shear strength measured inside the gouge track showed a slight increase (Fig. 44) over that measured before the experiment at the same depth and confirmed the other observations on a compression of the soil.

SOIL PRESSURE ON THE SIDES AND BOTTOM

In the experiments to determine the soil pressure on the sides, transducers #4, #2, and #6 were placed on the side of the model

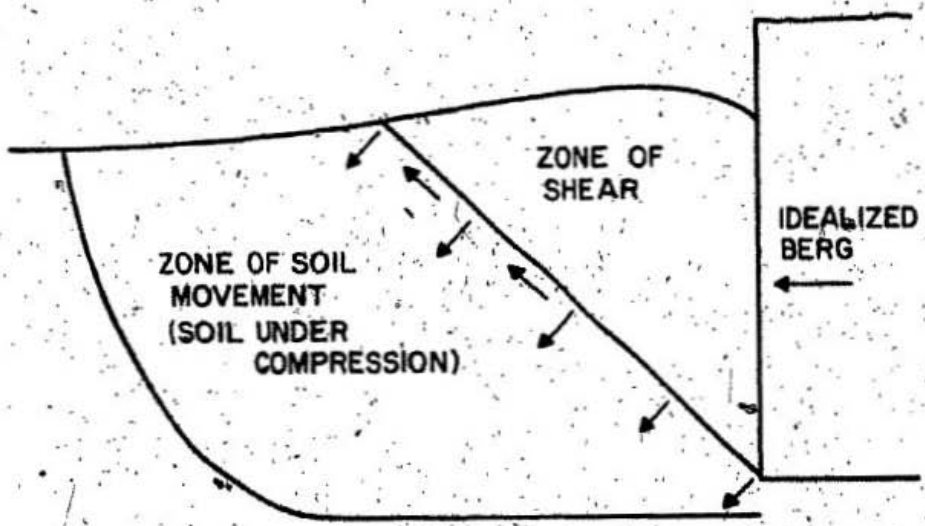

FIG. 76.- CONCEPTUAL SOIL MOVEMENT IN FRONT OF THE IDEALIZED BERG

and the transducer #3 was on the front face (Fig. 49). The maximum pressure on the side was about 58% of that on the front face. The active/passive pressure ratios depend on the type and the strength of the soil.

It was noticed that the displaced soil flowed around the model and there was slurry formation. The shear strength of the soil indicated a low adhesion between the model and the soil. This coupled with the pressures on the sides led to the conclusion that the resistance to the forward movement of the model was mostly from the front face.

Pressure variations on the bottom are shown in Fig. 50. The X-Y plane shows the variation of the pressure with time. The Y-Z plane gives the pressure distribution on the berg at different time intervals and is compared with the pressure on the front.

The uniform increase in pressure on the base of the model as far back as transducer #6 confirmed the formation of slurry below the model and a consequent increase in normal static pressure on the bottom face.

TOTAL FORCE ON THE MODEL

Since the pressures on the sides and base can be considered not contributing any resistance to the movement of the model, the total force on the model has to be through the frontal passive

pressure. The theoretical expression derived for the analytical model can be used to compute the resistance and this can be verified with the measured values, but the height of the displaced soil has to be known before calculating the total resistance.

Soil Surcharge: At the beginning of each experiment the soil line was marked on the glass face of the big tank. At the end of the experiment the actual depth of the gouge, the height of the surcharge and its shape in front of the model were observed and measured. In their experiments with agricultural blades, Nelson[57] and Payne[61] reported that the soil surcharge attained an equilibrium when it reached the blade top. The soil was found to flow around and above the blade, thus, maintaining a constant surcharge. Nelson measured its shape in cohesionless soils which was as shown in Fig. 77. The depth of cut was constant in those experiments. For an iceberg grounding in a uniform slope the depth of cut increases gradually. Unlike the tillage equipment where the height of the blade is restricted, the height of an iceberg extends far above the soil surface thus offering unlimited support in the vertical direction. The surcharge in front of a grounding iceberg is not likely to reach an equilibrium.

In the laboratory experiments with the idealized shape, the surcharge due to the soil flow took the shape of a fan as shown in Fig. 61. The gouged soil slid up the model face and curled forward as it reached the top. The height of the surcharge was a maximum at a short distance in front of the model.

It was not feasible to measure the surcharge at different

points during the experiment though this would have been desirable. If the surcharge is assumed to vary linearly, it can be calculated at any intermediate point from the measured value at the end of the test. However, this will lead to errors of large magnitude at the beginning of the test. The surcharge at the end of the experiment was nearly 64% of the gouge depth for a 7 foot scour length. To calculate the intermediate surcharges more correctly, equation [21] was used and with the measured values as boundary condition, curves as shown in Fig. 78 were drawn from which the intermediate surcharges were read.

Total force on the model: From the known gouge depth, the soil surcharge and the average shear strength, the theoretical frontal soil resistance was computed and compared with the measured pull recorded by the load cell. The computed forces were found to be less than the measured values (Figs. 79-82) by 29 to 34%. This proved that the soil was being compressed in front of the model and the force was reduced by a third in the compression process. To further confirm the phenomenon of soil compression, one experiment was conducted with a 9" wide by 19" long plexiglas plate and the forces were measured. A comparison of the computed and measured pulls showed a difference (Fig. 83) of about 25% towards the end of the experiment.

During the finalization of this thesis, an abstract of work done in Germany came to attention. Experiments were said to have been conducted with a horizontally pushed model earth-working machine. It was reported that 30% of the effort was lost in compacting

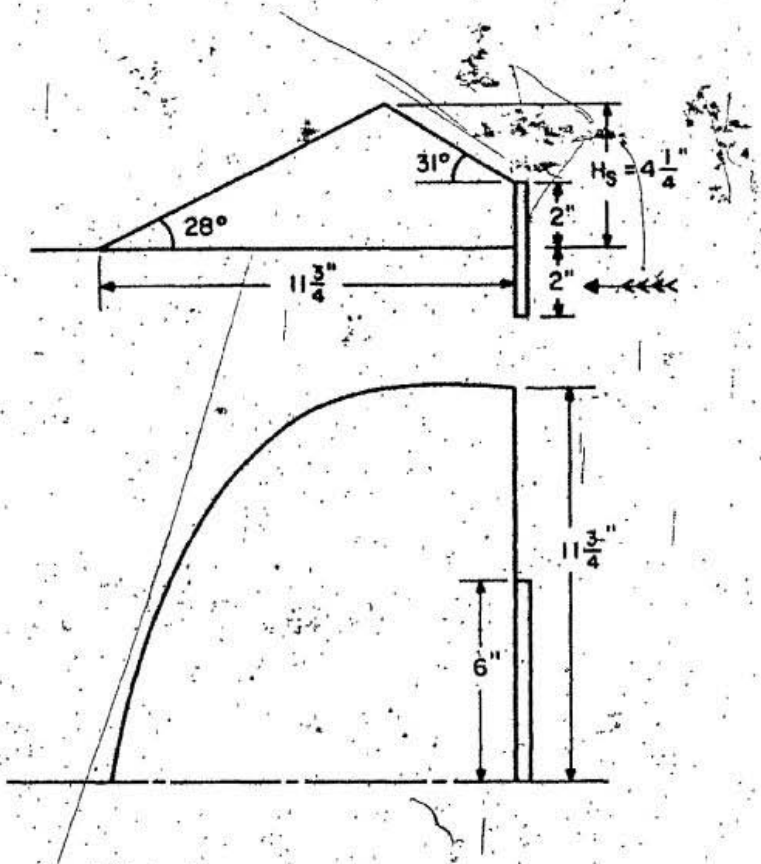

FIG. 77 - SURCHARGE IN SAND FOR A 12" WIDE BLADE
(From Nelson[57])

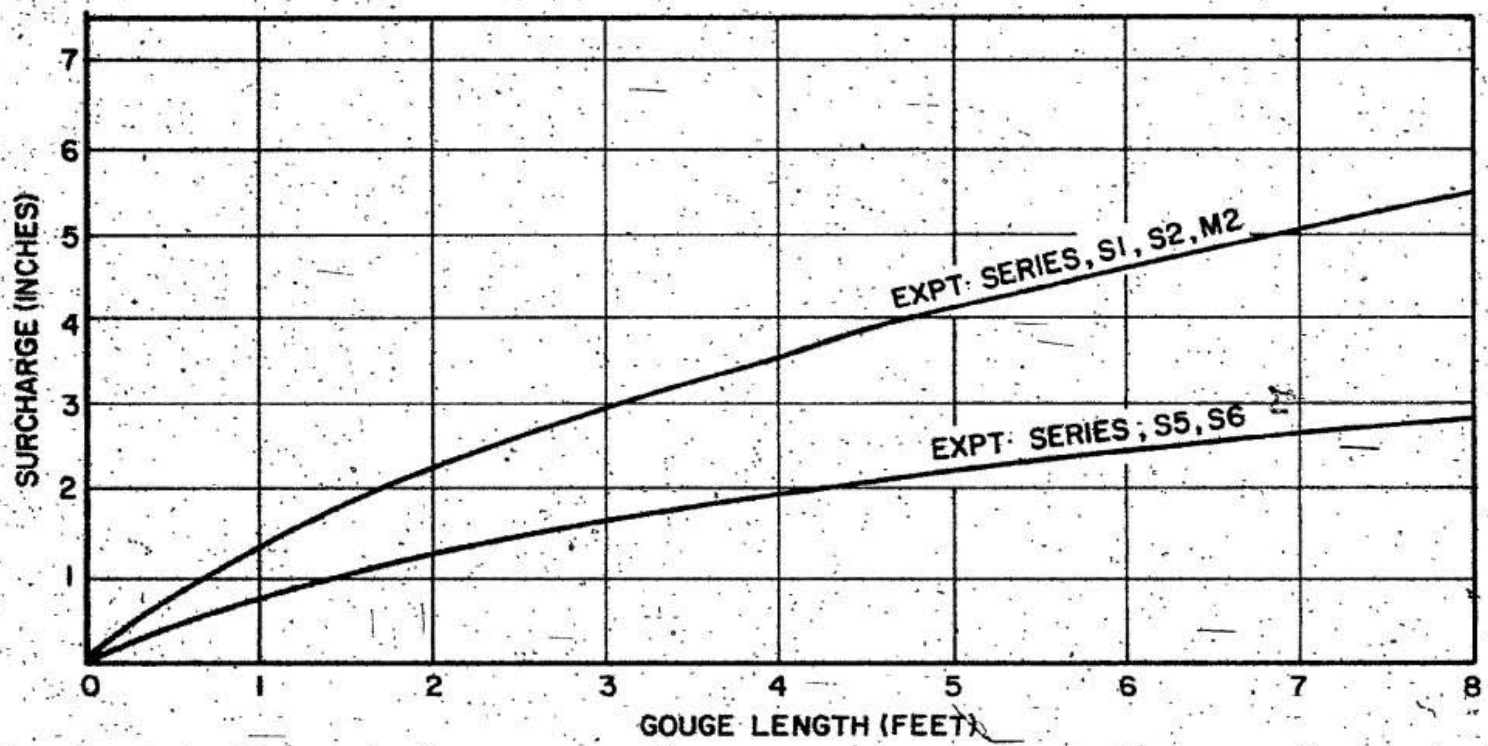

FIG. 78.- THEORETICAL SURCHARGE CURVES

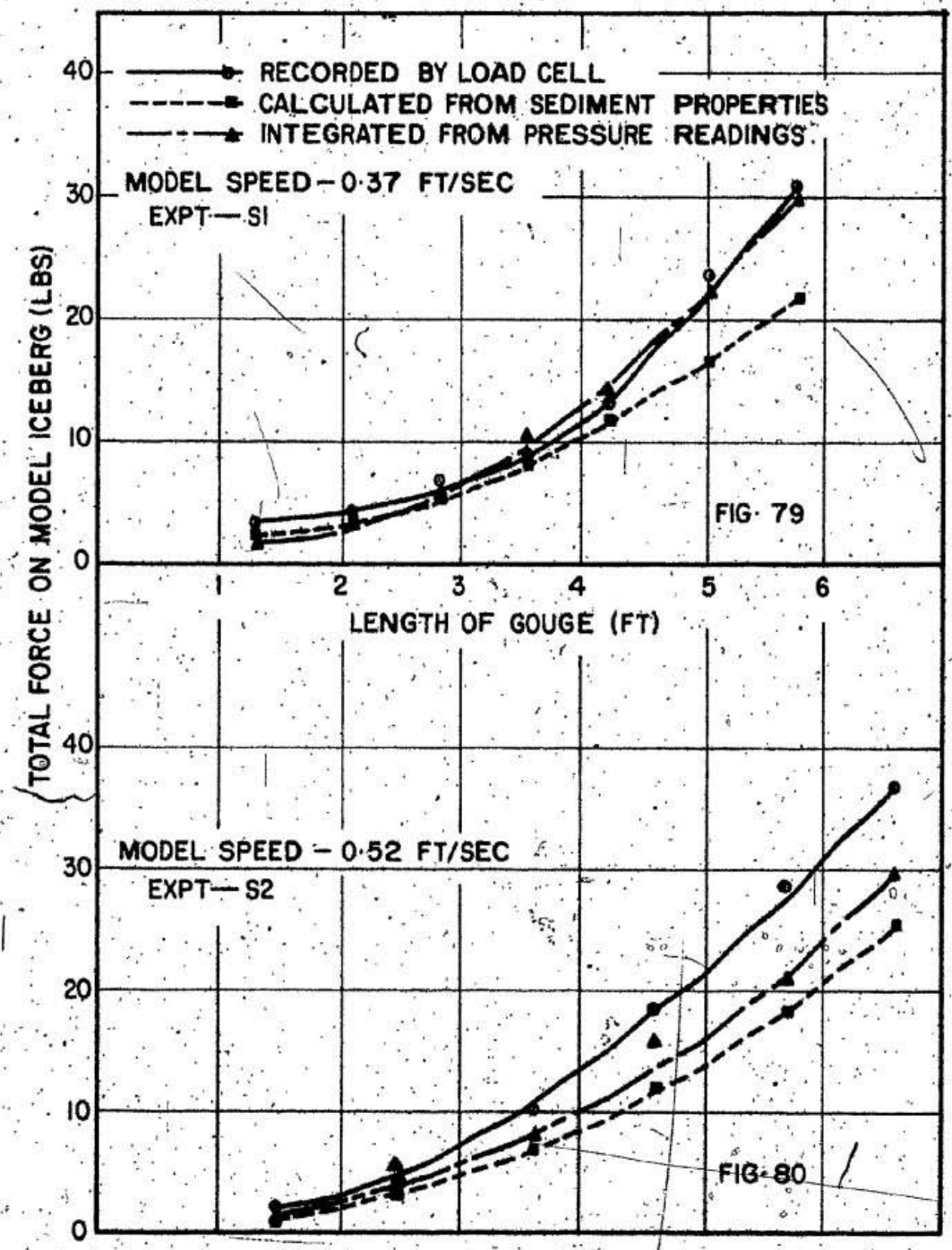

FIGS. 79 AND 80.- COMPUTED AND MEASURED TOTAL PULL ON THE IDEALIZED BERG MODEL

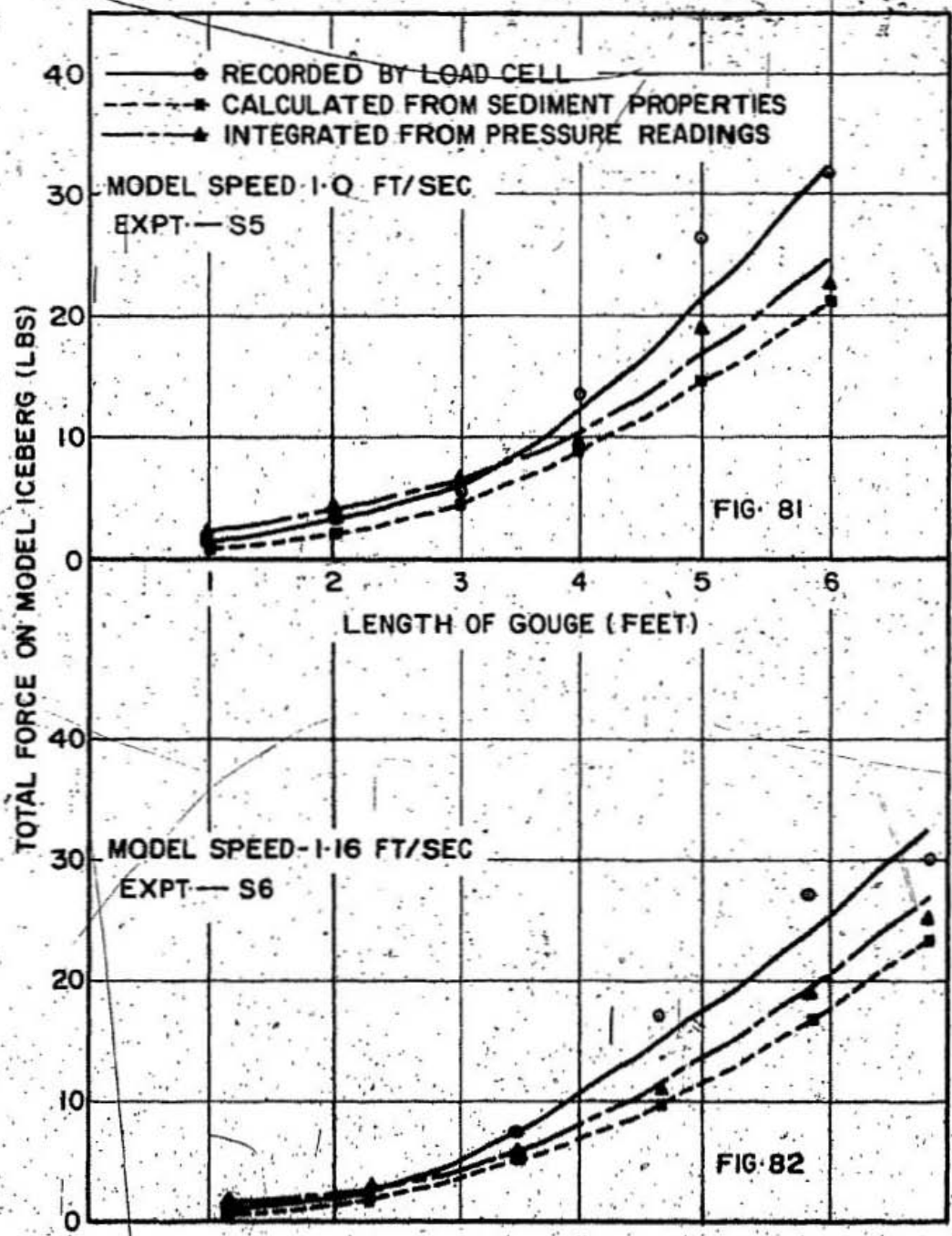

FIGS. 81 AND 82. - COMPUTED AND MEASURED TOTAL PULL ON THE IDEALIZED BERG MODEL

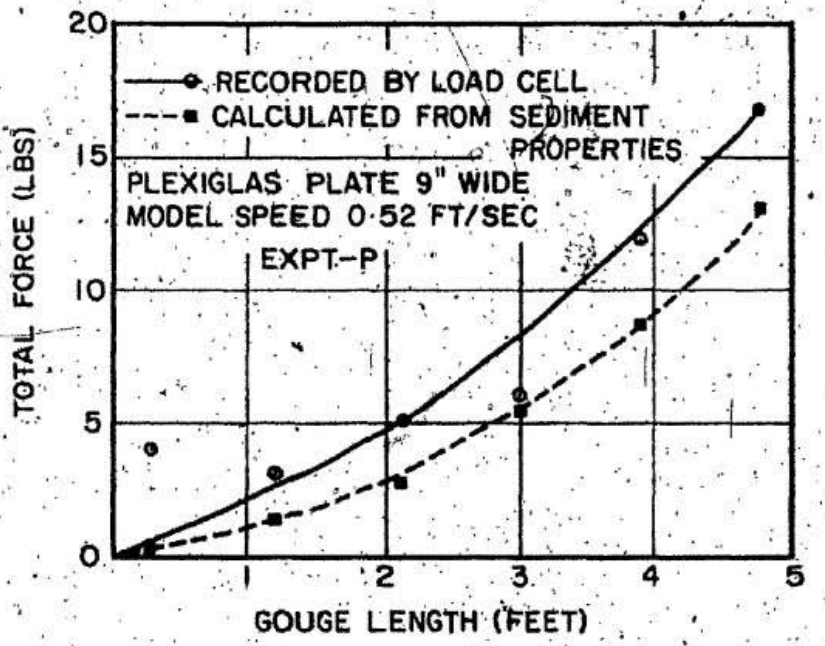

FIG. 83.- COMPUTED AND MEASURED TOTAL PULL ON A 9" WIDE PLATE

the soil. This coincides with the findings here of a difference between measured and computed pulls due to a zone of compression in front of the soil. The exact experimental conditions and details of the German work is not known yet.

The total force on the model was also computed from the recorded pressures on front face from the pressure variation and integration over the front face of the model. These forces were superimposed on the measured pulls and it was found that the correlation was good at the beginning of all the experiments, but as the length of gouge increased, the forces computed from the pressure readings were less by about 15%. From the limited number of pressure readings on the front, judging the variation of the pressure is subjective. But these computation substantiate the reliability of the other results.

EFFECT OF MODEL SPEED

Strain rate effect is a much researched topic in cohesive soils. To verify this effect in the soil used in this investigation, the total force on the model was recorded at six different speeds, as shown in Fig. 48. Forces were then computed at identical gouge lengths and the effect of speed on the total pull was compared (Fig. 84). The force at speed setting 2 was out of correlation. This particular sample had a vane shear strength varying from about 1 p.s.f. at the surface to about 2.5 p.s.f. at a depth of 6.5 inches while the other samples had shear strengths in the range of 5 to 7 p.s.f. at this depth and thus the soil resistance in this experiment was

very low.

For the range of speeds tested, no well defined rate effect was seen on the soil resistance. Sohne[71] observed that the total force on blades increased with speed for velocities greater than 2.5 feet/sec (about 1.5 knots) and the force was almost uniform within this range.

The average drift velocity for icebergs can be considered to be in the region of 1.25 feet/sec (about 0.75 knots) and for velocities of this magnitude the effect of speed is considered not to influence the sediment resistance.

SHAPE EFFECTS

The shape of an iceberg may be far from that of the idealized one considered here and is invariably random. A proper extension of the laboratory model to the actual grounding can be done only after studying the effect of different shapes.

Qualitative tests in the small tank with four different shapes showed that the soil movement was similar to that observed with the idealized shape. Published results of experiments with inclined blades could be used to logically infer the shape effects in iceberg grounding.

Payne and Tanner[62] conducted field studies to determine the shape of soil disturbance in front of blades of different inclinations. For blades of inclination greater than 120° the type of failure was as shown in Fig. 85 a.

Hettiaratchi et al[39] inferred after preliminary observations that for interfaces inclined greater than 90°, a soil wedge ABC (Fig. 85b) was formed in front. Photographic observations of Harrison[38] showed that actual formation of these wedges (Fig. 85e) for a sand with $\emptyset$ varying between 25° and 30°.

Formation of similar wedges in front of grounding icebergs could be conceived as converting the interface to an equivalent idealized shape. Failure surfaces were observed with the three smaller models (Fig. 71-73) of different shapes. In the model with the toe chamfered at 45°, the shear plane started at the top edge of the chamfer. The inclined surface itself acted as a continuation of the shear surface. In the model with a rounded toe and the one with a rounded front, the failure surface appeared to start very near the intersection of the base and the vertical face of the model.

The failure surface observed in the big tank with the model having a rounded toe (Fig. 56) also supports these observations.

Two tests were conducted with non-prismatic models. Assuming these to be idealized into equivalent prismatic shape, the measured and computed total force on the model were compared (Figs. 86, 87). No conclusions could be drawn from these limited observations, but towards the end of the test, the measured pull was greater by 37% for the model with rounded toe and by about 20% for the model with a twisted front face. Further work would be required before drawing any conclusion on the effect of shape.

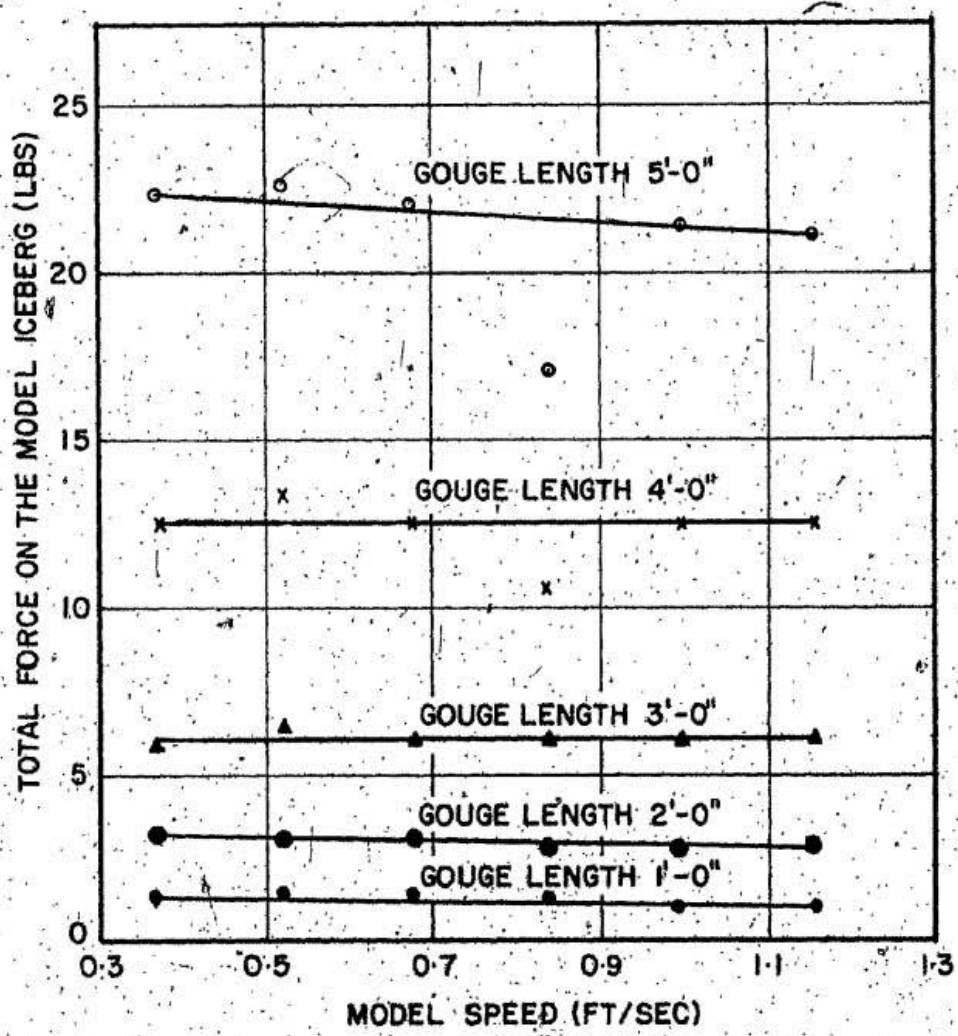

FIG. 84.- VARIATION OF TOTAL PULL WITH MODEL SPEED

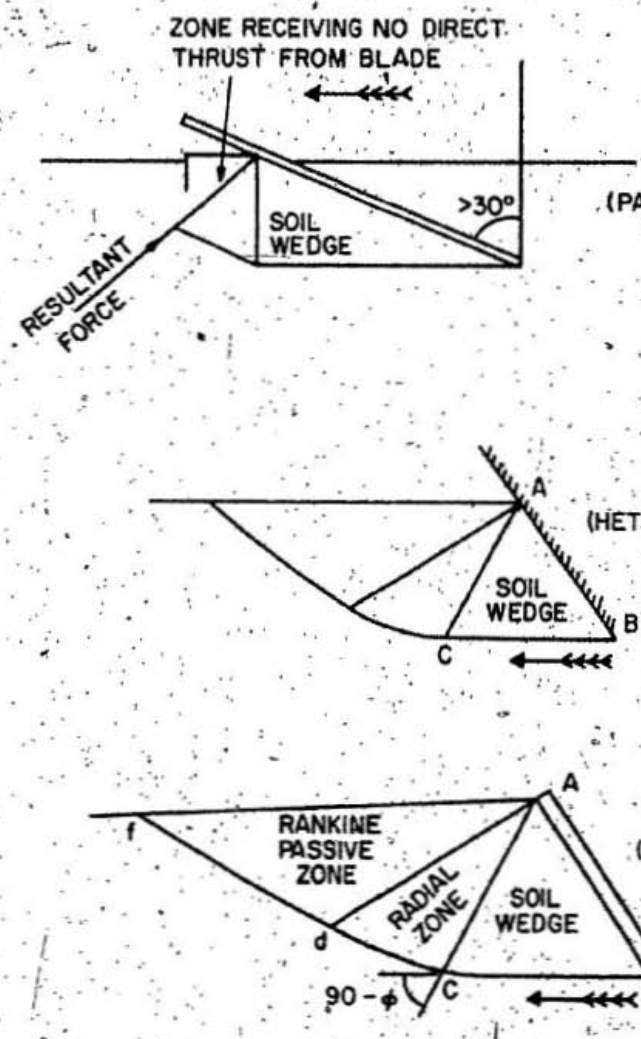

FIG. 85.- RUPTURE PATTERNS WITH INCLINED BLADES

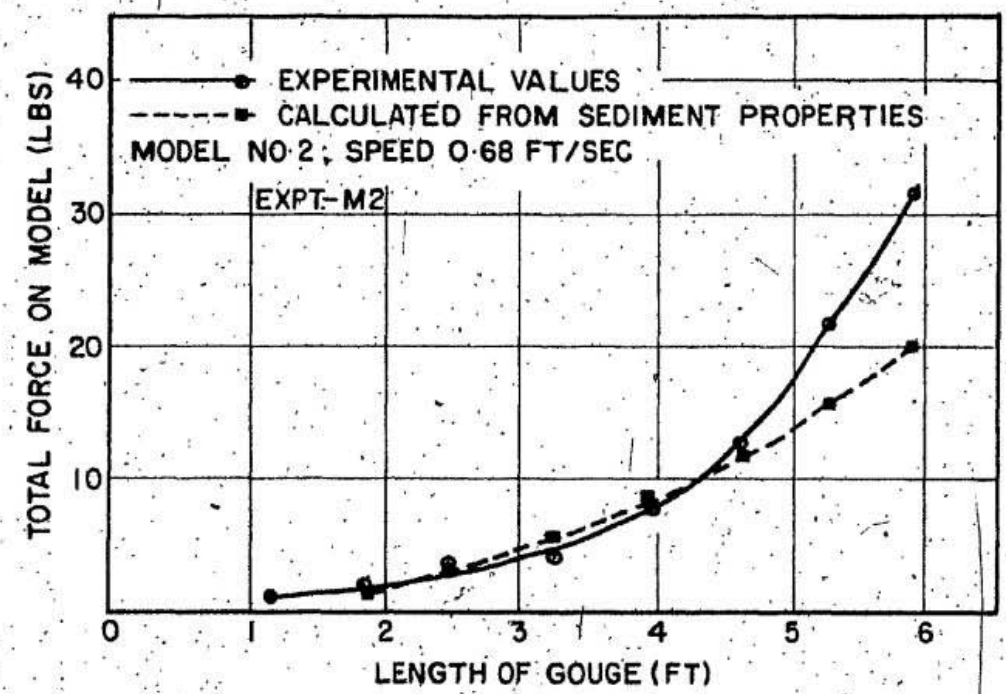

FIG. 86.- COMPUTED AND MEASURED TOTAL PULL FOR THE MODEL WITH A ROUNDED TOE

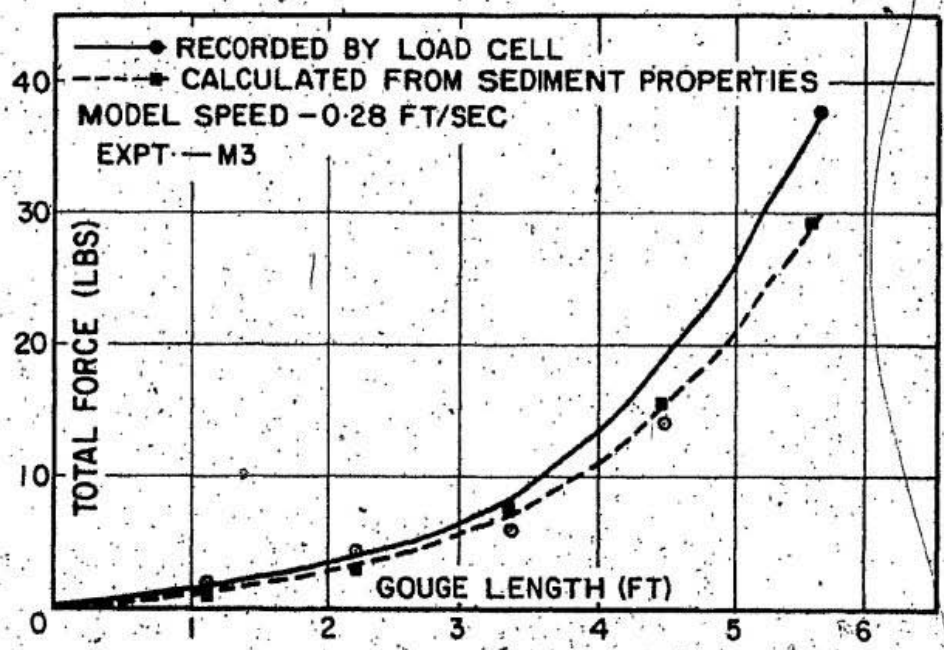

FIG. 87.- COMPUTED AND MEASURED PULLS FOR THE MODEL WITH A TWISTED FRONT FACE

APPLICATION OF THE RESULTS TO THE OCEAN ENVIRONMENT

The analytical model of the interaction of an iceberg with the continental shelf deposits was formulated assuming idealized conditions. Actual profiles of icebergs show[3] that the width of an iceberg is not constant below the water line. An ellipsoidal shape is very common at the bottom of a berg. In the computations of iceberg gouge size the effective width of the berg that comes in contact with the sediment has to be taken into account and not the width at the water line. In this thesis, a width of 100 feet was assumed in all the illustrative calculations as this appeared to be realistic at the soil-iceberg interface. The only recorded observation of gouge tracks off the Newfoundland coast was by Harris and Jollymore[37]. This revealed that the gouge widths were an average of 100 feet (30 meters) and the maximum length and depth of the observed tracks were about 9850 feet (3 Km) and 21 feet (6.5 m) respectively, including the shoulder height. However, these maximum measurements were not from the same track and the height of the shoulders was not reported. The sediment type in this area was said to be a mixture of sand, silt and clay, but no data on the engineering properties were given. The slope in this region varied from a steep 1:100 to a flat 1:1000 as computed from the bathymetric charts.

Icebergs of 20 million tons are not uncommon near Belle Isle where Harris and Jollymore did their survey. Assuming the sediment to be weak, with a shear strength of 50 lb/sft and bulk

density of 100 lb/cft, the theoretical gouge size can be computed using the analytical model. On a 1:1000 slope the maximum gouge length would be about 7800 feet. The assumed drift velocity is 1 ft/sec. Similarly, the maximum gouge depth on a 1:100 slope would be about 17.7 feet and hence, including the shoulders, the height of which depends on the slope of the surcharged soil, the total depth could be very close to the reported observations. These preliminary calculations show that the proposed analytical model is not unrealistic. When more field data are available together with the other parameters such as the soil property and the slope, a proper correlation is possible.

The continental shelves of Newfoundland and Labrador consist of a number of raised banks and the slope is not uniform as idealized. Submarine cables are laid under the protection of these natural banks in the ocean, and it is generally believed that cables laid in this manner are less susceptible to damage through scouring iceberg. Permanent or semi permanent installations such as pipe lines could perhaps be buried in a trench, far below the expected scour depths. Oil wells are normally plugged with a blowout preventer stack which might extend even up to 15 feet above the ocean floor. It is learnt that some of the blowout preventer stacks on exploration wells in the Labrador sea were severely damaged through icebergs moving across. A possible solution to this type of damage is to locate the drilling wells in the 'iceberg shadow' of a natural bank. Bunded protection to bottom structures is one of the solution that could be explored.

Construction of such a bund would necessitate a detailed knowledge of the soil bearing capacity, its consolidation characteristics and also the wave and current action on the bund material. It is therefore not feasible to examine this proposal in this thesis in detail. However, from this research it appears that such bunds could be effective in trapping and grounding deep-drafted bergs.

CHAPTER VII

SUMMARY AND CONCLUSIONS

Scouring of the ocean bed by icebergs is of regional interest in the Northwest Atlantic offshore and has attracted attention recently with the promising finds of natural gas. A number of factors such as currents, winds, iceberg size, the bathymetry of the ocean and the type of sediment influence the scouring phenomenon. Marine geotechnics is still in the developing process and so is the understanding of the shape, drift and size of icebergs.

This thesis was restricted to a study of the mechanics of the soil-iceberg interaction. The shape of an iceberg was idealized and assuming a uniformly sloping continental shelf with a deposit of very weak sediment whose properties were assumed determinable, an expression was derived for the size of the scour track that the idealized berg could cause. The gouging process is primarily one of a horizontal ploughing of the idealized berg into the sediment slope. The resistance to the berg motion is a frontal passive soil resistance. The effect of the surcharge of the displaced soil is significant and has been taken into account.

A laboratory tank was designed to enable a study to be made of the mechanics of iceberg scouring. This tank can be tilted up to a slope of 1:10 and sloping beds of soil can be conveniently laid

Apart from the determination of the soil properties for each experiment, the regular test program was both qualitative and quantitative. Observations at the end of the experiments showed a failure pattern in the soil which was local, and there was movement of the soil far ahead of the model. This was confirmed by placing pressure transducers in the soil. A soil front of about 5 feet was under compression and the soil below the toe of the model was also under compression. Pressures measured on the different faces of the model showed that the pressure on the base increased due to the increased buoyancy of the slurry formed in the process of scouring. The pressure on the sides was active. These pressures were considered insignificant in offering resistance to the iceberg movement.

A comparison of the analytically computed frontal soil resistance with the measured pulls showed the computed values to be less by 29 to 34%. It was concluded that icebergs scouring in sediments of low shear strength expend about a third of the effort in compressing the soil. Actual gouge lengths are, therefore, likely to be less than the computed lengths, but the soil below the iceberg would be subjected to some movement. Bottom structures will therefore have to be located below the computed maximum scour depths. It is felt that the iceberg push is transmitted to the soil ahead through the shear plane of the wedge in front. To determine the zone of movement in terms of the gouge size, experiments with bigger models are suggested.

Tests on models in the speed ranges of 0.36 ft/sec to 1.16 ft/sec showed that the model speed has no effect on the total soil resistance.

Limited measurements on models of different shape showed that an iceberg could be converted into an equivalent idealized shape. Further confirmative work is needed in this area before any final conclusion can be drawn.

A smaller tank was fabricated to obtain qualitative understanding of the soil movement with models of different shapes. Experiments with the idealized shape confirmed the soil movement in front and below the model. Tests with four other models showed failure planes which appeared to start from the junction of the front face and the bottom edge of the model.

Research on iceberg scouring is still in its initial phase and this work has dealt with one specialized aspect of the problem. Data on the continental shelf surface deposits and their engineering properties are at present limited. Much of the present research can be considered speculative unless the engineering properties of the surface deposits of the Labrador sea and also the behaviour of an actual berg in these deposits are determined.

From this research, it is felt that the following areas are to be examined before a safe design standard for sea bottom structures could be suggested:

1. Laboratory experiments with models of bigger sizes to determine the scaling effect, particularly in reference to the zone of soil movement below the scour bottom.

2. Further experiments with models of different shapes,

3. Field studies where icebergs of maneuverable sizes could be towed and artificially grounded in preselected locations,

4. Assessment of the technology to construct bunds around bottom structures or to use natural features such as banks on the ocean floor. Efforts in this direction will be necessary to keep the icebergs away from damaging the blowout preventer stacks which project out from the ocean floor.

5. Analytical studies of the iceberg soil interaction based on the finite element method.

BIBLIOGRAPHY

1. Allaire, P.E., "Stability of simply shaped icebergs", The Journal of Canadian petroleum technology, Vol. 11, no. 4, Oct - Dec, 1972, pp. 21-25.

2. Allen, J.H., "Cruise report, C.S.S. Dawson", Faculty of Engineering report, Memorial University of Newfoundland, St. John's, 1971.

3. Allen, J.H., "Iceberg study, Saglek, Labrador including cruise report C.S.S. Dawson", Faculty of Engineering report, Memorial University of Newfoundland, St. John's, 1972.

4. Anon., Herschel Island - Feasibility of a marine terminal, Department of Public works, Canada, 1971, pp. 29-32.

5. Anon., "Science seeks way to predict iceberg path", Offshore, Vol. 32, no. 1, Jan. 1972, pp. 32-33.

6. A.S.C.E. Committee on definitions and standards., "Nomenclature for soil mechanics", Journal of the Soil Mechanics & Foundations division, Proceedings ASCE, Vol. 88, no. SM3, June 1962, pp. 185-188.

7. Avilov, I.K., "Bottom contours and nature of grounds and their significance for trawl fishing", ICNAF special publication, No. 6, 1965, pp. 781-789.

8. Barnes, H.T., "Report on the influence of icebergs and land on the temperature of the sea", Forty fifth annual report of the department of marine and fisheries, sessional paper no. 21 C, pp. 523-542.

9. Barnes, H.T., "Iceberg and their location in navigation", Proceedings, Royal Institute of Great Britain, Vol. 20, May 1912, pp. 523-542.

10. Barnes, H.T., "Some physical properties of icebergs and a method for their destruction", Proceedings, Royal Society of London, Series A, Vol. 114, 1927, pp. 161-168.

11. Barnes, H.T., "Ice destruction", The Marine Observer, Vol. 5, no. 59, 1928, pp. 234-237.

12. Bartlett, R.A., "Ice navigation, Problems of polar research", American Geophysical Society Special publication no. 7, 1928, pp. 427-442.

13. Belderson, R.H., N.H. Kenyon and J.B. Wilson., "Iceberg plough marks in the Northeast Atlantic", Palaeogeography, Palaeoclimatology, Palaeoecology, Vol. 13, 1973, pp. 215-224.

14. Blenkarn, K.A., and A.E. Knapp, "Ice conditions on the Grand Banks", Ice Seminar, Canadian Institute of Mining and Mettallurgy, special vol. 10, 1969, pp. 61-72.

15. Bolz, R.E., and G.L. Tuve, Handbook of tables for applied engineering sciences, The Chemical Rubber Co., Cleveland, 1970.

16. Brooks, L.D., "Ice scour on the Northern continental shelf of Alaska", Preprint Proceedings, Fifth Offshore technology conference, Houston, May 1973, pp. 763-766.

17. Bruneau, A.A., "Icebergs over the Canadian continental shelf", Preprint, Canadian Soc. of exploration Geophysicists national convention, Calgary, April 1973.

18. Bruneau, A.A. and R.T. Dempster, "Iceberg dynamics, Vol 1 to 3", (Proprietory), Contract Report submitted to Eastcan Petroleum operators association, Calgary, 1971.

19. Bruneau, A.A., and R.T. Dempster, "Engineering and economic implications of icebergs in the North Atlantic", Conference Papers, Oceanology International, Brighton, March 1972, pp. 176-180.

20. Budinger, T.F., "Wind effect on icebergs", Report of the International Ice Patrol, July 1960.

21. Canadian Hydrographic Service, 1974 Canadian Tide and Current Tables, Atlantic coast, Vol 4, pp. 16-17.

22. Canizo, L., and C. Sagaseta, "Earth pressure of an elastoplastic soil upon a moving rigid wall", Proceedings, Fifth European conference on Soil Mechanics, Madrid, 1972, Translations of Spanish contributions, pp. 13-21.

23. Chari, T.R. and J.H. Allen, "Iceberg grounding - A preliminary theory", Applications of solid mechanics, Proceedings of the symposium held at the University of Waterloo, June 1972, (S.M. Study no. 7), pp. 81-95.

24. Chari, T.R. and J.H. Allen, "An analytical model and laboratory tests on iceberg sediment interaction", Proceedings, I.E.E.E. conference Ocean 74, Halifax, Aug. 1974, Vol. 1, pp. 133-136.

25. Chen, W.F. and C.R. Scawthorn, "Limit analysis and limit equilibrium solutions in soil mechanics", Soils and Foundations, Vol. 10, no. 3, Sept 1970, pp. 13-49.

26. Chen, W.F. and J.L. Rosenfarb, "Limit analysis solution of earth pressure problems", Soils and Foundations, Vol. 13, no. 4, Dec 1973, pp. 45-60.

27. Dempster, R.T., "The measurement and modeling of iceberg drift", Proceedings, I.E.E.E. conference Ocean 74, Halifax, Aug 1974, Vol. 1, pp. 125-129.

28. Dempster, R.T. and A.A. Bruneau, "Dangers presented by icebergs and protection against them", Preprint, Conference on Arctic oil and gas, Problems and possibilities, Le Havre, France, May 1973.

29. Dinsmore, R.P., "Ice and its drift into the North Atlantic ocean", Symposium on environmental conditions in the Northwest Atlantic, 1960-1969, ICNAF special publication no. 8, 1972, pp. 89-128.

30. Doyle, E.H., "Soil - Wave tank studies of marine soil instability", Preprint proceedings, Fifth offshore technology conference, Houston, 1973, pp. 753-766.

31. Drapeau, G., "Sedimentology of the Narrowest portion of the Strait of Belle Isle", Report, Bedford Institue of Oceanography, Dartmouth, 1971.

32. Dyson, J.L., The World of Ice, Alfred A. Knopf, New York, 1963, pp. 83-90.

33. Finn, W.D.L., "Application of limit plasticity in soil mechanics", Journal of the Soil Mechanics & Foundations division, Proceedings ASCE, Vol. 93, no. SM 5, Sept 1967, pp. 101-119.

34. Finn, W.D.L., P.M. Byrne and J.J. Emery, "Engineering properties of a marine sediment", Proceedings, International Symposium on the engineering properties of sea-floor soils and their geophysical identification, Seattle, July 1971, pp. 110-120.

35. Fisk, H.N. and B. McClelland, "Geology of continental shelf off Louisiana, its influence on offshore foundation design", Bulletin of the Geological society of America, Vol. 70, no. 10, Oct 1959, pp. 1369-1394.

36. Grant, A.C. "The continental margin off Labrador and Eastern Newfoundland - Morphology and Geology", Canadian Journal of earth sciences, Vol. 9, No. 11, Nov 1972, pp. 1394-1430.

37. Harris, I. McK. and P.G. Jollymore, "Iceberg furrow marks on the continental shelf Northeast of Belle Isle, Newfoundland", Canadian Journal of Earth Sciences, vol. 11, no. 1, Jan 1974, pp. 43-52.

38. Harrison, W.L., "Soil failure under inclined loads", Journal of Terramechanics, 1973, Vol. 9, no. 4, pp. 41-63, Vol. 10, no. 1, pp. 11-50.

39. Hettiaratchi, D.R.P., B.D. Witney, and A.R. Reece, "The calculation of passive pressure in two dimensional soil failure", Journal of Agricultural Engineering Research, Vol. 11, 1966, pp. 89-107.

40. Huntsman, A.G., "Arctic ice on our eastern coast", Biological board of Canada, Bulletin no. 13, Jan. 1930, pp. 1-12.

40a. Hvorslev, M.J., "Physical components of the shear strength of saturated clays", Shear strength of cohesive soils, Research Conference Proceedings, University of Colorado, Boulder, June 1960, pp. 169-273.

41. Janbu, N., "Earth pressure computations in theory and practice", Proceedings, Fifth European conference on Soil Mechanics, Madrid, 1972, pp. 47-54.

42. Keller, G.H., "Engineering properties of some sea-floor deposits", Journal of the Soil Mechanics & Foundations Division, Proceedings ASCE, Vol. 95, No. SM 6, Nov. 1969, pp. 1379-1392.

43. Kovacs, A., and M. Mellor, "Sea ice morphology and ice as a geologic agent in the Southern Beaufort Sea", Preprint. AINA symposium on Beaufort Sea coastal and shelf research, San Francisco, Jan. 1974.

44. Krause, R., "The displacement phenomenon around foundation tools in dry sand", Geotechnical abstracts, GA 82,92, Oct. 1974.

45. Langer, M., "Shearing resistance and rheologic properties of soft marine clays such as applying to subaquatic slides", Bulletin of the International Association of Engineering Geology, Paris, No. 5, 1972, pp. 127-134.

46. Ling, S.C., "State-of-the-art of marine soil mechanics and foundation engineering", Technical Report S-72-11, U.S. Army Engineer Waterways Experiment Station, Vicksburg, Aug. 1972.

47. Lysmer, J., "Limit analysis of plane problems in soil mechanics", Journal of the Soil Mechanics and Foundations Division, Proceedings ASCE, Vol. 96, No. SM 4, July 1970, pp. 1311-1334.

48. Maisey, G.H., "Geological properties of the Norwegian Continental Shelf relating to pipe lines", Northern Offshore, no. 8 1974, pp. 39-49.

49. Meyerhof, G.G., "The bearing capacity of foundations under eccentric and inclined loads", Proceedings, Third International Conference on Soil Mechanics and Foundation Engineering, Zurich, 1953, Vol. 1, pp. 440-445.

50. Meyerhof, G.G., "The mechanism of flow sides in cohesive soils", Technical Memorandum No. 50, National Research Council of Canada, Sept 1957.

51. Meyerhof, G.G., "Some problems in the design of rigid retaining walls," Proceedings, 15th Canadian Soil Mechanics Conference, Ottawa, 1961, pp. 59-79.

52. Milne, J., "Ice and ice-work in Newfoundland", Geological Magazine, Decade 2, Vol. 3, Nos. 7,8 and 9, July - Sept, 1876.

53. Moore, D.G., "Submarine slumps", Journal of sedimentary petrology, Vol. 31, no. 3, Sept 1961, pp. 343-357.

54. Morgenstern, N.R., "Submarine slumping and the initiation of turbidity currents", Marine Geotechnique, Ed. A.F. Richards, University of Illinois Press, 1967.

55. Murray, J.E., "The drift, deterioration and distribution of icebergs in the North Atlantic Ocean", Ice Seminar, Canadian Institute of Mining & Metallurgy special Vol. 10, 1969, pp. 3-18.

56. McMillan, N.J., "Surficial Geology of Labrador and Baffin Island shelves", Geological Survey of Canada, Earth Science symposium on offshore Eastern Canada, Paper 71-23, 1971, pp. 451-469.

57. Nelson, R.D., "Passive resistance of plane blades in cohesionless soil", Thesis submitted to the Illinois Institute of Technology in 1965 in partial fulfillment of the requirements for the degree of M.Sc. in Civil Engineering.

58. Noble, Rev. L.L., After an iceberg with a painter, Sampson Low, Son & Co., London, 1861.

59. Noorany, I.J., and S.F. Gizienski, "Engineering properties of submarine soils: State-of-the-art review", Journal of the Soil Mechanics and Foundations Division, Proceedings ASCE, Vol. 96, No. SM 5, Sept 1970, pp. 1735-1762.

60. Olsson, R.G., "Rigorous solution of a differential equation in soil mechanics," Quarterly of Applied Mathematics, Vol. 7, no. 3, October 1949, pp. 338-342.

61. Payne, P.C.J., "Relationship between the mechanical properties of soil and the performance of simple cultivation implements", Journal of Agricultural Engineering Research, Vol. 1, No. 1, 1956, pp. 23-50.

62. Payne, P.C.J. and D.W. Tanner, "The relationship between rake angle and the performance of simple cultivation implements", Journal of Agricultural Engineering Research, Vol. 4, No. 4, 1959, pp. 312-325.

63. Sanderson, R.M. and G.P. Davis, "Ice conditions through the Northwest passage", The Marine Observer, Vol. XLII, No. 236, April 1972, pp. 69-80.

64. Selig, E.T. and R.D. Nelson, "Observations of soil cutting with blades", Journal of Terramechanics, Vol. 1, No. 3, 1964, pp. 32-53.

65. Shearer, J.M., "Prelimipary interpretation of shallow seismic reflection profiles from the west side of MacKenzie Bay - Beaufort Sea", Geological survey of Canada, Report of activities - Nov 1970 to March 1971, Paper 71-1, part B, 1971, pp. 131-138.

66. Shields, D.H. and A.Z. Toluney, "Passive pressure coefficients by method of slices", Journal of the Soil Mechanics and Foundations Division, Proceedings ASCE, Vol. 99, No. SM12, Dec 1973, pp. 1043-1053.

67. Siemens, J.C., "Mechanics of soil under the influence of model tillage tools", Thesis presented to the University of Illinois at Urbana in 1963 in partial fulfillment of the requirements for the degree of Doctor of Philosophy.

68. Slatt, R.M. and A.B. Lew, "Provenance of quaternary sediments on the Labrador continental shelf and slope", Journal of Sedimentary Petrology, Vol. 43, No. 4, Dec 1973, pp. 1054-1060.

69. Smith, E.H., "The North Atlantic ice menance and the work of protection conducted by the U.S. Coast Guard", Proceedings of the U.S. Naval Institute, Vol. 5, No. 315, 1929, pp. 393-400.

70. Smith, E.H., "The Marion Expedition to Davis Strait and Baffin Bay", U.S. Coast Guard bulletin no. 19, Part 3, Scientific results, 1931, pp. 60-216.

71. Sohne, W., "Some basic considerations of soil mechanics as applied to agricultural engineering", Grundlagen der Landtechnik, 1956, Translation No. 53, U.K. National Institute of Agriculture, Silsoe.

72. Sokolovski, V.V., Statics of granular media, Translated from Russian, Pergamon Press, 1965.

73. Taylor, D.W., Fundamentals of soil mechanics, John Wiley and Sons Inc., New York, 1952.

74. Terzaghi, K., "Varieties of submarine slope failures", Proceedings, 8th Texas Conference on Soil Mechanics and Foundation Engineering, 1956.

75. Terzaghi, K., Theoretical Soil Mechanics, John Wiley and Sons, Inc. New York, 1959.

76. U.S. Naval Oceanographic Office, Oceanographic Atlas of the North Atlantic Ocean, Section III, Ice, 1968, pp. 94-117.

77. U.S. Naval Oceanographic Office, "Ice and its drift into the North Atlantic Ocean", Pilot Chart of the North Atlantic Ocean, April 1973.

78. U.S. Treasury Department, "Report of the International Ice Patrol Service in the North Atlantic Ocean", Coast Guard bulletin no. 45, Season of 1959, pp. 22-28.

79. U.S. Treasury Department, "Report of the International Ice Patrol Service in the North Atlantic Ocean", Coast Guard bulletin no. 46, Season of 1960, pp. 21-30.

80. Vesic, A.S., "Analysis of ultimate loads of shallow foundations", Journal of the Soil Mechanics and Foundations Division, Proceedings of the ASCE, Vol. 99, no. SM 1, Jan 1973, pp. 45-73.

81. Vey, E., and R.D. Nelson, "Environmental effects on properties of ocean sediments", Proceedings of the conference on Civil Engineering in the oceans, ASCE, San Francisco, Sept 1967, pp. 531-568.

82. Wells, A.A., "The mechanics of soil in relation to tillage", Doctoral thesis submitted to the Cambridge University, 1950.

83. Winterkorn, H.R. and H.Y. Fang, "Some lessons from other disciplines", Proceedings, International Symposium on the Engineering properties of sea-floor soils and their geophysical identifications, Seattle, July 1971, pp. 1-10.

84. Wismer, R.D. and Luth, H.J., "Performance of plane soil cutting blades in clay", Transactions, American Society of Agricultural Engineering, Vol. 15, No. 1, 1972, pp. 211-216.

85. Wismer, R.D. and H.J. Luth, "Rate effects in soil cutting", Journal of Terramechanics, Vol. 8, No. 3, 1972, pp. 11-21.

86. Witney, B.D., "The determination of soil particle movement in two dimensional failure", Journal of Terramechanics, Vol. 5, No. 1, 1968, pp. 39-52.

87. Zeusler, F.A., "Standing iceberg guard in the North Atlantic", The National Geographic Magazine, Vol. 50, No. 1, Jan 1926, pp. 1-28.

88. Zubrov, N.N., Arctic Ice, Translated by U.S. Navy Electronics Laboratory, San Diego, pp. 120-137.

APPENDIX A

SAMPLE CALCULATION

APPENDIX A

SAMPLE CALCULATIONS

Experiment No. S6; Model = idealized shape: B = 9"; γ' = 45.95 lb/cft

TIME (sec)	LENGTH OF TRAVEL L (feet)	GOUGE DEPTH d (inches)	SURCHARGE h (inches)	AVERAGE SHEAR STRENGTH τ_f (lb/sft)	CALCULATED FORCE ON MODEL $P = \gamma' \frac{(h+d)^2}{2} B + 2\tau_f d.B + 2\tau_f d^2$	MEASURED FORCE (pounds)	INTEGRATED FROM PRESSURE READINGS
1	1.15	1.3	0.8	1.0	0.53+0.16+0.02 = 0.71	1.0	0.94
2	2.32	2.65	1.3	1.0	1.86+0.33+0.99 = 2.28	1.5	2.84
3	3.50	4.03	1.6	1.75	3.79+0.88+0.39 = 5.06	7.5	5.85
4	4.65	5.35	2.0	2.5	6.46+1.57+0.99 = 9.12	17.5	11.09
5	5.85	6.72	2.3	4.5	9.74+3.78+2.82 =16.34	27.0	19.19
6	6.85	7.90	2.5	5.5	12.94+5.43+4.77 =23.14	30.0	24.45

APPENDIX B

COMPUTER PROGRAM FOR COMPUTING THE GOUGE SIZE BY ITERATION

```
C
C
C  ***************************************************************
C  PROGRAM FOR COMPUTING THE LENGTH OF A SCOUR TRACK
C  CAUSED BY AN ICEBERG.  THIS TAKES INTO ACCOUNT THE SOIL
C DISPLACED AND ASSUMES THAT THE DISPLACED SOIL
C SETTLES ON THE SIDES AND IN FRONT OF THE
C  GOUGE TRACK.  SHEAR FAILURE TAKES PLACE AT 45 DEGREES
C  IN THE UNDISTURBED SOIL.  THE WEIGHT OF THE DISPLACED SOIL
C  OFFERES RESISTANCE TO THE MOVING BERG.
C  ***************************************************************
C
C
      REAL L,LD,LNEW,LDN,V,C,K,SLP,REP,DENS,B,W
   10 WRITE (6,270)
   20 WRITE (6,280)
   21 WRITE (6,290)
   22 READ (5,255) B
   23 VI = 0.5
   24 CI = 10.0
   25 SLPI = 250.0
   26 REPI = 250.0
   27 DENSI = 10.0
   28 WI = 1000.0
   33 V = 0.5
   34 DENS = 100.0
   35 C = 10.0
   36 SLP = 250.0
   37 REP = 250.0
   38 W = 1000.0
C
C
C*************************************************
C  W= BERG WEIGHT IN THOUSAND TONS, V=VELOCITY IN FEET/SECOND
C  B=WIDTH OF BERG IN FEET, SLP=BED SLOPE 1 IN SLP,
C  REP=SLOPE OF DISPLACED SOIL 1 IN REP, DENS=UNIT WEIGHT IN AIR
C  OF THE OCEAN FLOOR SOIL, C=SHEAR STRENGTH OF SOIL
C  L=LENGTH OF GOUGE TRACK, LD=LENGTH OVER WHICH DISPLACED
C  SOIL SETTLES
C
C THIS CAN ALSO BE SOLVED ON A DO LOOP USING INTEGER=IFIX(REAL)
C
C  *************************************************
C
C
   39 CONTINUE
   40 K = 1.0/SLP + 1.0/REP
   50 GAMA = DENS - 64.0
   60 L = 100.0
   70 D = L/SLP
   80 LD = L/10.0
C
C  LD IS NOW OBTAINED BY NEWTON - RAPHSON METHOD
C
   90 FX = 2*K*K*LD**4 + 4*K*K*L*LD**3 + LD*LD*(2*K*K*L*L
     2 + 3*K*L*B/REP) - 3*L*L*D*B/REP
  100 FDX = 8*K*K*LD**3 + 12*K*K*L*LD*LD
     2 + 2*LD*(2*K*K*L*L + 3*K*L*B/REP)
  110 LDN = LD - FX/FDX
```

```
      IF(ABS(LD-LDN),LT,0,5) GO TO 150
      LD = LDN
      GO TO 90
      LD = LDN
      H = L/SLP  +  LD/REP + LD/SLP
      HD = LD/REP + LD/SLP
C
C  L IS NOW OBTAINED BY NEWTON - RAPHSON ITERATION
C
      FE = (GAMA*H*H*D*B/6000  + C*D*D*B/1000 + 2*C*D**3/3000)*SLP -
     2  W*V*V*2240/(2*32,2)
      FDE = GAMA*H**2*B/2000 + (2*C*D*B + 2*C*D*D)/1000
      LNEW = L - FE/FDE
      IF (ABS(L-LNEW),LT,5,0) GO TO 230
      L = LNEW
      GO TO 70
      L = LNEW
      RA = W/B
      WRITE (6,260) V,DENS,C,SLP,W,L,D,LD,HD,RA,B
      W = W + WI
      IF (W,LE,20000,0)GO TO 39
      WRITE (6,290)
      REP = REP + REPI
      SLP = SLP + SLPI
      IF(SLP,LE,1500,0) GO TO 38
      C = C + CI
      IF (C,LE,50,0) GO TO 36
      DENS = DENS + DENSI
      IF (DENS,LE,120,0)GO TO 35
      V = V + VI
      IF (V,LE,1,5) GO TO 34
      CONTINUE
      FORMAT (F5,1)
      FORMAT (' ',1X,F3,1,5X,F5,1,6X,F4,1,7X,F6,1,5X,F7,1,7X,F8,2,5X,
     2 F5,1,6X,F8,2,6X,F5,1,6X,F5,1,5X,F5,1)
      FORMAT (' ','VELCTY',3X,'DENSITY',3X,'SHEAR STRNG',3X,'SLOPE',
     2 3X,'BERG HEIGHT',3X,'GOUGE LENGTH',3X,'DEPTH',3X,
     3 'LNGT-DISPL FNNT')
      FORMAT(' ','FT/SEC',3X,'LB/CFT',5X,'LBS/SFT',4X,'ONE  IN',
     2 3X,'THSND TNS',8X,'FEET',8X,'FT.',9X,'FEET')
      FORMAT (' ',///)
      STOP
      END
/*
```

APPENDIX C

ESTIMATION BY GRAPHICAL AND NUMERICAL INTEGRATION OF THE ERROR IN ASSUMING A LINEAR VARIATION OF THE SURCHARGE HEIGHT

```
C
C THIS PROGRAM IS TO VERIFY THE DIFFERENCE IN VALUES BETWEEN THE
C ASSUMPTION THAT THE HEIGHT OF THE DISPLACED SOIL IS  A LINEAR
C PROPORTION OF THE GOUGE DEPTH AND THE MORE RIGOROUS METHOD BY THE
C METOD OF NUMERICAL INTEGRATION
      REAL HD,D,INT,DN,LD,LDN,L,LI,INTN,B,K,SLP,REP,HDN,
     2  W,RA,H,WAPP,RAAP
      SLP = 500.0
      REP = 500.0
      K = 1.0/SLP  +  1.0/REP
      V=1.0
      DENS = 100.0
      GAMA = DENS - 64.0
      C = 50.0
      DO 300 N=1,10
      HD = 0.0
      D=0.0
      INT = 0.0
   10 WRITE (6,250)
      WRITE (6,260)
      WRITE (6,270)
      READ (5,280) B
      L = 100.0
      LI = 100.0
   90 DN = L/SLP
C
C LD IS NOW OBTAINED BY NEWTON - RAPHSON METHOD
C
      LD = L/10.0
  110 FX = 2*K*K*LD**4 + 4*K*K*L*LD**3 + LD*LD*(2*K*K*L*L
     2  + 3*K*L*B/REP) - 3*L*L*DN*B/REP
      FDX = 8*K*K*LD**3 + 12*K*K*L*LD*LD
     2 + 2*LD*(2*K*K*L*L + 3*K*L*B/REP)
      LDN = LD - FX/FDX
  140 IF(ABS(LD-LDN).LT.2.0) GO TO 170
      LD = LDN
      GO TO 110
  170 LD = LDN
      HDN = LD/REP + LD/SLP
      ININ = ((HDN+DN)**2 -(HD+D)**2)*0.5
      INT = INT + ININ
      HD = HDN
      D = DN
      W = 2*32.2/(2240*V*V)*(GAMA*B*INT*LI/2000 +
     2 C*D*B*L/1000 + 2*C*D*D*L/3000)
      RA = W/B
      H = HD + D
      WAPP = 2*32.2/(2240*V*V) * (GAMA*B*H*HL/6000 +
     2 C*D*B*L/1000 + 2*C*D*D*L/3000)
      RAAP = WAPP/B
      WRITE (6,290) B,L,RA,RAAP,LD,D,HD
      L = L + LI
      IF(L.LE.5000.0) GO TO 90
      WRITE (6,270)
  300 CONTINUE
  250 FORMAT (' ','WIDTH',5X,'GOUGE LENGTH',3X,'WT RATIO',4X,
     2 'APPRX RATIO',4X,'DISPL FRNT',4X,'DEPTH',5X,'DISPL HGHT')
  260 FORMAT (' ','FEET',6X,'FEET',11X,'THOUSAND TONS/FT WIDTH',
     2 6X,'FEET',10X,'FEET',6X,'FEET')
```

```
270 FORMAT (' ',////)
280 FORMAT (F5.1)
290 FORMAT (' ',F5.1,7X,F8.2,7X,F7.2,8X,F7.2,6X,F8.2,8X,-
   2 F6.2,9X,F6.2)
    STOP
    END
```

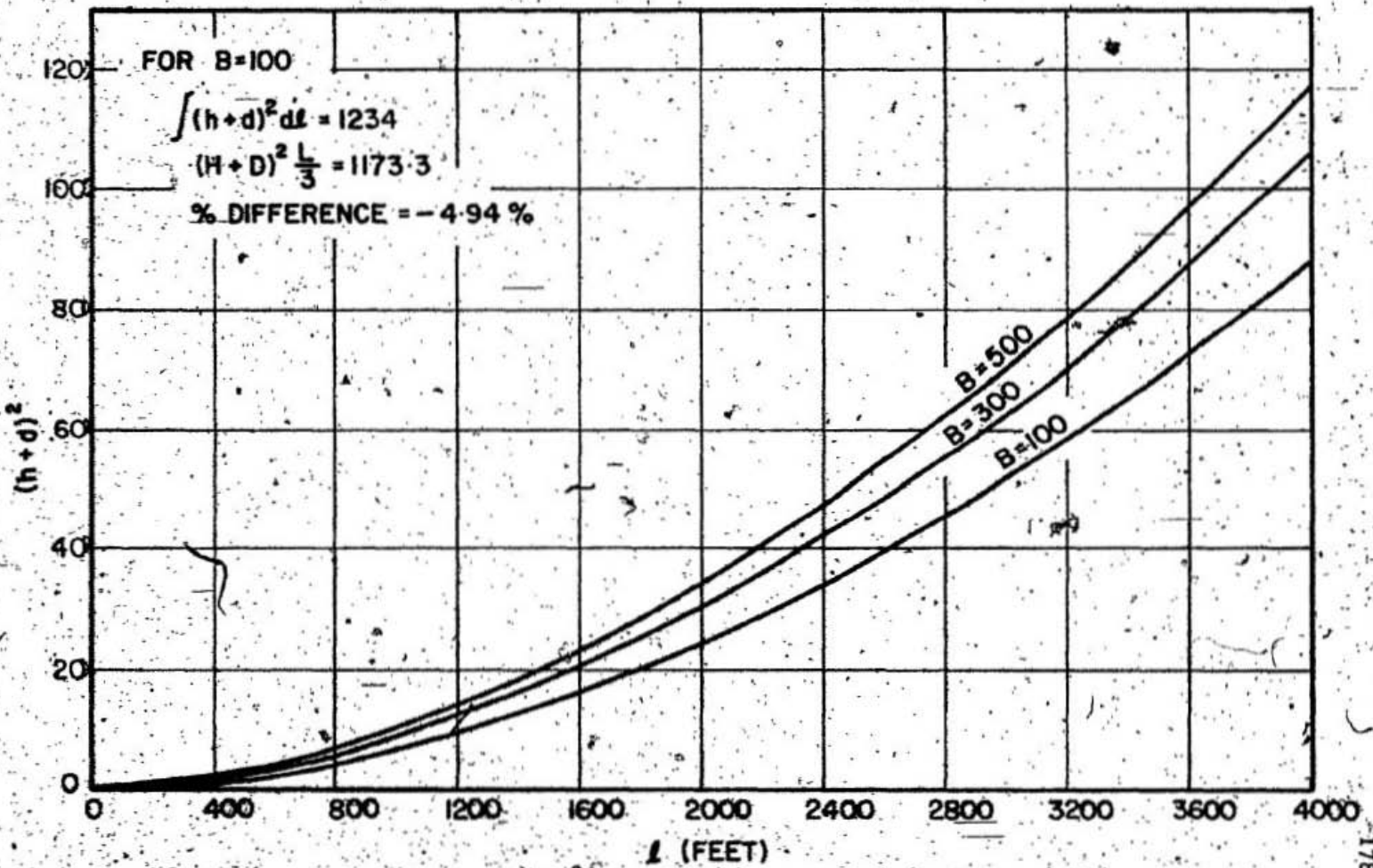

FIG. B1.- VARIATION OF $(h+d)^2$ WITH l

The error in the integral by assuming linear variation for h, is -4.94%

APPENDIX D

SPECIFICATIONS OF THE KISTLER QUARTZ PRESSURE TRANSDUCERS, MODEL 606-L

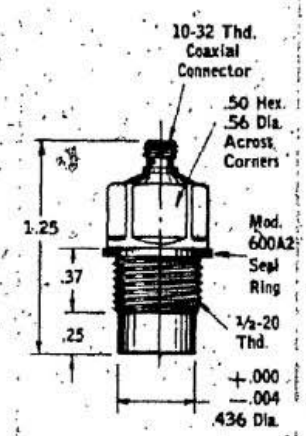

KISTLER QUARTZ PRESSURE TRANSDUCER
MODEL 606-L

SPECIFICATIONS:

Pressure range, full scale	30 psi
Resolution	0.005 psi
Maximum pressure	300 psi
Sensitivity (nominal)	5.5 picocoulomb/psi
Resonant frequency	>130 kHz
Rise time	3.0 microseconds
Linearity	±1%
Capacitance (nominal)	46 picofarads
Insulation resistance (at room temperature)	$>10^{13}$ ohms
Acceleration sensitivity - thru press. sens. axis	<.005 psi/g, <.001 psi/g special selection
Temperature effect on sensitivity	<0.03%/°F.
Temperature range	-350° to +450°F
Shock and vibration	1000 g
Cable connector	coaxial, 10-32
Case material	stainless steel
Weight	22 grams

CALIBRATION:

The sensitivity of the piezo gauge was factory checked and calibrated. Calibration charts were supplied with the gauges. However, to test check this, a static calibration arrangement was used in which the pressure was applied through a mercury column and the outputs at different sensitivity ranges of the amplifier were verified in long time constant.